

No. 113

December 1971

A RATIONAL STRIP THEORY OF SHIP MOTIONS: PART II

Odd Faltinsen

This research was carried out in part under the Naval Ship Systems Command General Hydromechanics Research Program Subproject SR 009 01 01, administered by the Naval Ship Research and Development Center. Contract No. N00014-67-A-0181-0016.

Reproduction in whole or in part is permitted for any purpose of the United States Government.

This document has been approved for public release and sale; its distribution is unlimited.



THE DEPARTMENT OF NAVAL ARCHITECTURE AND MARINE ENGINEERING

THE UNIVERSITY OF MICHIGAN
COLLEGE OF ENGINEERING

December 1971

A RATIONAL STRIP THEORY OF SHIP MOTIONS: PART II

Odd Faltinsen

This research was carried out under the
Naval Ship Systems Command
General Hydromechanics Research Program,
Subproject SR 009 01 01, administered by the
Naval Ship Research and Development Center.
Contract No. N00014-67-A-0181-0016
Reproduction in whole or in part is permitted
for any purpose of the United States Government.

This document has been approved for public release
and sale; its distribution is unlimited.



Department of Naval Architecture
and Marine Engineering
College of Engineering
The University of Michigan
Ann Arbor, Michigan 48104

ABSTRACT

The exact ideal-fluid boundary-value problem is formulated for the diffraction of head-sea regular waves by a restrained ship. The problem is then simplified by applying four restrictions: 1) the body must be slender; 2) the wave amplitude is small; 3) the wave length of the incoming waves is of the order of magnitude of the transverse dimensions of the ship; 4) the forward speed is zero or it is $O(\epsilon^{1/2-a})$, $0 < a \leq 1/2$, where ϵ is the slenderness parameter.

The problem is solved by using matched asymptotic expansions. The result shows that the wave is attenuated as it propagates along the ship. The result is not expected to be valid near the bow or stern of the ship.

The pressure distribution and force distribution along a ship model with circular cross-sections have been calculated. The total force on the ship has been compared with the value predicted by the Khaskind relation. The agreement is good.

The experimental and theoretical pressure distribution along a prolate spheroid have been compared. The predicted attenuation of the peak pressure is very well confirmed by the experiments. In addition, theory and experiment agree that the peak pressure near the ship generally leads the Froude-Kriloff pressure peak by 45° .

ACKNOWLEDGEMENT

I thank the members of my doctoral committee for their supervision of this thesis. My foremost acknowledgement goes to the chairman of the committee, Professor T. Francis Ogilvie.

My thanks go to Professor R. Timman, Technical University of Delft. The discussions with him were a break-through in my thesis work.

I thank Mr. Arthur M. Reed, University of Michigan, for giving valuable suggestions in the computational part of my thesis, and Dr. Choung Mook Lee, Naval Ship Research and Development Center, for providing me with experimental data.

I thank Dr. Nils Salvesen, Naval Ship Research and Development Center, for all his encouragement and help. Further, I am grateful to my employer, Det norske Veritas, for making my stay in the U.S.A. possible, and finally, my thanks go to The Royal Norwegian Council for Scientific and Industrial Research (NTNF) for supporting my stay.

CONTENTS

NOTATION	v
I INTRODUCTION	1
II GENERAL FORMULATION	2
III THE ZERO-SPEED PROBLEM	5
1. Far-field source solution	6
2. Inner expansion of far-field source solution	14
3. Comparison with another method	22
4. The near-field problem and the matching	24
IV THE FORWARD-SPEED PROBLEM	33
1. Far-field source solution	35
2. Inner expansion of far-field source solution	47
3. Comparison with another approach	58
4. The near-field problem and the matching	60
V NUMERICAL CALCULATIONS	67
1. Theoretical background	67
2. Numerical example	78
3. Comparison with experiments	81
VI REFERENCES	136

NOTATION

a	used in the description of the order of magnitude of the velocity U ; $U = O(\epsilon^{1/2-a})$, $0 < a \leq 1/2$
B	beam at midships when used in the figures
C =	$\frac{gh}{\omega_0}$
Fn =	U/\sqrt{Lg} , Froude number
g =	acceleration of gravity
$G(k_Y, k_Z; k_\xi, k_\eta)$	See (88)
h	wave amplitude of the incoming wave
$h(x, y)$	function defining the wetted surface of the ship
I(k)	See (19) for zero-speed problem. See (112) for forward-speed problem.
k	equal to $v \cdot \epsilon$ in the sections about the near-field problem and the matching. Otherwise integration variable in the Fourier transform.
$k_1 =$	0
$k_2 =$	$-\frac{g}{U^2} (2\omega_0 U/g + 1)$
L	length of ship
n	coordinate-axis in the direction of the outward normal on the wetted surface of the ship.
N	See (66)
n_{2D}	coordinate-axis normal to and out of a cylinder with the same cross-section as the ship at a given section.
n_i	$i = 1, 2, 3$: the x-, y-, z- component of the unit normal vector to the wetted surface of the ship.
r	radial coordinate used in the chapter: "Numerical Calculations" (see Fig. 8).

t	time variable
T	draft of the ship midships
U	forward speed of the ship
x,y,z	Cartesian coordinates (see Fig. 1). (The ship moves in the direction of the negative x-axis, z is measured upwards, y to starboard.).
X,Y,Z	Stretched coordinates (see (66) or (169)).
$\alpha =$	$\left \frac{v-k}{v} \right $ where k is an integration variable
β	very small positive number
δ_1	very small positive number
δ_2	very small positive number
ϵ	slenderness parameter
$\zeta(x,y,t)$	free-surface displacement
θ	angular coordinate used in the chapter: "Numerical Calculations" (see Fig. 8). $\theta = 0$ is a point on the centerplane.
λ	wave length of the incoming wave
μ	fictitious (Rayleigh) viscosity. (Note that $\mu(\arg)$ has another meaning.)
$v =$	$\frac{\omega^2}{g} = \frac{2\pi}{\lambda}$
ρ	density of water (mass per unit volume)
$\sigma(x)e^{i(\omega t - vx)}$	source density per unit length in line distribution of sources.
$\sigma^*(k) =$	$\int_{-\infty}^{\infty} dx e^{-ikx} \sigma(x)$
$\tau =$	$\frac{\omega U}{g}$
$\phi(x,y,z,t)$	velocity potential in forward-speed problem and in zero-speed problem *
$\phi_I(x,y,z,t)$	velocity potential of the incoming wave
$\phi_D(x,y,z,t)$	velocity potential of the diffracted wave

* Note, however, that it means the time dependent part of the velocity potential in the Chapter "Numerical calculations".

$\phi_s(x,y,z)$ $(1/U)$ * perturbation-velocity in steady motion problem

$\phi_T(x,y,z,t)$ time-dependent part of velocity potential

$\Phi(x,y,z)$ see (16) and (17) for zero-speed problem. See (109) and (110) for forward-speed problem.

$\psi(x,y,z)$ see (62) in zero-speed problem. See (164) in forward-speed problem.

ψ_i $i = 1, 2, \dots, N$, $\psi \sim \sum_{i=1}^N \psi_i$.

ω_0 wave frequency of the incoming wave

$\omega = \omega_0 + \nu U$

I. INTRODUCTION

The intention in this thesis is to derive a method to find the pressure distribution along a ship due to head-sea regular waves. The ship is restrained from oscillating, and the ship meets the waves with a high frequency. The wave length of the incoming waves is assumed to be of the order of magnitude of the transverse dimensions of the ship. For the zero-speed case, the frequency of the wave is the same order of magnitude as the frequency of oscillation used in Ogilvie & Tuck (1969). Ogilvie & Tuck considered the forced heave and pitch oscillation of a ship when there were no incoming waves. Due to linearity, the forces obtained in Ogilvie & Tuck and the forces obtained in this thesis can be superimposed to give the hydrodynamical forces on a ship which oscillates in a steady-state condition in regular head-sea waves. In the forward-speed case, the assumptions in Ogilvie & Tuck (1969) and in this thesis are different.

Ogilvie & Tuck got a strip theory result and it is well-known that strip theory gives good results for a wider range of wave lengths than Ogilvie & Tuck restricted themselves to (see Salvesen, Tuck, & Faltinsen (1970)). So it is the hope that the theory presented in this thesis also will cover a wider range of wave lengths. But it is only our experience that is going to tell us for how large wave lengths our theory is capable of predicting the pressure distribution along the ship. The theory predicts that head-sea waves of small wave length are deformed as they propagate along the ship. Abels (1959) observed this fact for a wave length which was half of the length of the ship, but he did not observe it for a wave length which was three-fourths of the length of the ship.

By integrating the pressure in an appropriate way over the submerged part of the ship, we are able to predict the exciting force and moment on the ship. For the zero-speed case there is another way to obtain the exciting force and moment on a ship, namely to use the Khaskind relation (see Newman (1962)). The disadvantage of the Khaskind relation is that it cannot predict

the pressure distribution along the ship. Further it is a formula derived on the basis of a general mathematical relationship, and so it does not give us much insight into the physical problem.

The method of matched asymptotic expansions has been used in solving our problem, and an important part of our solution in the near-field problem is Ursell's solution (1968 a) of a closely related problem: He obtained a general expression describing wave motions which can exist in the presence of an infinitely long horizontal cylinder, the wave motion being periodic along the cylinder. Our solution for the total potential in the near-field can be written as Ursell's solution multiplied with a function of x (x is the longitudinal coordinate. See Fig. 1). The function of x contains the factor $(x + L/2)^{-1/2}$, where $-L/2$ is the x -coordinate of the forward perpendicular. Our solution is not assumed to be valid near the bow or stern. Ursell was somewhat discouraged with his solution because it became unbounded laterally at infinity (when $y \rightarrow \pm \infty$. See Fig. 1). But in our case this does not matter because Ursell's solution is only a part of our near-field solution, which is not assumed to be valid at infinity. The only important thing is that our near-field solution should match with the far-field solution, which it does.

II. GENERAL FORMULATION

The coordinate system which is going to be used is shown in Figure 1.

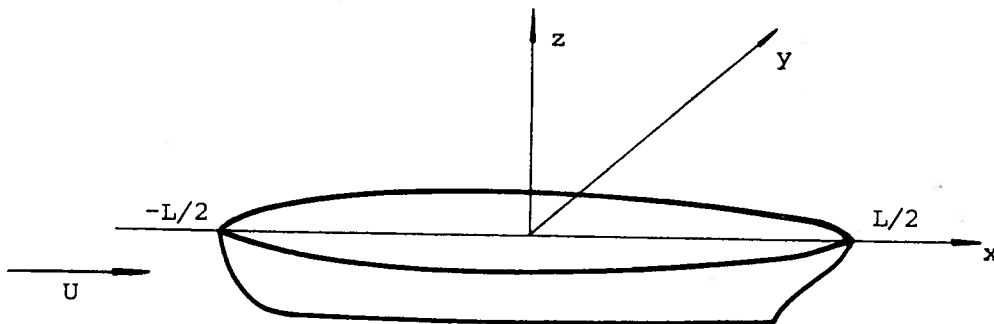


FIGURE 1
COORDINATE SYSTEM

The coordinate system is fixed to the ship. The plane $z = 0$ represents the undisturbed free surface. The z -axis is positive upwards and the positive y -direction is in the starboard direction. It is assumed that the ship moves with a constant velocity U in the direction of the negative x -axis. Since we will refer everything to the coordinate system in the ship it will look as if there is an incident, undisturbed flow with velocity U in the direction of the positive x -axis.

It is assumed that the fluid is incompressible and the flow irrotational, so that there exists a velocity potential ϕ which satisfies the three-dimensional Laplace equation,

$$\frac{\partial^2 \phi}{\partial x^2} + \frac{\partial^2 \phi}{\partial y^2} + \frac{\partial^2 \phi}{\partial z^2} = 0 \quad (1)$$

in the fluid domain. The ship is restrained from performing any oscillatory motions, and so the boundary condition on the wetted surface of the ship will be

$$\frac{\partial \phi}{\partial n} = 0 \quad \text{on } z = h(x, y) \quad (2)$$

Here $z = h(x, y)$ is the mathematical description of the wetted surface of the ship. $\partial/\partial n$ denotes the derivative in the direction of the outwards normal on the surface of the ship.

The conditions on the free surface, $z = \zeta(x, y, t)$, are, neglecting surface tension,

(A), the dynamic free surface condition

$$g\zeta + \phi_t + 1/2 [\phi_x^2 + \phi_y^2 + \phi_z^2] = 1/2 U^2 \quad \text{on } z = \zeta(x, y, t) \quad (3)$$

(B), the kinematic free surface condition

$$\phi_x \zeta_x + \phi_y \zeta_y - \phi_z + \zeta_t = 0 \quad \text{on } z = \zeta(x, y, t). \quad (4)$$

g is the acceleration of gravity.

We must also satisfy a radiation condition. We will be more specific about that later.

It is assumed that the fluid has infinite depth, the free surface has infinite extent, and there are no bodies other than the ship.

We will assume that there are incoming, regular gravity waves propagating along the positive x-axis. The wave amplitude is assumed to be small so that the classical linear free-surface theory is applicable. We will later linearize the problem with respect to the wave amplitude. The potential ϕ_I of the incoming waves will be given by

$$\phi_I = \underline{\text{Re}} \left[\frac{gh}{\omega_0} e^{\nu z} e^{i(\omega t - \nu x)} \right] \quad (5)$$

Here Re means the real part. As is usual we are going to drop the notation Re. We will write the potential in complex form, and it should be understood that we should take the real part. This is only a matter of convenience.

h is the wave amplitude, ω_0 is the wave frequency, ν is the wave number, ω the frequency of encounter and t is the time variable. The wave number ν can be written as

$$\nu = \frac{2\pi}{\lambda} = \frac{\omega_0^2}{g} \quad (6)$$

where λ is the wave length. The relation between ν, ω_0, ω , and U for head-sea waves is

$$\omega = \omega_0 + \nu U \quad (7)$$

We will assume that the ship is slender, and we will introduce the slenderness parameter ϵ . It is a measure of the transverse dimensions of the ship compared with the length of the ship. So ϵ is a small quantity. If we denote the x, y, z -components of the normal \underline{n} on the wetted surface of the ship by n_1, n_2, n_3 respectively, then we can set

$$n_1 = O(\epsilon), \quad n_2 = O(1), \quad n_3 = O(1) \quad (8)$$

We will assume that the frequency of the wave has the following asymptotic behavior

$$\omega_0 = O(\epsilon^{-1/2}) \quad (9)$$

Using (6) this means that

$$\lambda = O(\epsilon) \quad (10)$$

III. THE ZERO-SPEED PROBLEM

The frequency of encounter, ω , is the same as the frequency of the waves, ω_0 , for the zero-speed case (see (7)). The time dependence of the incident wave is given by $e^{i\omega t}$ (see (5)). It is expected that the time dependence for the total potential is also given by $e^{i\omega t}$. This means that $\partial/\partial t$ is equivalent to multiplying by $i\omega$. We will use this fact and now write down the equations to determine the velocity potential. From (1), (2), (3), (4) and the assumption about linearity it follows that ϕ satisfies

$$\frac{\partial^2 \phi}{\partial x^2} + \frac{\partial^2 \phi}{\partial y^2} + \frac{\partial^2 \phi}{\partial z^2} = 0 \quad \text{in the fluid domain,} \quad (1)$$

$$\frac{\partial \phi}{\partial n} = 0 \quad \text{on } z = h(x, y), \quad (2)$$

$$-\omega^2 \phi + g \frac{\partial \phi}{\partial z} = 0 \quad \text{on } z = 0 \quad \text{outside the body.} \quad (11)$$

In addition, the diffraction part of the potential must satisfy a radiation condition.

We will write ϕ as

$$\phi = \phi_I + \phi_D = \frac{gh}{\omega} e^{vz} e^{i(\omega t - vx)} + \phi_D \quad (12)$$

Here ϕ_D denotes the diffraction potential. To find ϕ_D we are going to use the method of matched asymptotic expansions (Van Dyke (1964), Ogilvie (1970)). As is usual, we introduce a far-field description and a near-field description. The far-field description is expected to be valid at distances which are $O(1)$ and larger from the ship. The near-field description is valid near the ship at distances which are $O(\epsilon)$.

There are four parts in this chapter: (1) derivation of the far-field source solution due to a line of pulsating sources located on the x-axis between $-L/2$ and $L/2$ (see Fig. 1); (2) derivation of a two-term inner expansion of the far-field source solution; (3) comparison of the expression found in part (2) with the result obtained by another method; (4) formulation of the near-field problem, and the matching of a two-term near-field solution with the far-field solution.

1. Far-field source solution

In the far-field description, we expect to have waves. In order to have waves, we must satisfy the condition (11). This means that the two terms in (11) must be of the same order of magnitude in the far-field, and so $\partial/\partial z = O(\epsilon^{-1})$. The existence of a surface wave implies that $\partial/\partial z$ and, say, $\partial/\partial s$ are the same order of magnitude, where s is measured normal to wave fronts. In the far-field, we cannot in general say that the normal to the wave fronts should be neither along the x-axis nor along the y-axis. This implies that $\partial/\partial x$ and $\partial/\partial y$ must also be of order ϵ^{-1} in the far-field.

From a far-field point of view, one cannot see the shape of the hull. As $\epsilon \rightarrow 0$ the disturbance from the hull to the far-field seems to emanate from a line of singularities located on the x-axis between $-L/2$ and $L/2$. The dominant far-away effect is expected to appear to be due to a line of sources. Since the incoming waves vary as $e^{i(\omega t - \nu x)}$, it is expected that the line of sources has a source density of the form

$$\sigma(x) e^{i(\omega t - \nu x)}.$$

Due to the slenderness of the ship we assume $\frac{\partial \sigma}{\partial x} = O(\sigma)$.

These physical arguments can be given a mathematical formulation. We can replace the Laplace equation (1) by the Poisson equation

$$\frac{\partial^2 \phi_D}{\partial x^2} + \frac{\partial^2 \phi_D}{\partial y^2} + \frac{\partial^2 \phi_D}{\partial z^2} = \sigma(x) e^{i(\omega t - \nu x)} \delta(y) \delta(z - z_0). \quad (13)$$

Here δ is the Dirac-delta function, and initially we take $z_0 < 0$. When the solution of ϕ_D is found, z_0 will be set equal to zero. If we set $z_0 = 0$ first, we would be in difficulties solving the problem.

We cannot expect that the far-field solution will satisfy the boundary condition on the hull given by (2), but it must satisfy a proper radiation condition. We must be sure that the diffraction potential ϕ_D does not contain an incoming wave. This is most easily taken care of by introducing the artificial Rayleigh viscosity μ (see Ogilvie & Tuck (1969)). The free-surface condition (11) will then be modified to

$$(i\omega + \mu)^2 \phi_D + g \frac{\partial \phi_D}{\partial z} = 0 \quad \text{on } z = 0 \quad (14)$$

At an appropriate later point, we will let μ go to zero.

The solution to (13) and (14) with $z_0 = 0$ can be found in Ogilvie & Tuck (1969) and is

$$\begin{aligned} \phi_D(x, y, z, t) &= -\frac{1}{4\pi^2} e^{i\omega t} \int_{-\infty}^{\infty} dk e^{ikx} F\{\sigma(x) e^{-i\nu x}\} \\ &\cdot \lim_{\mu \rightarrow 0} \int_{-\infty}^{\infty} \frac{d\ell e^{i\ell y} + z\sqrt{k^2 + \ell^2}}{\sqrt{k^2 + \ell^2} - \frac{1}{g}(\omega - i\mu)^2} \end{aligned} \quad (15)$$

Here

$$F\{\sigma(x) e^{-i\nu x}\} = \int_{-\infty}^{\infty} dx e^{-ikx} \sigma(x) e^{-i\nu x} = \sigma^*(k + \nu)$$

Expression (15) can be rewritten in a form which is more convenient to handle for our purposes. I will follow a procedure described by Ogilvie (1969), and what I am going to do is based on his work.

We first introduce

$$k' = k + v$$

in (15). We can then write

$$\phi_D(x, y, z, t) = -\frac{1}{4\pi^2} e^{i(\omega t - vx)} \int_{-\infty}^{\infty} dk' e^{ik'x} \sigma^*(k')$$

$$\cdot \lim_{\mu' \rightarrow 0} \int_{-\infty}^{\infty} \frac{d\ell e^{i\ell y + z\sqrt{(k'-v)^2 + \ell^2}}}{\sqrt{(k'-v)^2 + \ell^2} - (v - i\mu')}$$

Here $\mu' = \frac{2\omega\mu}{g}$. We drop the primes and write

$$\phi_D(x, y, z, t) = \Phi(x, y, z) e^{i(\omega t - vx)} \quad (16)$$

where

$$\Phi(x, y, z) = -\frac{1}{4\pi^2} \int_{-\infty}^{\infty} dk e^{ikx} \sigma^*(k)$$

$$\cdot \lim_{\mu \rightarrow 0} \int_{-\infty}^{\infty} \frac{d\ell e^{i\ell y + z\sqrt{\ell^2 + (v-k)^2}}}{\sqrt{\ell^2 + (v-k)^2} - (v - i\mu)} \quad (17)$$

We will let $y = O(1)$ and we are going to assume that $y > 0$. The derivation for $y < 0$ will be quite similar, and we are not going to go through that. Since we are operating with sources, we can later use the fact that

$$\phi_D(x, -y, z, t) = \phi_D(x, y, z, t) \quad (18)$$

We now define

$$I(k) = \lim_{\mu \rightarrow 0} \int_{-\infty}^{\infty} \frac{d\ell e^{i\ell y + z\sqrt{\ell^2 + (\nu-k)^2}}}{\sqrt{\ell^2 + (\nu-k)^2} - (\nu - i\mu)} \quad (19)$$

The poles of the integrand are important in the evaluation of $I(k)$. They are given in the limit $\mu \rightarrow 0$ by:

$$\ell^2 = (2\nu - k)k.$$

Let us first study the case in which these singularities are imaginary, which means $k < 0$ or $k > 2\nu$. Then we study case II, in which $0 < k < 2\nu$.

Case I: $k < 0$ or $k > 2\nu$. We define

$$\ell_0 = i\sqrt{k(k-2\nu)}$$

We introduce a closed curve ABCDEA in the complex ℓ -plane, as shown in Figure 2.

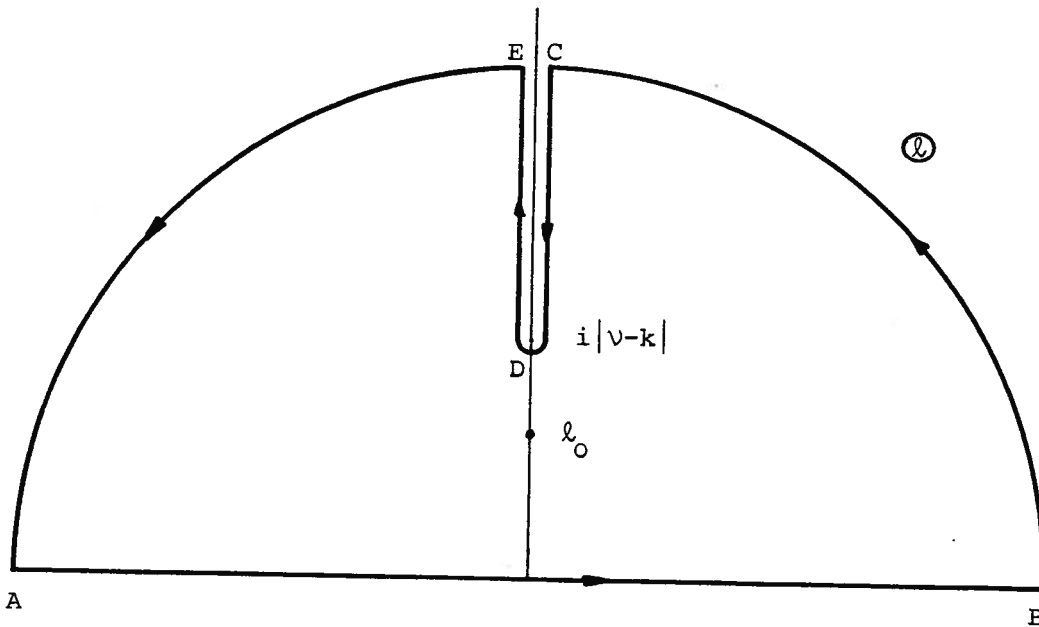


FIGURE 2
COMPLEX INTEGRATION PATH

The integrand in (19) has a branch point at $i|v-k|$, and we choose the branch cut along the positive imaginary axis. By using the residue theorem, letting $B \rightarrow +\infty$, $C \rightarrow +i\infty$, $E \rightarrow +i\infty$, $A \rightarrow -\infty$, we will get

$$\begin{aligned}
 I(k) &= 2\pi i \operatorname{Res} (l_0) \\
 &+ \int_{|v-k|}^{\infty} i \, dl \, e^{-ly} \left[\frac{e^{iz\sqrt{l^2-(v-k)^2}}}{i\sqrt{l^2-(v-k)^2-v}} - \frac{e^{-iz\sqrt{l^2-(v-k)^2}}}{-i\sqrt{l^2-(v-k)^2-v}} \right] \\
 &= \frac{2\pi v e^{vz - y\sqrt{k(k-2v)}}}{\sqrt{k(k-2v)}} + \int_{\alpha}^{\infty} dl \, e^{-vy l} \left[\frac{e^{ivz\sqrt{l^2-\alpha^2}}}{\sqrt{l^2-\alpha^2+i}} + \frac{e^{-ivz\sqrt{l^2-\alpha^2}}}{\sqrt{l^2-\alpha^2-i}} \right] \quad (20)
 \end{aligned}$$

where $\alpha = \left| \frac{v-k}{v} \right|$. α will be greater than 1, since we are considering the case $k < 0$ or $k > 2v$.

We want to show that the integral in (20) is exponentially small as $\varepsilon \rightarrow 0$. The following inequality must be valid

$$\left| \int_{\alpha}^{\infty} \frac{dl \, e^{-vy l \pm ivz\sqrt{l^2-\alpha^2}}}{\sqrt{l^2-\alpha^2 \pm i}} \right| < \int_{\alpha}^{\infty} \frac{dl \, e^{-vy l}}{\sqrt{l^2-\alpha^2}} \quad (21)$$

This can be written as

$$\int_{\alpha}^{\infty} \frac{dl \, e^{-vy l}}{\sqrt{l^2-\alpha^2}} = \int_0^{\infty} \frac{dm}{\sqrt{m^2+\alpha^2}} e^{-vy\sqrt{m^2+\alpha^2}} = \int_0^{\infty} e^{-vy\alpha \cosh u} \, du = K_0(vy\alpha) \quad (22)$$

See Abramowitz and Stegun (1964). K_0 is a modified Bessel function of the second kind. Since $v = O(\varepsilon^{-1})$, $y = O(1)$ and $\alpha > 1$, the argument of K_0 is large. By using the asymptotic expansion of K_0 for large arguments, we can show that the integral term in (20) is bounded by a quantity which is $O(e^{-1/\varepsilon})$. So we can write

$$I(k) = \frac{2\pi v e^{vz - y\sqrt{k(k-2v)}}}{\sqrt{k(k-2v)}} + O(e^{-1/\varepsilon}) \quad (23)$$

for $k < 0$ or $k > 2v$, and $y=O(1)$

Case II: $0 < k < 2\nu$. The poles of the integrand of (19) are now real. The Rayleigh viscosity will help us to determine how to indent the integration path of $I(k)$ around the poles. If we define

$$l_0 = \sqrt{k(2\nu - k)}, \quad (24)$$

the poles will be at $\pm l_0$ when $\mu = 0$. The integration path will be as shown in Figure 3.

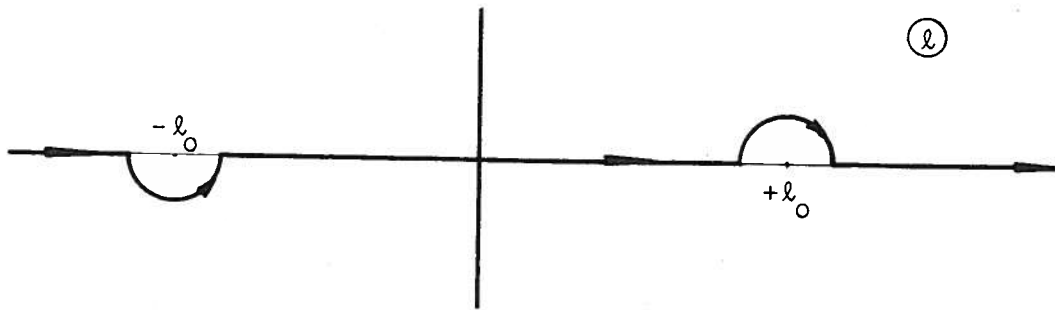


FIGURE 3
COMPLEX INTEGRATION PATH

In the same way as we did for Case I, we introduce a closed curve ABCDEA in the complex l -plane and use the residue theorem to evaluate $I(k)$. The closed curve is shown in Figure 4.

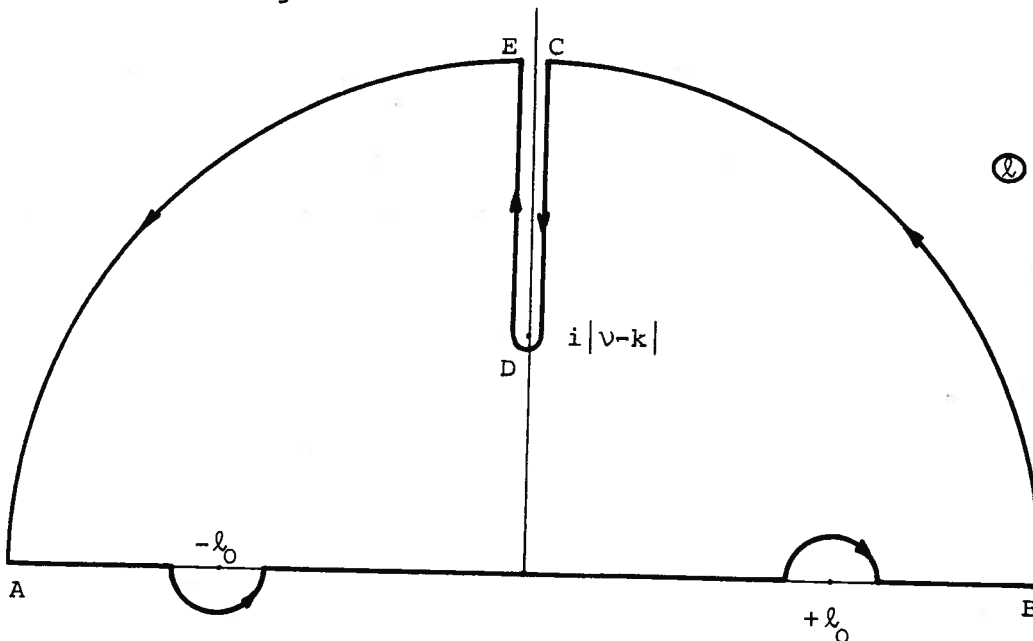


FIGURE 4
COMPLEX INTEGRATION PATH

Noting that

$$\text{Res } (-l_0) = \frac{v e^{vz - iy\sqrt{k(2v-k)}}}{-\sqrt{k(2v-k)}}, \quad (25)$$

we get by use of the residue theorem in the same way as for Case I that

$$I(k) = -\frac{2\pi i v e^{vz - iy\sqrt{k(2v-k)}}}{\sqrt{k(2v-k)}} + \int_{\alpha}^{\infty} dl e^{-vy l} \left[\frac{e^{ivz\sqrt{l^2 - \alpha^2}}}{\sqrt{l^2 - \alpha^2} + i} + \frac{e^{-ivz\sqrt{l^2 - \alpha^2}}}{\sqrt{l^2 - \alpha^2} - i} \right] \quad (26)$$

Here $\alpha = \left| \frac{v-k}{v} \right| < 1$.

As long as α is not of order ϵ or less, we can use the same argument as for Case I to show that the integral in (26) is exponentially small with respect to ϵ as $\epsilon \rightarrow 0^*$. But when $\alpha = O(\epsilon)$ we see from (22) that the argument of the bounding function K_0 is of order 1. We therefore have to use another procedure.

We can write

$$\left| \int_{\alpha}^{\infty} dl e^{-vy l} \frac{e^{\pm ivz\sqrt{l^2 - \alpha^2}}}{\sqrt{l^2 - \alpha^2} \pm i} \right| < \int_{\alpha}^{\infty} dl e^{-vy l} = \frac{e^{-vy\alpha}}{vy} = O(\epsilon)$$

When $\alpha = 0$ it can be shown that the integral term is of $O(\epsilon)$. Since k is $O(v) = O(\epsilon^{-1})$ when $\alpha = O(\epsilon)$ or less, it is easily seen that the first term in (26) is $O(1)$. So the integral will be of higher order than the first term in (26) when $\alpha = O(\epsilon)$, as well as when $\alpha = O(1)$. We now have the results ($0 < y = O(1)$).

$$I(k) = \begin{cases} \frac{2\pi v e^{vz - y\sqrt{k(k-2v)}}}{\sqrt{k(k-2v)}} + \dots & \text{for } k < 0 \\ -\frac{2\pi i v e^{vz - iy\sqrt{k(2v-k)}}}{\sqrt{k(2v-k)}} + \dots & \text{for } 0 < k < 2v \\ \dots & \text{for } k > 2v \end{cases} \quad (27)$$

* It will be evident later why k is related to ϵ , and therefore why α is related to ϵ .

By using equation (17) and (19), we can write

$$\begin{aligned}
 \Phi(x, y, z) = & -\frac{ve^{vz}}{2\pi} \left[\int_{-\infty}^0 \frac{dk e^{ikx - y\sqrt{k(k-2v)}} \sigma^*(k)}{\sqrt{k(k-2v)}} \right. \\
 & -i \int_0^{2v} \frac{dk e^{ikx - iy\sqrt{k(2v-k)}} \sigma^*(k)}{\sqrt{k(2v-k)}} \\
 & \left. + \int_{2v}^{\infty} \frac{dk e^{ikx - y\sqrt{k(k-2v)}} \sigma^*(k)}{\sqrt{k(k-2v)}} \right] \\
 & + \text{higher order terms}
 \end{aligned} \tag{28}$$

We rewrite (28) as

$$\begin{aligned}
 \Phi(x, y, z) = & -\frac{ve^{vz}}{2\pi} \left[\int_{-\infty}^{-\epsilon^{-(1-\delta_1)}} \frac{dk e^{ikx - y\sqrt{k(k-2v)}} \sigma^*(k)}{\sqrt{k(k-2v)}} \right. \\
 & + \int_{-\epsilon^{-(1-\delta_1)}}^0 \frac{dk e^{ikx - y\sqrt{k(k-2v)}} \sigma^*(k)}{\sqrt{k(k-2v)}} \\
 & -i \int_0^{\epsilon^{-(1-\delta_1)}} \frac{dk e^{ikx - iy\sqrt{k(2v-k)}} \sigma^*(k)}{\sqrt{k(2v-k)}} \\
 & -i \int_{\epsilon^{-(1-\delta_1)}}^{2v} \frac{dk e^{ikx - iy\sqrt{k(2v-k)}} \sigma^*(k)}{\sqrt{k(2v-k)}} \\
 & \left. + \int_{2v}^{\infty} \frac{dk e^{ikx - y\sqrt{k(k-2v)}} \sigma^*(k)}{\sqrt{k(k-2v)}} + \dots \right]
 \end{aligned} \tag{29}$$

Here δ_1 is some very small positive number. It will be evident in the next section why we have introduced $\epsilon^{-(1-\delta_1)}$.

It can easily be shown that the first integral in (29) is exponentially small. So we drop that term.

We prefer to write the last two terms in another way by introducing the new variable $u = k-2\nu$. After introducing the new variable in the last integral, we drop the contribution from integrating from $\varepsilon^{-(1-\delta_1)}$ to ∞ ; the argument is the same as that used above in dropping the first integral in (29). Equation (29) can now be written as

$$\begin{aligned} \Phi(x,y,z) \approx & -\frac{\nu e^{\nu z}}{2\pi} \left[\int_{-\varepsilon^{-(1-\delta_1)}}^0 \frac{dk e^{ikx - y\sqrt{k(k-2\nu)}}}{\sqrt{k(k-2\nu)}} \sigma^*(k) \right. \\ & -i \int_0^{\varepsilon^{-(1-\delta_1)}} \frac{dk e^{ikx - iy\sqrt{k(2\nu-k)}}}{\sqrt{k(2\nu-k)}} \sigma^*(k) \\ & -i \int_{\varepsilon^{-(1-\delta_1)}-2\nu}^0 \frac{du e^{iux + i2\nu x - iy\sqrt{(u+2\nu)(-u)}}}{\sqrt{(u+2\nu)(-u)}} \sigma^*(u+2\nu) \\ & \left. + \int_0^{\varepsilon^{-(1-\delta_1)}} \frac{du e^{iux + i2\nu x - y\sqrt{(u+2\nu)u}}}{\sqrt{(u+2\nu)u}} \sigma^*(u+2\nu) \right] \end{aligned} \quad (30)$$

This is the final form of the far-field source solution. It is valid for $y = O(1)$.

2. Inner expansion of far-field source solution

We are now going to find a two-term inner expansion of the far-field source solution. The result is given by equation (54).

We now let y be of order ε , and we reorder the terms in (30).

In the first integrand we want an expansion of

$$\frac{e^{-y\sqrt{k(k-2\nu)}}}{\sqrt{k(k-2\nu)}} \quad (31)$$

It will now be evident why we introduced $\varepsilon^{-(1-\delta_1)}$ in the previous section. Since k cannot be greater than $\varepsilon^{-(1-\delta_1)}$, $y\sqrt{k(k-2\nu)}$ will be $O(1)$. We expand (31) and keep two terms

$$\frac{e^{-y\sqrt{k(k-2\nu)}}}{\sqrt{k(k-2\nu)}} = \frac{1}{\sqrt{k(k-2\nu)}} - y + \dots \quad (32)$$

The omitted terms are higher order. Further, we expand

$$\frac{1}{\sqrt{k(k-2\nu)}} .$$

We can then write (31) as follows

$$\frac{e^{-y\sqrt{k(k-2\nu)}}}{\sqrt{k(k-2\nu)}} = \frac{1}{\sqrt{2\nu|k|}} \left[1 + \frac{k}{4\nu} + \dots \right] - y + \dots \quad (33)$$

We want to keep only the two lowest-order terms in the first integral in (30). k in the first integral will be $O(\varepsilon^{\alpha_1-1})$, where α_1 can be greater than or equal to δ_1 , depending on k . So the first term in (33) will be $O(\varepsilon^{1-\alpha_1/2})$, the second term $O(\varepsilon^{1+\alpha_1/2})$, and the third term $O(\varepsilon)$. When (33) is put into the first integral in (30), the second term in (33) will give the highest-order term. The two lowest-order terms in the first integral in (30) will be

$$- \frac{\nu e^{\nu z}}{2\pi} \int_{-\varepsilon^{-(1-\delta_1)}}^0 dk e^{ikx} \sigma^*(k) \left[\frac{1}{\sqrt{2\nu|k|}} - y \right]. \quad (34)$$

In a similar way we will find that the second integral in (30) can be written as

$$\frac{\nu e^{\nu z}}{2\pi} i \int_0^{\varepsilon^{-(1-\delta_1)}} dk e^{ikx} \sigma^*(k) \left[\frac{1}{\sqrt{2\nu k}} - iy \right]. \quad (35)$$

We are going to follow the same procedure as above to evaluate the third and fourth integrals in (30). It will be evident later that the latter will give a contribution which is of the same order of magnitude as the higher-order terms in (34) and (35). We will therefore keep only the lowest-order terms in the two last integrals. But we must be careful with the third integral. The lower integration limit is $O(\nu) = O(\varepsilon^{-1})$. For the integration variable u of order ν we cannot truncate the series expansion of

$$\frac{e^{-iy\sqrt{(u+2v)(-u)}}}{\sqrt{(u+2v)(-u)}}$$

after two terms in the same manner as we did in (32). But let us set the lower integration limit in the third integral equal to $-\epsilon^{-(1-\delta_1)}$. The difference between

$$\int_{-\epsilon^{-(1-\delta_1)} - 2v}^0 \frac{du e^{iux} e^{-iy\sqrt{(u+2v)(-u)}} \sigma^*(u+2v)}{\sqrt{(u+2v)(-u)}} \quad (36)$$

and

$$\int_{-\epsilon^{-(1-\delta_1)}}^0 \frac{du e^{iux} e^{-iy\sqrt{(u+2v)(-u)}} \sigma^*(u+2v)}{\sqrt{(u+2v)(-u)}} \quad (37)$$

is higher order. As long as we only want the lowest-order term of (36), we should be safe in changing (36) to (37).

We now do for the third integral as we did for the first integral. We will get

$$i \frac{ve^{vz}}{2\pi} e^{i2vx} \int_{-\epsilon^{-(1-\delta_1)}}^0 du e^{iux} \frac{\sigma^*(u+2v)}{\sqrt{2v|u|}} \quad (38)$$

And for the fourth integral we will get

$$- \frac{ve^{vz}}{2\pi} e^{i2vx} \int_0^{\epsilon^{-(1-\delta_1)}} du e^{iux} \frac{\sigma^*(u+2v)}{\sqrt{2vu}} \quad (39)$$

By now putting the expressions (34), (35), (38) and (39) for each of the four integrals into (30), we can write

$$\begin{aligned}
 \Phi(x, y, z) = & \left[-\frac{ve^{vz}}{2\pi} \int_{-\epsilon}^0 dk e^{ikx} \frac{\sigma^*(k)}{\sqrt{2v|k|}} \right. \\
 & \left. + \frac{ve^{vz}}{2\pi} i \int_0^{\epsilon^{-(1-\delta_1)}} dk e^{ikx} \frac{\sigma^*(k)}{\sqrt{2vk}} \right] \\
 & + \left[\frac{ve^{vz}}{2\pi} y \int_{-\epsilon}^{\epsilon^{-(1-\delta_1)}} dk e^{ikx} \sigma^*(k) \right. \\
 & + i \frac{ve^{vz}}{2\pi} e^{i2vx} \int_{-\epsilon}^0 du e^{iux} \frac{\sigma^*(u+2v)}{\sqrt{2v|u|}} \\
 & \left. - \frac{ve^{vz}}{2\pi} e^{i2vx} \int_0^{\epsilon^{-(1-\delta_1)}} du e^{iux} \frac{\sigma^*(u+2v)}{\sqrt{2vu}} \right] \\
 & + \text{higher order terms}
 \end{aligned} \tag{40}$$

Note that the first brackets contain the lowest-order terms, the second brackets the next-lowest-order terms.

Because we want to apply Fourier-transform techniques, we want to set $\epsilon^{-(1-\delta_1)}$ equal to ∞ . For the three higher-order terms in (40) we could do that; the effect would be only to introduce higher-order, negligible effects. But we must be careful with the lower order terms:

$$\int_{-\epsilon}^0 dk e^{ikx} \frac{\sigma^*(k)}{\sqrt{2v|k|}} \tag{41}$$

and

$$\int_0^{\epsilon^{-(1-\delta_1)}} dk e^{ikx} \frac{\sigma^*(k)}{\sqrt{2vk}} \tag{42}$$

We will consider especially the integral (42). We can write it as

$$\int_0^{\infty} dk e^{ikx} \frac{\sigma^*(k)}{\sqrt{2vk}} - \int_{\epsilon^{-(1-\delta_1)}}^{\infty} dk e^{ikx} \frac{\sigma^*(k)}{\sqrt{2vk}}. \quad (43)$$

We will try to find the order of magnitude of the second integral. We then need to know how $\sigma^*(k)$ behaves for large k . We will assume that $\sigma(x)$ and $\sigma'(x)$ are continuous in the interval $-L/2 \leq x \leq L/2$ [including the end points] (see Fig. 1). Outside $-L/2 \leq x \leq L/2$, $\sigma(x) \equiv 0^*$. It can then be shown (see Lighthill (1958)) that $|kL|^3 \sigma^*(k)$ remains bounded as $k \rightarrow \pm\infty$. So the second integral in (43) can be bounded by

$$\left| \int_{\epsilon^{-(1-\delta_1)}}^{\infty} dk e^{ikx} \frac{\sigma^*(k)}{\sqrt{2vk}} \right| < \frac{C_1}{\sqrt{v}} \int_{\epsilon^{-(1-\delta_1)}}^{\infty} \frac{dk}{k^{7/2}} = \frac{2C_1}{5\sqrt{v}} \epsilon^{(1-\delta_1) \cdot 5/2}.$$

C_1 is a constant determined so that the inequality above is satisfied.

If we now put (43) into (40) and use the estimate above of the order of magnitude of

$$\int_{\epsilon^{-(1-\delta_1)}}^{\infty} dk e^{ikx} \frac{\sigma^*(k)}{\sqrt{2vk}},$$

it should be obvious that we can replace

$$\int_0^{\epsilon^{-(1-\delta_1)}} dk e^{ikx} \frac{\sigma^*(k)}{\sqrt{2vk}}$$

by

$$\int_0^{\infty} dk e^{ikx} \frac{\sigma^*(k)}{\sqrt{2vk}}$$

in (40).

In a similar way, we can show that we can replace

* It should be noted specifically that we assume $\sigma(\pm L/2) = 0$, $\sigma'(\pm L/2) = 0$, and continuity in the neighborhood of $x = \pm L/2$.

$$\int_{-\epsilon}^0 \frac{dk}{(1-\delta_1)} e^{ikx} \frac{\sigma^*(k)}{\sqrt{2\nu|k|}}$$

by

$$\int_{-\infty}^0 dk e^{ikx} \frac{\sigma^*(k)}{\sqrt{2\nu|k|}}$$

in (40).

We can now write (40) as follows:

$$\begin{aligned} \phi(x,y,z) = & -\frac{\nu}{2\pi} e^{\nu z} \left[\int_{-\infty}^0 \frac{dk e^{ikx} \sigma^*(k)}{\sqrt{2\nu|k|}} - i \int_0^{\infty} \frac{dk e^{ikx} \sigma^*(k)}{\sqrt{2\nu k}} \right. \\ & - y \int_{-\infty}^{\infty} dk e^{ikx} \sigma^*(k) \\ & - i e^{i2\nu x} \int_{-\infty}^0 \frac{du e^{iux} \sigma^*(u+2\nu)}{\sqrt{2\nu|u|}} \\ & \left. + e^{i2\nu x} \int_0^{\infty} \frac{du e^{iux} \sigma^*(u+2\nu)}{\sqrt{2\nu u}} \right] \end{aligned} \quad (44)$$

+ higher order terms.

This is now in a form that can be greatly simplified through use of the properties of Fourier transforms.

We define

$$F^*(k) = \begin{cases} \frac{1}{\sqrt{|k|}} & k < 0 \\ \frac{-i}{\sqrt{k}} & k > 0 \end{cases} \quad (45)$$

$F^*(k)$ denotes the Fourier transform of a function $F(x)$. So

$$\begin{aligned}
 F(x) &= \frac{1}{2\pi} \int_{-\infty}^0 \frac{dk e^{ikx}}{\sqrt{|k|}} - \frac{i}{2\pi} \int_0^{\infty} \frac{dk e^{ikx}}{\sqrt{k}} \\
 &= \frac{1-i}{2\pi} \int_0^{\infty} \frac{dk}{\sqrt{k}} \{ \cos kx + \sin kx \} \\
 &= \frac{1-i}{2\pi} \sqrt{\frac{\pi}{2|x|}} \{1 + \operatorname{sgn} x\} = \frac{e^{-i\pi/4}}{\sqrt{\pi|x|}} H(x) ,
 \end{aligned} \tag{46}$$

where $H(x)$ is Heaviside step function.

We also define

$$G^*(u) = \begin{cases} -\frac{i}{\sqrt{|u|}} & u < 0 \\ \frac{1}{\sqrt{u}} & u > 0 \end{cases} \tag{47}$$

So

$$\begin{aligned}
 G(x) &= -\frac{i}{2\pi} \int_{-\infty}^0 \frac{du e^{iux}}{\sqrt{|u|}} + \frac{1}{2\pi} \int_0^{\infty} \frac{du e^{iux}}{\sqrt{u}} \\
 &= \frac{1-i}{2\pi} \int_0^{\infty} \frac{du}{\sqrt{u}} \{ \cos ux - \sin ux \} = \frac{e^{-i\pi/4}}{\sqrt{\pi|x|}} H(-x)
 \end{aligned} \tag{48}$$

By using (45) and (47) we can rewrite (44) as follows:

$$\begin{aligned}
 \phi(x, y, z) &= -\frac{ve^{vz}}{2\pi\sqrt{2v}} \int_{-\infty}^{\infty} dk e^{ikx} \sigma^*(k) F^*(k) + vye^{vz} \sigma(x) \\
 &\quad - \frac{ve^{vz} e^{i2vx}}{2\pi\sqrt{2v}} \int_{-\infty}^{\infty} du e^{iux} \sigma^*(u+2v) G^*(u) .
 \end{aligned} \tag{49}$$

We now apply the convolution theorem to (49) and use (46) and (48). We get

$$\begin{aligned}
 \Phi(x, y, z) &= -ve^{vz} \int_{-\infty}^{\infty} d\xi \sigma(\xi) \frac{e^{-i\pi/4}}{\sqrt{2\pi v|x-\xi|}} H(x-\xi) + vye^{vz} \sigma(x) \\
 &\quad - ve^{vz} e^{i2vx} \int_{-\infty}^{\infty} d\xi \sigma(\xi) e^{-i2v\xi} \frac{e^{-i\pi/4}}{\sqrt{2\pi v|x-\xi|}} H(\xi-x) \\
 &= -ve^{vz} e^{-i\pi/4} \int_{-L/2}^x \frac{d\xi \sigma(\xi)}{\sqrt{2\pi v|x-\xi|}} + vy e^{vz} \sigma(x) \\
 &\quad - ve^{vz} e^{i2vx} e^{-i\pi/4} \int_x^{L/2} \frac{d\xi \sigma(\xi) e^{-i2v\xi}}{\sqrt{2\pi v|x-\xi|}} .
 \end{aligned} \tag{50}$$

In the last expression we have used the definition of the Heaviside step function and the fact that the source density σ is zero outside the ship.

The integral

$$\int_x^{L/2} \frac{d\xi \sigma(\xi) e^{-i2v\xi}}{\sqrt{|x-\xi|}} \tag{51}$$

can be further simplified. It is a Fourier integral. The integrand has a singularity at the lower integration limit, x , and it is zero at the upper integration limit. (See discussion following (43).) The theory for finding asymptotic expansions of such integrals can be found in Erdélyi (1956). We find that (51) can be written

$$\int_x^{L/2} \frac{d\xi \sigma(\xi) e^{-i2v\xi}}{\sqrt{|x-\xi|}} = \sqrt{\frac{\pi}{2v}} e^{-i2vx} e^{-i\pi/4} \sigma(x) + o\left(\frac{1}{v}\right) . \tag{52}$$

So, by putting (52) into (50), we get

$$\Phi(x,y,z) = -ve^{vz} e^{-i\pi/4} \int_{-L/2}^x \frac{d\xi\sigma(\xi)}{\sqrt{2\pi v|x-\xi|}} + vye^{vz} \sigma(x) - e^{vz} e^{-i\pi/2} \frac{\sigma(x)}{2} \quad (53)$$

+ higher order terms.

We remember that we have assumed $y > 0$. But we can use (18) together with (16),

$$\phi_D(x,y,z,t) = \Phi(x,y,z) e^{i(\omega t - vx)} \quad , \quad (16)$$

so that we can write down a two-term inner expansion of the far-field source solution

$$\begin{aligned} \phi_D(x,y,z,t) \sim e^{i(\omega t - vx)} e^{vz} \left[-ve^{-i\pi/4} \int_{-L/2}^x \frac{d\xi\sigma(\xi)}{\sqrt{2\pi v|x-\xi|}} \right. \\ \left. + v|y|\sigma(x) - e^{-i\pi/2} \frac{\sigma(x)}{2} \right] \end{aligned} \quad (54)$$

3. Comparison with another method

The method applied above by using Fourier transforms is a very good method and has been applied to many problems in ship hydrodynamics. (Ogilvie (1970)). Other methods can also be applied to find inner expansions of far-field expansions, but generally speaking it is very difficult to obtain the inner expansion by other methods than the Fourier transform method as used above. Sometimes it even seems to be impossible.

Below I will attack the above problem by another method. I cannot obtain all three terms in (54), but I will obtain the two terms which remain when $y = 0$. These two terms will agree with the two relevant terms in (54). This is a good check on our result.

In Ogilvie & Tuck (1969), it is described how a far-field solution of the velocity potential, $\phi(x,y,z,t)$, of a line distribution of sources of

density $\mu(x)e^{i\omega t}$ spread along the line $y = z = 0$, $-L/2 \leq x \leq L/2$, in the presence of a free surface, can be written as

$$\phi(x, y, z, t) = \text{Re}[\phi(x, y, z)e^{i\omega t}] , \quad (55)$$

where

$$\phi(x, y, z) = -2 \int_{-L/2}^{L/2} d\xi \mu(\xi) \int_{0 \rightarrow \infty} \frac{dk k e^{kz}}{k - v} J_0 [k\sqrt{(x-\xi)^2 + y^2}] . \quad (56)$$

(55) is a solution of (1) and (11), and it satisfies a proper radiation condition. The inner integral is a contour integral, indented at the pole as indicated. J_0 is a Bessel function of the first kind.

In our problem we must set

$$4\pi\mu(\xi) = \sigma(\xi) e^{-i\nu\xi} , \quad (57)$$

in accordance with what we did in the previous chapters. The factor 4π is needed because of the different normalization of source strength here and in Ogilvie & Tuck (1969).

Ogilvie & Tuck (1969) simplified the expression (56) for $y = O(1)$ and we only state the result here. We get:

$$\phi(x, y, z) \approx -\sqrt{\frac{\nu}{2\pi}} e^{\nu z - i\pi/4} \int_{-L/2}^{L/2} d\xi \frac{\sigma(\xi) e^{-i\nu\xi} e^{-i\nu\sqrt{(x-\xi)^2 + y^2}}}{((x-\xi)^2 + y^2)^{1/4}} . \quad (58)$$

We want an inner expansion of (58), which means that $y = O(\epsilon)$. It is difficult to do anything with (58) when $y = O(\epsilon)$, but, if we simply set $y = 0$, we can get a special case of the inner expansion of (58). By setting $y = 0$, we get

$$-\sqrt{\frac{\nu}{2\pi}} e^{\nu z - i\pi/4} \left[\int_{-L/2}^x \frac{d\xi \sigma(\xi) e^{-i\nu\xi}}{\sqrt{|x-\xi|}} + \int_x^{L/2} \frac{d\xi \sigma(\xi) e^{-i2\nu\xi + i\nu x}}{\sqrt{|x-\xi|}} \right] . \quad (59)$$

By using (52) in the last integral, we can write (59) as

$$- \sqrt{\frac{\nu}{2\pi}} e^{\nu z - i\pi/4} \left[\int_{-L/2}^x \frac{d\xi \sigma(\xi) e^{-i\nu x}}{\sqrt{|x-\xi|}} + \sqrt{\frac{\pi}{2\nu}} e^{-i\nu x - i\pi/4} \sigma(x) \right] \quad (60)$$

By combining this with (55) we get two of the terms in the inner expansion of the far-field solution:

$$e^{i(\omega t - \nu x)} e^{\nu z} \left[-\nu e^{-i\pi/4} \int_{-L/2}^x \frac{d\xi \sigma(\xi)}{\sqrt{2\pi\nu|x-\xi|}} - e^{-i\pi/2} \frac{\sigma(x)}{2} \right] \quad (61)$$

We see that (61) agrees with the two terms in (54) that remain when $y = 0$. Since we set $y = 0$, we could not get the y -term in (54), and, as said above, it is very difficult to get the y -dependent term by this method. I will not go further with this method, but I think we have a good check on our result.

4. The near-field problem and the matching

We are now going to formulate the near-field problem and perform the matching between the near-field and the far-field solutions. A one-term far-field solution is found to be due to a line of sources with source density

$$\sigma_1(x) e^{i(\omega t - \nu x)}$$

spread along the line $y = z = 0$, $-L/2 \leq x \leq L/2$ (see Fig.1), and a one-term near-field solution will be found to be the negative of the incident wave. The matching between the lowest-order term in the near-field problem and the lowest-order term in the far-field problem gives an integral equation for $\sigma_1(x)$ (see (78)). σ_1 is needed in the second order near-field solution. The two-term near-field solution is given by (94).

It should be noted that "Near-field" means the region near the body, where the distance from the body is $O(\epsilon)$. However, we do not expect the near-field approximations to be valid near the bow and stern.

We will express the potential of the diffracted wave as follows:

$$\phi_D = e^{i(\omega t - v x)} \psi(x, y, z) \quad (62)$$

By putting (62) into the Laplace equation, (1), we get

$$\frac{\partial^2 \psi}{\partial y^2} + \frac{\partial^2 \psi}{\partial z^2} - v^2 \psi - 2iv \frac{\partial \psi}{\partial x} + \frac{\partial^2 \psi}{\partial x^2} = 0 \quad (63)$$

in the fluid region. The free-surface condition, (11), is:

$$\frac{\partial \psi}{\partial z} - v \psi = 0 \quad \text{on } z = 0 \quad (64)$$

The body boundary condition, (2), together with (12), gives

$$\left[n_2 \frac{\partial \psi}{\partial y} + n_3 \frac{\partial \psi}{\partial z} - iv n_1 \psi + n_1 \frac{\partial \psi}{\partial x} \right] = [iv n_1 - v n_3] \frac{gh}{\omega} e^{vz} \quad (65)$$

on $z = h(x, y)$.

n_1 , n_2 , and n_3 have been explained before equation (8). A last condition on ψ is that it must match with the far-field solution.

We will assume that ψ varies very slowly in the x -direction compared with the variation of ψ in the transverse plane. We assume that the rate of change of ψ in the transverse plane is governed by the order of magnitude of the transverse dimensions of the body and that the rate of change of ψ in the x -direction is governed by the order of magnitude of the longitudinal dimensions of the body.

We therefore stretch the coordinates

$$y = \epsilon Y, \quad z = \epsilon Z, \quad n_{2D} = \epsilon N, \quad x = X \quad (66)$$

Here $\partial/\partial n_{2D}$ denotes the directional derivative normal to and out of a cylinder with the same cross-section as the ship at a given section.

We assume that, in the near-field

$$\frac{\partial \psi}{\partial Y} = o(\psi) , \quad \frac{\partial \psi}{\partial Z} = o(\psi) , \quad \frac{\partial \psi}{\partial N} = o(\psi) , \quad \frac{\partial \psi}{\partial X} = o(\psi) \quad (67)$$

It should be noted, however, that the rate of change in the x-direction of the diffraction potential, ϕ_D , as given by (62), is of the same order of magnitude as the rate of change of ϕ_D in the transverse dimensions.

We will assume an asymptotic expansion of ψ of the form

$$\psi \sim \sum_{n=1}^N \psi_n(X, Y, Z; \epsilon) \quad (68)$$

where $\psi_{n+1} = o(\psi_n)$ as $\epsilon \rightarrow 0$ for fixed X, Y, Z . By putting (68) into (63) we get

$$\left(\frac{\partial^2}{\partial Y^2} + \frac{\partial^2}{\partial Z^2} - v^2 \epsilon^2 \right) (\psi_1 + \psi_2 + \dots) = 2iv\epsilon^2 \frac{\partial}{\partial X} (\psi_1 + \dots) + \dots \quad (69)$$

The free-surface condition, (64), gives

$$\frac{\partial}{\partial Z} (\psi_1 + \psi_2 + \dots) - v\epsilon (\psi_1 + \psi_2 + \dots) = 0 \quad \text{on } z = 0. \quad (70)$$

The body boundary condition, (65), becomes

$$\begin{aligned} \frac{1}{\epsilon} \frac{\partial}{\partial N} (\psi_1 + \psi_2 + \dots) &= (ivn_1 - n_1 \frac{\partial}{\partial X}) (\psi_1 + \dots) \\ &+ ivn_1 \frac{gh}{\omega} e^{vz} - vn_3 \frac{gh}{\omega} e^{vz} \quad \text{on } z = h(x, y). \end{aligned} \quad (71)$$

We introduce

$$v\epsilon = k = o(1). \quad (72)$$

We will set

$$\frac{gh}{\omega} = C . \quad (73)$$

Since the problem is linear in C , we shall not be bothered with the order of magnitude of C .

The lowest-order equations become:

$$\left(\frac{\partial}{\partial Y^2} + \frac{\partial}{\partial Z^2} - k^2 \right) \psi_1 = 0 ; \quad (74)$$

$$\left(\frac{\partial}{\partial Z} - k \right) \psi_1 = 0 \text{ on } Z = 0 ; \quad (75)$$

$$\frac{\partial}{\partial N} (\psi_1) = - C n_3 k e^{kZ} \text{ on the body.} \quad (76)$$

In addition, ψ_1 must match with the far-field solution.

A one-term far-field solution is assumed to be the potential associated with a line distribution of sources of density

$$\sigma_1(x) e^{i(\omega t - \nu x)}$$

spread along the line $y = z = 0$, $-L/2 \leq x \leq L/2$. That solution has been obtained in a previous chapter, and a one-term inner expansion of a one-term far-field solution can be found from (54). For any fixed x greater than $-L/2$, it is obvious that a one-term inner expansion is

$$e^{i(\omega t - \nu x)} \left[-\epsilon^{-1/2} \sqrt{\frac{k}{2\pi}} e^{kZ} e^{-i\pi/4} \int_{-L/2}^x \frac{d\xi \sigma_1(\xi)}{\sqrt{|x-\xi|}} \right] \quad (77)$$

and that the second-order term in the inner expansion is of order $\epsilon^{1/2}$ compared with the first-order term.

(77) should match with a one-term outer expansion of $\psi_1 e^{i(\omega t - \nu x)}$, as determined from (74), (75) and (76). Ursell (1968a)* has given a solution to that problem, but it does not appear to match with (77). However, if we say that the one-term near-field solution is just the negative of the incident wave (this is a special case of Ursell's solution), then (74), (75) and (76) are satisfied, and if we require that

$$\sqrt{\frac{k}{2\pi}} \varepsilon^{-1/2} e^{kZ} e^{-i\pi/4} \int_{-L/2}^x \frac{d\xi \sigma_1(\xi)}{\sqrt{|x-\xi|}} = C e^{kZ} \quad (78)$$

then we see that a one-term outer expansion of the one-term near-field solution matches with a one-term inner expansion of a one-term far-field solution.

So we have the solution

$$\begin{aligned} \psi_1(X, Y, Z; \varepsilon) &= -\varepsilon^{-1/2} \sqrt{\frac{k}{2\pi}} e^{kZ} e^{-i\pi/4} \int_{-L/2}^x \frac{d\xi \sigma_1(\xi)}{\sqrt{|x-\xi|}} \\ &= -C e^{kZ} \end{aligned} \quad (79)$$

We solve (78) for $\sigma_1(x)$ formally by letting it be an equality for all $x \geq -L/2$. We recognize (78) as Abel's integral equation (see Dettman 1965)), which has the solution

$$\sigma_1(x) = \varepsilon^{1/2} \sqrt{\frac{2}{\pi k (x+L/2)}} e^{i\pi/4} \cdot C \quad (80)$$

This solution is singular at $x = -L/2$, which is a violation of the assumptions made earlier. However, this is not a serious difficulty if we do not try to use our results very near the bow of the ship. The near-field expansion of which (79) gives the first term, is not uniformly valid near $x = -L/2$. In order to examine the solution precisely in the neighborhood of $x = -L/2$, we should construct a separate expansion for a region in which $x + L/2 = O(\varepsilon^\gamma)$, for some $\gamma > 0$. One may expect then that $\sigma_1(x)$ is not given in that region by (80); rather, $\sigma_1(x)$ will decrease continuously to zero at $x = -L/2$,

* Ursell's solution will be needed in the second order term and will be discussed then.

as physical considerations require that it must. Using (80) to express $\sigma_1(x)$ produces a higher-order, i.e., negligible, error in the velocity potential, provided that we restrict our attention to a region in which $\epsilon^Y = o(x+L/2)$.

We wish next to find ψ_2 , but first we need to say some more about the far-field.

We expect that a two-term far-field expansion is obtained by a line distribution of sources of density

$$(\sigma_1(x) + \sigma_2(x)) e^{i(\omega t - \nu x)} \quad (81)$$

spread along the line $y = z = 0$, $-L/2 \leq x \leq L/2$. It is assumed that

$$\sigma_2 = o(\sigma_1) \quad (82)$$

A two-term inner expansion of this two-term far-field expansion can be obtained from (54), and it is

$$\begin{aligned} e^{i(\omega t - \nu x)} \left[-\epsilon^{-1/2} \sqrt{\frac{k}{2\pi}} e^{kz} e^{-i\pi/4} \int_{-L/2}^x \frac{d\xi \sigma_1(\xi)}{\sqrt{|x-\xi|}} \right. \\ \left. -\epsilon^{-1/2} \sqrt{\frac{k}{2\pi}} e^{kz} e^{-i\pi/4} \int_{-L/2}^x \frac{d\xi \sigma_2(\xi)}{\sqrt{|x-\xi|}} \right. \\ \left. + e^{kz} k|Y| \sigma_1(x) - e^{-i\pi/2} \frac{\sigma_1(x)}{2} e^{kz} \right] \quad (83) \end{aligned}$$

Let us now look at the second term, $\psi_2 e^{i(\omega t - \nu x)}$, in the near-field. Since $\partial\psi_1/\partial x = 0$, it follows from (69) that ψ_2 has to satisfy the Helmholtz equation

$$\left(\frac{\partial^2}{\partial Y^2} + \frac{\partial^2}{\partial Z^2} - k^2 \right) \psi_2 = 0 \quad (84)$$

From (70) it follows that ψ_2 satisfies the free-surface condition

$$\left(\frac{\partial}{\partial Z} - k \right) \psi_2 = 0 \quad \text{on } Z = 0. \quad (85)$$

In the body boundary condition, (71), we know that $i\nabla n_1 \psi_1$ cancels $i\nabla n_1 \left(\frac{gh}{\omega} \right) e^{\nu z}$. Further $\partial \psi_1 / \partial x = 0$, and so the only possibility is

$$\frac{\partial \psi_2}{\partial N} = 0 \quad \text{on the body.} \quad (86)$$

In addition ψ_2 must match with the far-field solution.

Ursell (1968a) has derived a solution of (84), (85) and (86). It can be written as

$$\begin{aligned} \psi_2 = A_2(x) \left[e^{kZ} + \int_{C(+)} k\mu(s;k) \cdot [G(kY, kZ; k\xi(s), k\eta(s)) \right. \\ \left. + G(kY, kZ; -k\xi(s), k\eta(s))] ds \right] \end{aligned} \quad (87)$$

where

$$\begin{aligned} G(kY, kZ; k\xi, k\eta) = K_0 [k \sqrt{(Y-\xi)^2 + (Z-\eta)^2}] \\ + \frac{1}{4} \left[\int_{-\infty}^{\infty} + \int_{-\infty}^{\infty} \right] \frac{\cosh \mu + 1}{\cosh \mu - 1} \exp [ik(Y-\xi) \sinh \mu + k(Z+\eta) \cosh \mu] d\mu \end{aligned} \quad (88)$$

The symbol \int denotes integration along a contour passing below the double pole at $\mu = 0$, with a corresponding meaning for \int . K_0 is a modified Bessel function of the second kind. In (87) $C(+)$ denotes the half of the boundary curve of the submerged cross-section at x for which $y > 0$;

$Y = \xi(s)$, $Z = \eta(s)$ are the parametric equations of the curve $C(+)$. $\mu(s,k)$ is determined from satisfaction of the body boundary condition (86). It should be noted that (84), (85) and (86) will be satisfied for an arbitrary $A_2(x)$ in (87). The reasons are that 1) none of the equations (84), (85), and (86) involve differentiation with respect to x , and 2) (84), (85), and (86) are homogeneous. $A_2(x)$ has to be determined by the matching procedure.

In order to match, we need an outer expansion of (87). Ursell (1968a) has done that. The result is

$$A_2(x) \left[e^{kZ} - 4k^2\pi \frac{|y|}{\epsilon} e^{kZ} \int_{C(+)} \mu(s,k) e^{k\eta(s)} ds \right] \quad (89)$$

A three-term outer expansion of the two-term near-field solution,

$$(\psi_1 + \psi_2) e^{i(\omega t - \nu x)} \quad , \quad (90)$$

can now be written down. It is

$$e^{i(\omega t - \nu x)} \left[-\epsilon^{-1/2} \sqrt{\frac{k}{2\pi}} e^{kZ} e^{-i\pi/4} \int_{-L/2}^x \frac{d\xi \sigma_1(\xi)}{\sqrt{|x-\xi|}} \right. \\ \left. + A_2(x) e^{kZ} - A_2(x) 4k^2\pi \frac{|y|}{\epsilon} e^{kZ} \int_{C(+)} \mu(s,k) e^{k\eta(s)} ds \right] \quad (91)$$

The last term is the lowest-order term and the first term is the next lowest-order term. (91) should match with (83) and we see that it does if we set

$$A_2(x) = - \frac{\sigma_1(x)}{4k\pi \int_{C(+)} \mu(s,k) e^{k\eta(s)} ds} \\ = - \frac{\epsilon^{1/2} \sqrt{\frac{2}{\pi k(x+L/2)}} e^{i\pi/4} C}{4k\pi \int_{C(+)} \mu(s,k) e^{k\eta(s)} ds} \quad (92)$$

(σ_1 is given by (80)), and if also

$$\begin{aligned}
 & -\epsilon^{-1/2} \sqrt{\frac{k}{2\pi}} e^{-i\pi/4} \int_{-L/2}^x \frac{d\xi \sigma_2(\xi)}{\sqrt{|x-\xi|}} \\
 & = A_2(x) + e^{-i\pi/2} \frac{\sigma_1(x)}{2} \tag{93} \\
 & = \left[-\frac{1}{4k\pi} \int_{C(+)} \frac{1}{\mu(s,k) e^{k\eta(s)}} ds + \frac{e^{-i\pi/2}}{2} \right] \\
 & \cdot \epsilon^{1/2} \sqrt{\frac{2}{\pi k(x+L/2)}} e^{i\pi/4} C,
 \end{aligned}$$

which is a condition to be satisfied by σ_2 . Equation (93) gives us Abel's integral equation, and it can be solved in principle. It is to be noted that the term in the brackets is a function of x , which is determined in practice by numerical computation.

It is the near-field solution that has the primary interest. So let us summarize our result: A two-term near-field solution of the diffraction potential is given by

$$\begin{aligned}
 (\psi_1 + \psi_2) e^{i(\omega t - vx)} & = e^{i(\omega t - vx)} \left[-C e^{kZ} - \frac{\epsilon^{1/2} \sqrt{\frac{2}{\pi k(x+L/2)}} e^{i\pi/4} C}{4k\pi \int_{C(+)} \frac{1}{\mu(s,k) e^{k\eta(s)}} ds} \right. \\
 & \left. \cdot \left[e^{kZ} + \int_{C(+)} k\mu(s,k) [G(kY, kZ; k\xi(s), k\eta(s)) + G(kY, kZ; -k\xi(s), k\eta(s))] ds \right] \right] \tag{94}
 \end{aligned}$$

where k and C are given by (72) and (73), and G is given by (88). The first term in (94) is just the negative of the incident wave and so (94) tells us that the total (incident- plus diffracted-wave) potential near the body (except near the bow and stern) will have a decay factor

$$(x+L/2)^{-1/2} \quad (95)$$

in the x-direction. But note that μ in (94) is also a function of x , and so (95) does not give the total x-dependence. However, μ will be the same for similar cross-sections. So, if the cross-sections are not varying much in the x-direction, the potential will, roughly speaking, drop off with the factor $(x+L/2)^{-1/2}$ in the lengthwise direction. Note that we have assumed that the wave length is of the order of magnitude of the transverse dimensions of the ship.

IV. THE FORWARD-SPEED PROBLEM

We write the total potential ϕ as follows:

$$\phi(x,y,z,t) = Ux + U\phi_s(x,y,z) + \phi_T(x,y,z,t) \quad , \quad (96)$$

where $U\phi_s$ is the perturbation velocity potential in the steady motion problem. ϕ_s satisfies the three-dimensional Laplace equation

$$\frac{\partial^2 \phi_s}{\partial x^2} + \frac{\partial^2 \phi_s}{\partial y^2} + \frac{\partial^2 \phi_s}{\partial z^2} = 0 \quad (97)$$

in the fluid domain and the body boundary condition

$$\frac{\partial}{\partial n} (Ux + U\phi_s) = 0 \quad \text{on } z = h(x,y) \quad . \quad (98)$$

Since ϕ satisfies (1) and (2), this implies that ϕ_T satisfies

$$\frac{\partial^2 \phi_T}{\partial x^2} + \frac{\partial^2 \phi_T}{\partial y^2} + \frac{\partial^2 \phi_T}{\partial z^2} = 0 \quad (99)$$

in the fluid domain and the body boundary condition

$$\frac{\partial \phi_T}{\partial n} = 0 \quad \text{on } z = h(x,y) \quad (100)$$

By combining (3) and (4) and using the assumption about linearity, it can be shown that ϕ_T satisfies the free-surface condition

$$\left[\frac{\partial}{\partial t} + U \frac{\partial}{\partial x} \right]^2 \phi_T + g \frac{\partial \phi_T}{\partial z} = 0 \quad \text{on } z=0 \quad (101)$$

(see Ogilvie & Tuck (1969)). Since the time dependence of the incident wave is given by $e^{i\omega t}$ (see (5)), it is expected that the time dependence for the potential ϕ_T is also given by $e^{i\omega t}$. This implies that we can write equation (101) as

$$\left[i\omega + U \frac{\partial}{\partial x} \right]^2 \phi_T + g \frac{\partial \phi_T}{\partial z} = 0 \quad \text{on } z=0. \quad (102)$$

We will write ϕ_T as

$$\phi_T = \phi_I + \phi_D = \frac{gh}{\omega_0} e^{vz} e^{i(\omega t - vx)} + \phi_D, \quad (103)$$

where ϕ_D denotes the diffraction potential. ϕ_D must satisfy a radiation condition. As in the zero-speed problem we are going to use the method of matched asymptotic expansions to find ϕ_D .

We will assume that

$$U = O(\epsilon^{1/2 - a}), \quad 0 < a \leq 1/2 \quad (104)$$

In the steady forward-motion problem we know that there is a length scale in the x-direction which is connected with the wave length $2\pi U^2/g$. So (104) implies that this length scale is large compared with the transverse dimensions of the ship, and that it can be of the same order of magnitude as the length of the ship. In some way, I expect this length scale will enter our diffraction problem and affect the rate of change of the variables in the x-direction. But it turns out that it will not have any influence on the first two approximations of the diffraction potential. The important length

scale in the x-direction will be connected with the wave length of the incoming wave, in the same way as for the zero-speed problem. As we remember from equation (10), this wave length is assumed to be of order ϵ .

If, however, we had assumed that a were zero in (104), we would have been in difficulties finding the second approximation to the diffraction potential. The reason must be that there then are two important length scales of order ϵ in the x-direction, one connected with the wave length of the incoming wave and one connected with the forward speed, and it is difficult to separate out the effect of one of the length scales from the other.

Using (7) and (9), we can show that (104) implies that the order of magnitude of the frequency of encounter, ω will be

$$\omega = O(\epsilon^{-1/2-a}), \quad 0 < a \leq 1/2 \quad . \quad (105)$$

We then see that the order of magnitude of $\tau = \frac{\omega U}{g}$ is

$$\tau = \frac{\omega U}{g} = O(\epsilon^{-2a}), \quad 0 < a \leq 1/2 \quad (106)$$

It is obvious that τ will be larger than 1/4. This is important, because the solution will be singular when $\tau = 1/4$ (see Ogilvie and Tuck (1969)).

There are four parts in this chapter: (1) derivation of the far-field source solution due to a line of pulsating, translating sources located on the x-axis between $-L/2$ and $L/2$ (see Fig. 1); (2) a two-term inner expansion of the far-field source solution; (3) comparison of the expression found in part (2) with the result obtained by another approach; (4) formulation of the near-field problem, and the matching of a two-term near-field solution with the far-field solution.

1. Far-field source solution

In the far-field description we expect to have waves. It is difficult to say how differentiation changes order of magnitudes in the far-field. So, to be careful, we would rather keep too many terms in the far-field. But we

have to be sure that we have a system of equations that describes a wave motion.

Using arguments similar to those in the section "Far-field source solution" in the chapter on the zero-speed problem, we can find that ϕ_D must satisfy the Poisson equation,

$$\frac{\partial^2 \phi_D}{\partial x^2} + \frac{\partial^2 \phi_D}{\partial y^2} + \frac{\partial^2 \phi_D}{\partial z^2} = \sigma(x) e^{i(\omega t - vx)} \delta(y) \delta(z - z_0) ,$$

where $z_0 < 0$. We write the free-surface condition as follows:

$$(i\omega + U \frac{\partial}{\partial x} + \mu)^2 \phi_D + g \frac{\partial \phi_D}{\partial z} = 0 \quad \text{on } z = 0 ,$$

where μ is the artificial Rayleigh viscosity, which will approach zero at a proper later point. This equation system does give waves.

The solution to the equation system with $z_0 = 0$ can be found in Ogilvie & Tuck (1969). It is

$$\begin{aligned} \phi_D(x, y, z, t) = & -\frac{1}{4\pi^2} e^{i\omega t} \int_{-\infty}^{\infty} dk e^{ikx} F\{\sigma(x) e^{-ivx}\} \\ & \cdot \lim_{\mu \rightarrow 0} \int_{-\infty}^{\infty} \frac{d\ell e^{i\ell y + z\sqrt{k^2 + \ell^2}}}{\sqrt{k^2 + \ell^2} - \frac{1}{g} (\omega + Uk - i\mu)^2} , \end{aligned} \quad (107)$$

where

$$\begin{aligned} F\{\sigma(x) e^{-ivx}\} &= \int_{-\infty}^{\infty} dx e^{-ikx} \sigma(x) e^{-ivx} \\ &= \sigma^*(k+v) . \end{aligned}$$

We will rewrite (107) in a way similar to the way we did with (15) in the zero speed problem. We introduce:

$$k' = k + v .$$

(107) can then be written:

$$\begin{aligned} \phi_D(x, y, z, t) &= -\frac{1}{4\pi^2} e^{i(\omega t - vx)} \int_{-\infty}^{\infty} dk' e^{ik'x} \sigma^*(k') \\ &\cdot \lim_{\mu \rightarrow 0} \int_{-\infty}^{\infty} \frac{d\ell e^{i\ell y + z\sqrt{(k'-v)^2 + \ell^2}}}{\sqrt{(k'-v)^2 + \ell^2} - \frac{1}{g} (\omega + U(k'-v) - i\mu)^2} . \end{aligned} \quad (108)$$

We drop the primes and write

$$\phi_D(x, y, z, t) = \Phi(x, y, z) e^{i(\omega t - vx)} , \quad (109)$$

where

$$\begin{aligned} \Phi(x, y, z) &= -\frac{1}{4\pi^2} \int_{-\infty}^{\infty} dk e^{ikx} \sigma^*(k) \\ &\cdot \lim_{\mu \rightarrow 0} \int_{-\infty}^{\infty} \frac{d\ell e^{i\ell y + z\sqrt{(v-k)^2 + \ell^2}}}{\sqrt{(v-k)^2 + \ell^2} - \frac{1}{g} (\omega_0 + Uk - i\mu)^2} . \end{aligned} \quad (110)$$

We will let $y = O(1) > 0$. The derivation for $y = O(1) < 0$ will be similar and, instead of going through that, we use the fact that ϕ_D is a source solution, which implies that

$$\phi_D(x, -y, z, t) = \phi_D(x, y, z, t) . \quad (111)$$

We now define

$$I(k) = \lim_{\mu \rightarrow 0} \int_{-\infty}^{\infty} \frac{d\ell e^{i\ell y + z\sqrt{\ell^2 + (v-k)^2}}}{\sqrt{\ell^2 + (v-k)^2} - \frac{1}{g} (\omega_0 + Uk - i\mu)^2} . \quad (112)$$

The poles of the integrand of (112) are important. They are given in the limit by:

$$\ell = \pm \sqrt{\frac{1}{g^2} (\omega_0 + Uk)^4 - (\nu - k)^2} . \quad (113)$$

We have to study the sign of the radicand in order to determine the location of the poles in the complex ℓ -plane. We study therefore the equation:

$$\frac{1}{g^2} (\omega_0 + Uk)^4 - (\nu - k)^2 = 0 ,$$

which is the same as

$$\left[\frac{1}{g} (\omega_0 + Uk)^2 - (\nu - k) \right] \left[\frac{1}{g} (\omega_0 + Uk)^2 + \nu - k \right] = 0 . \quad (114)$$

The zeroes of the first factor are:

$$k = k_1 = 0 , \quad (115)$$

$$k = k_2 = -\frac{g}{U^2} \left[\frac{2\omega_0 U}{g} + 1 \right] , \quad (116)$$

and the zeroes of the second factor are:

$$\begin{aligned} k &= \frac{-\frac{g}{U^2} \left[\frac{2\omega_0 U}{g} - 1 \right] \pm \sqrt{\frac{g^2}{U^4} \left[\frac{2\omega_0 U}{g} - 1 \right]^2 - 8 \frac{g}{U^2} \frac{\omega_0^2}{g}}}{2} \\ &= \frac{-\frac{g}{U^2} \left[\frac{2\omega_0 U}{g} - 1 \right] \pm \frac{g}{U^2} \sqrt{1 - 4 \frac{U\omega_0}{g}}}{2} \end{aligned}$$

But from (106) and the text that followed (106), we know that $\tau = \frac{\omega U}{g} > 1/4$. This means that the latter pair of zeroes of (114) are imaginary. But k is a real variable, and so this means that the quantity

$$f(k) = \frac{1}{g} (\omega_0 + Uk)^2 + \nu - k \quad (117)$$

can never be zero. And since expression (117) for large k behaves like

$$\frac{1}{g} (\omega_0 + Uk)^2 ,$$

we see that (117) has to be a positive quantity.

Going back now to expression (113) we can conclude:

a) when $k > k_1 = 0$ or $k < k_2 = -\frac{g}{U^2} (2\omega_0 U/g + 1)$, the poles of the integrand of (112) are real;

b) when $k_2 < k < 0$ the poles of the integrand of (112) are imaginary.

The integration path in (112) is along the real l -axis, and so, when the poles of the integrand are real, we have to know how to indent the integration path at those poles. The Rayleigh viscosity μ helps us to do that. For $\mu \neq 0$, the poles of the integrand are given by

$$\begin{aligned} l^2 &= \frac{1}{g^2} (\omega_0 + Uk - i\mu)^4 - (k - \nu)^2 \\ &= (k - k_1) (k - k_2) f(k) U^2 / g - 4(\omega_0 + Uk)^3 i\mu / g^2 + o(\mu) . \end{aligned}$$

where k_1, k_2 , and $f(k)$ are given by (115), (116), and (117), respectively. The poles of the integrand of (112) are then given by

$$l = \pm \sqrt{(k - k_1) (k - k_2) f(k) U^2 / g} \left[1 - \frac{2(\omega_0 + Uk)^3 i\mu}{gU^2 (k - k_1) (k - k_2) f(k)} + o(\mu) \right] \quad (118)$$

for $k \neq k_1$ and $k \neq k_2$

For the case $k > k_1$, the imaginary part of the factor in parenthesis in (118) is negative. This means that the integration path of (112) for $k > k_1$ will be shown in Figure 5, where $+|\ell_0|$ and $-|\ell_0|$ are the poles of the integrand

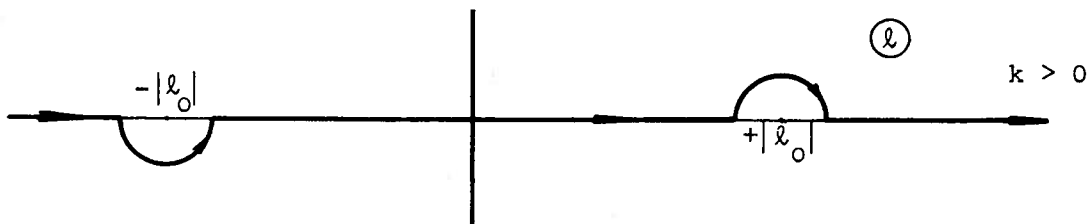


FIGURE 5
COMPLEX INTEGRATION PATH

When $k < k_2$, the imaginary part of the term in the parenthesis in (118) is positive. This means that the integration path of (112) will be as shown in Figure 6.

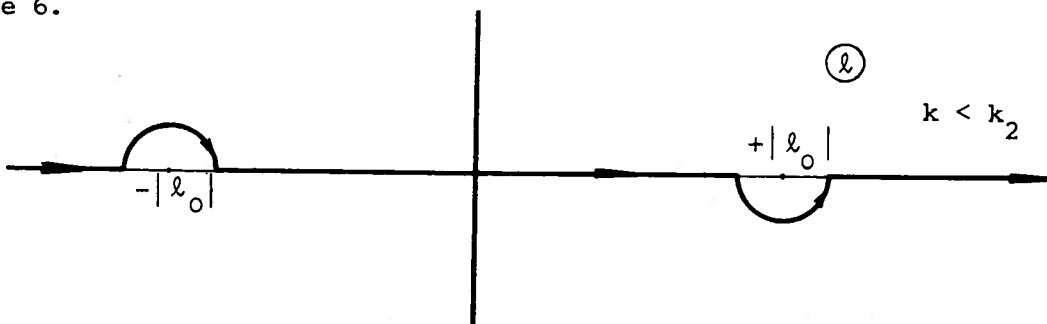


FIGURE 6
COMPLEX INTEGRATION PATH

Let us now study $I(k)$, given by (112), for different ranges of k :

Case I: $k_2 < k < k_1$. This is the case in which the poles are imaginary. We define:

$$\ell_0 = i\sqrt{(\nu-k)^2 - (\omega_0 + Uk)^4/g^2}$$

We introduce a closed curve ABCDE in the complex ℓ -plane in the same way as we did for the zero-speed case. See Figure 2. The residue at $\ell = \ell_0$ is

$$\begin{aligned} \text{Res}(\ell_0) &= \lim_{\ell \rightarrow \ell_0} (\ell - \ell_0) \frac{e^{i\ell y + z\sqrt{\ell^2 + (\nu-k)^2}}}{\sqrt{\ell^2 + (\nu-k)^2} - (\omega_0 + Uk)^2/g} \\ &= \frac{e^{i\ell_0 y} e^{\nu z(1+Uk/\omega_0)^2} \nu(1+Uk/\omega_0)^2}{\ell_0} \end{aligned}$$

By using the residue theorem we can write

$$\begin{aligned} I(k) &= 2\pi i \text{Res}(\ell_0) + \int_{\alpha}^{\infty} d\ell e^{-\nu y \ell} \left[\frac{e^{i\nu z \sqrt{\ell^2 - \alpha^2}}}{\sqrt{\ell^2 - \alpha^2} + i \left[1 + \frac{Uk}{\omega_0}\right]^2} \right. \\ &\quad \left. + \frac{e^{-i\nu z \sqrt{\ell^2 - \alpha^2}}}{\sqrt{\ell^2 - \alpha^2} - i \left[1 + \frac{Uk}{\omega_0}\right]^2} \right] , \end{aligned} \quad (119)$$

where $\alpha = \left| \frac{\nu-k}{\nu} \right| > 1$, since k is negative.

The integral terms in (119) can be bounded by

$$\left| \int_{\alpha}^{\infty} \frac{d\ell e^{-\nu y \ell \pm i\nu z \sqrt{\ell^2 - \alpha^2}}}{\sqrt{\ell^2 - \alpha^2} \pm i \left[1 + \frac{Uk}{\omega_0}\right]^2} \right| < \int_{\alpha}^{\infty} \frac{d\ell e^{-\nu y \ell}}{\sqrt{\ell^2 - \alpha^2}} .$$

Using 1) equation (22) ,

$$\int_{\alpha}^{\infty} \frac{d\ell e^{-\nu y \ell}}{\sqrt{\ell^2 - \alpha^2}} = K_0(\nu y \alpha) , \quad (22)$$

2) the fact that $\nu = O(\varepsilon^{-1})$, $y = O(1)$, $\alpha > 1$, and 3) the asymptotic expansion of K_0 for large arguments, we see that the integral terms in (119) are exponentially small with respect to ε . So we can write

$$I(k) = \frac{2\pi i v \left[1 + \frac{Uk}{\omega_0}\right]^2 e^{i\ell_0 y} e^{vz} \left[1 + \frac{Uk}{\omega_0}\right]^2}{\ell_0} + o(e^{-1/\epsilon}) \quad (120)$$

for $k_2 < k < k_1$

Case II: $k > k_1$. Let us define

$$\ell_0 = -\sqrt{(\omega_0 + Uk)^4/g^2 - (v-k)^2} .$$

We have earlier studied how to indent the integration path of the expression for $I(k)$ at the poles $\pm\ell_0$. See Fig. 5. In the same way as before, we introduce a closed curve ABCDEA in the complex ℓ -plane. We can use Fig. 4, noting that $-\ell_0$ in Fig. 4 is the same as ℓ_0 defined above.

We have to evaluate the residue at $\ell = \ell_0$. It is given by

$$\text{Res } (\ell_0) = \frac{v \left[1 + \frac{Uk}{\omega_0}\right]^2 e^{i\ell_0 y} e^{vz} \left[1 + \frac{Uk}{\omega_0}\right]^2}{\ell_0} .$$

By the residue theorem

$$I(k) = 2\pi i \text{Res } (\ell_0) + \int_{\alpha}^{\infty} d\ell e^{-vy\ell} \left[\frac{e^{ivz\sqrt{\ell^2 - \alpha^2}}}{\sqrt{\ell^2 - \alpha^2} + i \left[1 + \frac{Uk}{\omega_0}\right]^2} + \frac{e^{-ivz\sqrt{\ell^2 - \alpha^2}}}{\sqrt{\ell^2 - \alpha^2} - i \left[1 + \frac{Uk}{\omega_0}\right]^2} \right] . \quad (121)$$

As before, $K_0(vy\alpha)$ is a bounding function for the integral terms. But when $k = O(v) = O(\epsilon^{-1})$, $\alpha = \left|\frac{v-k}{v}\right|$ is of $O(\epsilon)$. This means that the argument of the K_0 function is $O(1)$, and so we cannot say that the integral terms are exponentially small when $\alpha = O(\epsilon)$, and it does not seem

probable that there exists any such bounding function when $\alpha = O(\epsilon)$. We should note that

$$\frac{Uk}{\omega_0} = O(\epsilon^{-a}) \quad , \quad 0 < a \leq 1/2$$

when $k = O(\epsilon^{-1})$ (see (104) and (9)). This means that

$$e^{-\nu z \left[1 + \frac{Uk}{\omega_0}\right]^2}$$

is exponentially small when $k = O(\epsilon^{-1})$, which makes the first term in (121) exponentially small when $k = O(\epsilon^{-1})$. So we should be careful to keep the integral term in (121) when $k = O(\epsilon^{-1})$. We can write

$$I(k) = \frac{2\pi i \nu \left[1 + \frac{Uk}{\omega_0}\right]^2 e^{i l_0 y} e^{-\nu z \left[1 + \frac{Uk}{\omega_0}\right]^2}}{l_0}$$

+ exponentially small terms

for $0 < k < \epsilon^{-(1-a+\delta_2)}$, $0 < a \leq 1/2$.

(δ_2 is some very small positive number) (122)

$$I(k) = \int_{\alpha}^{\infty} d\ell e^{-\nu y \ell} \left[\frac{e^{i \nu z \sqrt{\ell^2 - \alpha^2}}}{\sqrt{\ell^2 - \alpha^2} + i \left[1 + \frac{Uk}{\omega_0}\right]^2} + \frac{e^{-i \nu z \sqrt{\ell^2 - \alpha^2}}}{\sqrt{\ell^2 - \alpha^2} - i \left[1 + \frac{Uk}{\omega_0}\right]^2} \right]$$

+ exponentially small terms

for $\alpha = \left|\frac{\nu-k}{\nu}\right| < \epsilon^{(1-\delta_1)}$.

(δ_1 is some very small positive number)

For all other values of k in Case II, $I(k)$ will be exponentially small.

Case III: $k < k_2$. We define

$$l_0 = \sqrt{(\omega_0 + Uk)^4 / g^2 - (\nu - k)^2}$$

We have earlier studied how to indent the integration path of $I(k)$ at the poles $\pm l_0$. See Fig. 6. In the same way as before, we introduce a closed curve ABCDEA in the complex l -plane . See Fig. 7.

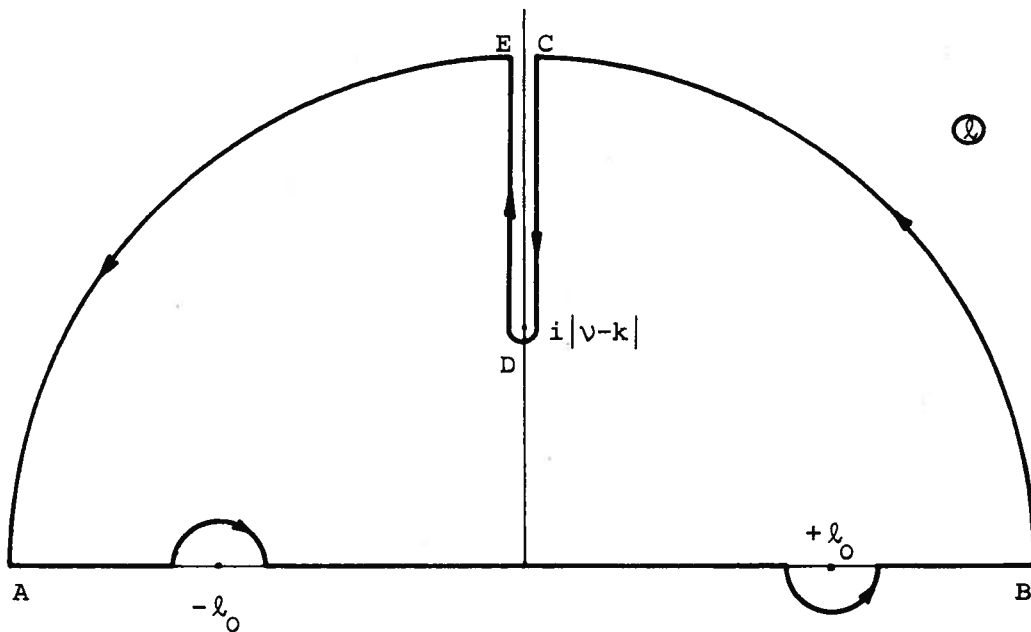


FIGURE 7
COMPLEX INTEGRATION PATH

The residue at $l = l_0$ is

$$\text{Res}(l_0) = \frac{\nu \left[1 + \frac{Uk}{\omega_0}\right]^2 e^{il_0 y} e^{\nu z} \left[1 + \frac{Uk}{\omega_0}\right]^2}{l_0}$$

By means of the residue theorem we get

$$I(k) = 2\pi i \operatorname{Res}(\ell_0) + \int_{\alpha}^{\infty} d\ell e^{-vY\ell} \left[\frac{e^{ivz\sqrt{\ell^2-\alpha^2}}}{\sqrt{\ell^2-\alpha^2} + i \left[1 + \frac{Uk}{\omega_0}\right]^2} + \frac{e^{-ivz\sqrt{\ell^2-\alpha^2}}}{\sqrt{\ell^2-\alpha^2} - i \left[1 + \frac{Uk}{\omega_0}\right]^2} \right].$$

As before, $K_0(vy\alpha)$ is a bounding function for the integral terms. For this case, $\alpha = \left|\frac{v-k}{v}\right| > 1$, and so the integral terms are exponentially small. So we can write

$$I(k) = \frac{2\pi i v \left[1 + \frac{Uk}{\omega_0}\right]^2 e^{i\ell_0 y} e^{vz \left[1 + \frac{Uk}{\omega_0}\right]^2}}{\ell_0} + \text{exponentially small terms} \quad (123)$$

for $k < k_2$.

By using (110), (112), (120), (122), (123), and the fact that the exponentially small terms in $I(k)$ will only give exponentially small terms in the expression for Φ , we can write

$$\begin{aligned} \Phi(x, y, z) \approx & -\frac{i}{2\pi} \left[\int_{-\infty}^{k_2} + \int_{k_2}^{-\epsilon^{-(1-a-\beta)}} + \int_{-\epsilon^{-(1-a-\beta)}}^0 + \int_0^{\epsilon^{-(1-a-\beta)}} \right. \\ & \left. + \int_{\epsilon^{-(1-a-\beta)}}^{\epsilon^{-(1-a+\delta_2)}} \right] \frac{dk e^{ikx} \sigma^*(k) \left[1 + \frac{Uk}{\omega_0}\right]^2 e^{i\ell_0 y} e^{vz \left[1 + \frac{Uk}{\omega_0}\right]^2}}{\ell_0/v} \\ & + I_{\alpha} \end{aligned} \quad (124)$$

In the first integral, $l_0 = \sqrt{(\omega_0 + Uk)^4/g^2 - (\nu - k)^2}$. In the second and third integrals, $l_0 = i\sqrt{(\nu - k)^2 - (\omega_0 + Uk)^4/g^2}$. In the fourth and fifth integrals, $l_0 = -\sqrt{(\omega_0 + Uk)^4/g^2 - (\nu - k)^2}$.

Further, β is some very small number, $0 < a \leq 1/2$, and

$$I_\alpha = -\frac{1}{4\pi^2} \int_{k_3(\alpha_1)}^{k_4(\alpha_1)} dk e^{ikx} \sigma^*(k) \int_\alpha^\infty dl e^{-\nu y l} \left[\frac{e^{i\nu z \sqrt{l^2 - \alpha^2}}}{\sqrt{l^2 - \alpha^2 + i \left[1 + \frac{Uk}{\omega_0}\right]^2}} + \frac{e^{-i\nu z \sqrt{l^2 - \alpha^2}}}{\sqrt{l^2 - \alpha^2 - i \left[1 + \frac{Uk}{\omega_0}\right]^2}} \right] \quad (125)$$

Here $k_3(\alpha_1) < \nu$ and $k_4(\alpha_1) > \nu$. α_1 is chosen in accordance with (122), and we choose

$$\alpha_1 = \varepsilon^{1-\delta_1} \quad (126)$$

We will write

$$I_\alpha = I_{\alpha 1} + I_{\alpha 2} \quad (127)$$

where the integration in $I_{\alpha 1}$ is from $k = k_3(\alpha_1)$ to $k = \nu$, and the integration in $I_{\alpha 2}$ is from $k = \nu$ to $k = k_4(\alpha_1)$.

We introduce $\alpha = \left| \frac{\nu - k}{\nu} \right|$ as a new integration variable in (125). So, for $I_{\alpha 1}$,

$$\alpha = \frac{\nu - k}{\nu} \quad .$$

This means:

$$I_{\alpha 1} = \frac{v e^{i v x}}{4 \pi^2} \int_{\epsilon^{1-\delta_1}}^0 d\alpha e^{-i v \alpha x} \sigma^*(v-\alpha v) \int_{\alpha}^{\infty} d\ell e^{-v y \ell} \quad (128)$$

$$\cdot \left[\frac{e^{i v z \sqrt{\ell^2 - \alpha^2}}}{\sqrt{\ell^2 - \alpha^2} + i \left[1 + \frac{U \omega_0}{g} (1-\alpha) \right]^2} + \frac{e^{-i v z \sqrt{\ell^2 - \alpha^2}}}{\sqrt{\ell^2 - \alpha^2} - i \left[1 + \frac{U \omega_0}{g} (1-\alpha) \right]^2} \right].$$

For $I_{\alpha 2}$,

$$\alpha = \frac{k-v}{v} .$$

This means:

$$I_{\alpha 2} = - \frac{v e^{i v x}}{4 \pi^2} \int_0^{\epsilon^{1-\delta_1}} d\alpha e^{i v \alpha x} \sigma^*(v+v\alpha) \int_{\alpha}^{\infty} d\ell e^{-v y \ell} \quad (129)$$

$$\cdot \left[\frac{e^{i v z \sqrt{\ell^2 - \alpha^2}}}{\sqrt{\ell^2 - \alpha^2} + i \left[1 + \frac{U \omega_0}{g} (1+\alpha) \right]^2} + \frac{e^{-i v z \sqrt{\ell^2 - \alpha^2}}}{\sqrt{\ell^2 - \alpha^2} - i \left[1 + \frac{U \omega_0}{g} (1+\alpha) \right]^2} \right].$$

We note that the second and third integrals in (124) could be written as one integral. The reason for not doing so will be obvious in the next section. The same is true for the fourth and fifth integrals in (124).

2. Inner expansion of far-field source solution

We are now going to find a two-term inner expansion of the far-field source solution. The result is given by equation (161).

We now let y be of order ϵ , and we reorder the terms in (124). We will first take a look on the integrand of the fourth integral in (124).

We note that

$$\sqrt{\left[1 + \frac{Uk}{\omega_0} \right]^4 - \left[1 - \frac{k}{v} \right]^2} = o(1) \quad (130)$$

This is because $4 \frac{Uk}{\omega_0}$ is the lowest order term in (130) and that the lowest possible order of $\frac{Uk}{\omega_0}$ is

$$o\left(\frac{Uk}{\omega_0}\right) = o\left(\frac{\epsilon^{1/2-a}}{\epsilon^{-1/2}} \epsilon^{a+\beta-1}\right) = o(\epsilon^\beta) = o(1) \quad (131)$$

This means we can write

$$e^{-ivy} \sqrt{\left[1 + \frac{Uk}{\omega_0}\right]^4 - \left[1 - \frac{k}{v}\right]^2} = 1 - ivy \sqrt{\left[1 + \frac{Uk}{\omega_0}\right]^4 - \left[1 - \frac{k}{v}\right]^2} + \text{higher order terms} \quad (132)$$

Further

$$\frac{\left[1 + \frac{Uk}{\omega_0}\right]^2}{\sqrt{\left[1 + \frac{Uk}{\omega_0}\right]^4 - \left[1 - \frac{k}{v}\right]^2}} = \frac{1}{\sqrt{1 - \frac{\left[1 - \frac{k}{v}\right]^2}{\left[1 + \frac{Uk}{\omega_0}\right]^4}}}$$

Since $\frac{Uk}{\omega_0} = o(1)$ (see (131)) we get by Taylor expansion

$$\begin{aligned} \frac{1}{\sqrt{1 - \frac{\left[1 - \frac{k}{v}\right]^2}{\left[1 + \frac{Uk}{\omega_0}\right]^4}}} &= \frac{1}{\sqrt{k \left[\frac{2\omega + 4U}{v\omega_0} \right] - k^2 \left[\frac{1}{v^2} + 8 \frac{U}{\omega_0 v} + 10 \frac{U^2}{\omega_0^2} \right] + \text{higher order terms}}} \\ &= \frac{1}{\sqrt{k \left[\frac{2\omega + 2UV}{v\omega_0} \right]}} \left[1 + \frac{1}{2} k \frac{(\omega^2 + 6U\omega v + 3U^2 v^2)}{v\omega_0 (2\omega + 2UV)} + \dots \right] \\ &= \frac{1}{\sqrt{k \left[\frac{2\omega + 2UV}{v\omega_0} \right]}} \left[1 + o(\epsilon^{\beta 1}) \right] \end{aligned}$$

Here $\beta_1 \geq \beta > 0$. Further

$$\frac{1}{\sqrt{k \left[\frac{2\omega + 2UV}{v\omega_0} \right]}} = o\left(\epsilon^{-\beta_1/2}\right)$$

and

$$e^{vz \left[1 + \frac{Uk}{\omega_0} \right]^2} = e^{vz} (1 + o(\epsilon^{\beta_1}))$$

This means that, in the integrand of the inner expansion of the fourth integral in (124), we can write

$$\begin{aligned} & \frac{\left[1 + \frac{Uk}{\omega_0} \right]^2 e^{-ivy \sqrt{\left[1 + \frac{Uk}{\omega_0} \right]^4 - \left[1 - \frac{k}{v} \right]^2}} e^{vz \left[1 + \frac{Uk}{\omega_0} \right]^2}}{\sqrt{\left[1 + \frac{Uk}{\omega_0} \right]^4 - \left[1 - \frac{k}{v} \right]^2}} \\ &= \frac{\left[1 + \frac{Uk}{\omega_0} \right]^2 e^{vz \left[1 + \frac{Uk}{\omega_0} \right]^2}}{\sqrt{\left[1 + \frac{Uk}{\omega_0} \right]^4 - \left[1 - \frac{k}{v} \right]^2}} - ivy \left[1 + \frac{Uk}{\omega_0} \right]^2 e^{vz \left[1 + \frac{Uk}{\omega_0} \right]^2} + \dots \\ &= \frac{e^{vz}}{\sqrt{\frac{2\omega+2UV}{v\omega_0} k}} - ivye^{vz} + o(\epsilon^{\beta_1/2}), \quad \beta_1 \geq \beta > 0 \end{aligned}$$

Thus, the inner expansion of the fourth integral in (124) can be written:

$$\begin{aligned} & \frac{1}{2\pi} \int_0^{\epsilon^{-(1-a-\beta)}} dk e^{ikx} \sigma^*(k) \frac{i \left[1 + \frac{Uk}{\omega_0} \right]^2 e^{-ivy \sqrt{\left[1 + \frac{Uk}{\omega_0} \right]^4 - \left[1 - \frac{k}{v} \right]^2}} e^{vz \left[1 + \frac{Uk}{\omega_0} \right]^2}}{\sqrt{\left[1 + \frac{Uk}{\omega_0} \right]^4 - \left[1 - \frac{k}{v} \right]^2}} \\ &= \frac{e^{vz} i}{2\pi} \int_0^{\epsilon^{-(1-a-\beta)}} dk e^{ikx} \sigma^*(k) \left[\frac{1}{\sqrt{\frac{2\omega+2UV}{v\omega_0} k}} - ivy \right] + \text{higher order terms} \end{aligned} \quad (133)$$

Let us now study the inner expansion of the third integral in (124). The derivation is quite similar to that for the fourth integral in (124), and so we only state the result

$$\begin{aligned}
 & -\frac{1}{2\pi} \int_{-\epsilon}^0 \frac{dk e^{ikx} \sigma^*(k) \left[1 + \frac{Uk}{\omega_0}\right]^2 e^{-vy} \sqrt{\left[1 - \frac{k}{v}\right]^2 - \left[1 + \frac{Uk}{\omega_0}\right]^4} e^{vz} \left[1 + \frac{Uk}{\omega_0}\right]^2}{\sqrt{\left[1 - \frac{k}{v}\right]^2 - \left[1 + \frac{Uk}{\omega_0}\right]^4}} \\
 & = -\frac{e^{vz}}{2\pi} \int_{-\epsilon}^0 dk e^{ikx} \sigma^*(k) \left[\frac{1}{\sqrt{\frac{2\omega+2Uv}{v\omega_0} |k|}} - vy \right] + \text{higher order terms}
 \end{aligned} \tag{134}$$

We will now study the inner expansion of the fifth integral in (124). We then need an asymptotic formula for $\sigma^*(k)$ as $k \rightarrow \infty$. We will assume that $\sigma(x)$ and $\sigma'(x)$ are continuous in the interval $-L/2 \leq x \leq L/2$ [including the end points] (see Fig. 1). Outside $-L/2 \leq x \leq L/2$, $\sigma(x) \equiv 0$. It can then be shown (see Lighthill (1958)) that $|kL|^3 \sigma^*(k)$ remains bounded as $k \rightarrow \pm \infty$.

The fifth integral in (124) can be bounded by

$$\int_{-\epsilon}^{\epsilon} e^{-(1-a+\delta_2)} dk |\sigma^*(k)| \leq C_1 \int_{-\epsilon}^{\epsilon} e^{-(1-a+\delta_2)} \frac{dk}{k^3} \tag{135}$$

C_1 is a constant determined so that the inequality above is satisfied. It is obvious from (133), (134), and (135) that the inner expansion of the fifth integral in (124) will give a term of higher order of magnitude than the highest-order terms already retained in the inner expansion of the third and fourth integral in (124). So we can drop the contribution from the fifth integral in (124).

Let us now study the inner expansion of I_α in (124). I_α is given by (127) as

$$I_{\alpha} = I_{\alpha 1} + I_{\alpha 2} \quad (127)$$

where $I_{\alpha 1}$ and $I_{\alpha 2}$ are given by (128) and (129), respectively. Since the argument of σ^* is large both in (128) and (129) we can use the previously stated fact that $|kL|^3 \sigma^*(k)$ remains bounded as $|k| \rightarrow \infty$. For the inner integrals in (128) and (129) we can write

$$\left| \int_{\alpha}^{\infty} d\ell e^{-vy\ell} \frac{e^{\pm i v z \sqrt{\ell^2 - \alpha^2}}}{\sqrt{\ell^2 - \alpha^2} \pm i \left[1 + \frac{U\omega_0}{g} (1 \pm \alpha) \right]^2} \right| < \int_{\alpha}^{\infty} d\ell e^{-vy\ell} \quad (136)$$

$$= \frac{e^{-vy\alpha}}{vy} < \frac{1}{vy} = o(1)$$

So the inner expansion of (128) can be bounded by

$$\frac{C_1 \cdot v}{vy \cdot 2\pi^2} \int_{\epsilon}^0 \frac{d\alpha}{(v-\alpha)^3} \quad (137)$$

A similar bounding function can be found for the inner expansion of (129). It should be obvious, for the same reasons used to drop the contribution from the inner expansion of the fifth integral in (124), that we can drop the contribution from the inner expansion of I_{α} in (124).

Let us now look at the first two integrals in (124). We have to be careful since the integrands have a pole at

$$k = k_2$$

where

$$k_2 = -\frac{g}{U^2} (2\omega_0 U/g + 1)$$

We will study the first integral first. We introduce the new variable

$$v = k - k_2$$

This means that

$$(1+Uk/\omega_0)^4 = H_3^4 H_2^4$$

$$(1-k/v)^2 = H_3^4 H_1^2$$

where

$$H_1 = 1 - \frac{v}{vH_3^2} \tag{138}$$

$$H_2 = 1 - \frac{Uv}{\omega_0 H_3} \tag{139}$$

$$H_3 = 1 + \frac{g}{\omega_0 U} \tag{140}$$

We can now write the first integral in (124) as

$$-\frac{e^{ik_2 x}}{2\pi} i \int_{-\infty}^0 \frac{dv e^{ivx} \sigma^*(v+k_2)}{\sqrt{1-H_1^2/H_2^4}} e^{i\sqrt{v}H_3^2 \sqrt{H_2^4-H_1^2} + vZH_3^2 H_2^2} \tag{141}$$

We write this integral as a sum of two integrals. The first integral is from $-\infty$ to $-\epsilon^{-(1-a-\beta)}$. The integrand is well-behaved, and the upper limit is a large number. So, since the infinite integral from $-\infty$ to 0 necessarily has to converge, the first integral has to be of higher order than the second integral from $-\epsilon^{-(1-a-\beta)}$ to 0. It will be evident later on that the integral from $-\epsilon^{-(1-a-\beta)}$ to 0 will give a term which is of the same order of magnitude as the highest order terms already retained in the inner expansion of the far-field source solution. So we drop the integral from $-\infty$ to $-\epsilon^{-(1-a-\beta)}$.

We therefore write (141) as

$$-\frac{e^{ik_2 x}}{2\pi} i \int_{-\epsilon^{-(1-a-\beta)}}^0 \frac{dv e^{ivx} \sigma^*(v+k_2)}{\sqrt{1-H_1^2/H_2^4}} e^{i\sqrt{v}H_3^2 \sqrt{H_2^4-H_1^2} + vZH_3^2 H_2^2} \tag{142}$$

We note that

$$v_y H_3^2 \sqrt{H_2^4 - H_1^2} = o(1) \quad (143)$$

This is because

$$o\left(\frac{g}{\omega_0 U}\right) = o(\epsilon^a) = o(1) \quad (144)$$

and that the order of magnitude of the lowest order term under the square root sign in (143) is

$$o\left(\frac{Uv}{\omega_0 H_3}\right) = o(\epsilon^{\beta_1}) = o(1) \quad (145)$$

Here $\beta_1 \geq \beta > 0$

We can therefore write

$$e^{i v_y H_3^2 \sqrt{H_2^4 - H_1^2}} = 1 + \text{higher order terms} \quad (146)$$

in the integrand of (142). Further using (144), (145), and the fact that $o(vz) = o(1)$, we can also write

$$e^{v_z H_3^2 H_2^2} = e^{v_z} + \text{higher order terms}$$

in the integrand of (142).

By using (144), (145), Taylor expansion and the fact that

$$o\left(\frac{v}{v H_3}\right) = o(\epsilon^{a+\beta_1}), \quad \beta_1 \geq \beta > 0 \quad (147)$$

we can write the expression

$$\frac{1}{\sqrt{1 - H_1^2/H_2^4}} \quad (148)$$

in (142) as

$$\frac{1}{\sqrt{\left[\frac{2\omega+2Uv}{v\omega_0}\right]v}} + \text{higher order terms} \quad (149)$$

This means we can write (142) as

$$- \frac{e^{ik_2x + vz}}{2\pi} i \int_{-\epsilon}^0 (1-a-\beta) \frac{dv e^{ivx} \sigma^*(v+k_2)}{\sqrt{\frac{2\omega+2Uv}{v\omega_0} |v|}} \quad (150)$$

+ higher order terms

Setting the lower integration limit equal to $-\infty$ can only introduce higher order terms. This means that the inner expansion of the first integral in (124) can be written as

$$\begin{aligned} & - \frac{1}{2\pi} \int_{-\infty}^{k_2} dk e^{ikx} \frac{\sigma^*(k) i (1+Uk/\omega_0)^2 e^{i\sqrt{v} \sqrt{(1+Uk/\omega_0)^4 - (1-k/v)^2} + vz} (1+Uk/\omega_0)^2}{\sqrt{(1+Uk/\omega_0)^4 - (1-k/v)^2}} \\ & = - \frac{e^{ik_2x + vz}}{2\pi} i \int_{-\infty}^0 \frac{dv e^{ivx} \sigma^*(v+k_2)}{\sqrt{\frac{2\omega+2Uv}{v\omega_0} |v|}} + \text{higher order terms} \end{aligned} \quad (151)$$

Let us now study the inner expansion of the second integral in (124). As for the first integral we introduce

$$v = k - k_2$$

as a new integration variable. We then set the upper integration limit equal to $\epsilon^{-(1-a-\beta)}$ instead of $-k_2 - \epsilon^{-(1-a-\beta)}$ using the argument that this will only introduce higher order negligible effects. Then we expand the integrand in the same way as we did for the inner expansion of the first integral in (124). We will find that we can write the inner expansion of the second integral in (124) as

$$- \frac{e^{ik_2 x + \nu z}}{2\pi} \int_0^{\epsilon^{-(1-a-\beta)}} \frac{dv e^{i\nu x} \sigma^*(\nu+k_2)}{\sqrt{\frac{2\omega+2U\nu}{\nu\omega_0}} \nu} \quad (152)$$

Since it will only introduce higher order negligible effects to set the upper integration limit equal to ∞ , we can now write the inner expansion of the second integral as

$$\begin{aligned} & - \frac{1}{2\pi} \int_{k_2}^{\epsilon^{-(1-a-\beta)}} \frac{dk e^{ikx} \sigma^*(k) (1+Uk/\omega_0)^2 e^{-\nu y \sqrt{(1-k/\nu)^2 - (1+Uk/\omega_0)^4} + \nu z (1+Uk/\omega_0)^2}}{\sqrt{(1-k/\nu)^2 - (1+Uk/\omega_0)^4}} \\ & = - \frac{e^{ik_2 x + \nu z}}{2\pi} \int_0^{\infty} \frac{dv e^{i\nu x} \sigma^*(\nu+k_2)}{\sqrt{\frac{2\omega+2U\nu}{\nu\omega_0}} \nu} + \text{higher order terms} \end{aligned} \quad (153)$$

So by using (133), (134), (151), (153), and the fact that the last two terms in (124) gave higher order terms, we can write the inner expansion of the far-field source solution (124) as

$$\begin{aligned} \Phi(x, y, z) \approx & - \frac{e^{\nu z}}{2\pi} \left[\int_{-\epsilon^{-(1-a-\beta)}}^0 \frac{dk e^{ikx} \sigma^*(k)}{\sqrt{\frac{2\omega+2U\nu}{\nu\omega_0}} |k|} - i \int_0^{\epsilon^{-(1-a-\beta)}} \frac{dk e^{ikx} \sigma^*(k)}{\sqrt{\frac{2\omega+2U\nu}{\nu\omega_0}} k} \right] \\ & + \frac{\nu y e^{\nu z}}{2\pi} \int_{-\infty}^{\infty} dk e^{ikx} \sigma^*(k) \end{aligned} \quad (154)$$

$$- \frac{e^{ik_2 x + \nu z}}{2\pi} i \left[\int_{-\infty}^0 \frac{dv e^{i\nu x} \sigma^*(\nu+k_2)}{\sqrt{\frac{2\omega+2U\nu}{\nu\omega_0}} |\nu|} - i \int_0^{\infty} \frac{dv e^{i\nu x} \sigma^*(\nu+k_2)}{\sqrt{\frac{2\omega+2U\nu}{\nu\omega_0}} \nu} \right]$$

We note that in the third integral we have set the integration limits equal to $\pm\infty$. We could do that because the third integral is one of the terms

of highest order magnitude retained in (154) and because the integration limits were large and equal to $\pm \varepsilon^{-(1-a-\beta)}$ before we set them equal to $\pm \infty$.

We must be careful in setting $\pm \varepsilon^{-(1-a-\beta)}$ equal to $\pm \infty$ in the first two terms in (154). The reason is that those two terms are the two lowest order terms in (154).

We write the second integral as

$$\int_0^{\varepsilon^{-(1-a-\beta)}} dk \frac{e^{ikx} \sigma^*(k)}{\sqrt{\frac{2\omega+2UV}{v\omega_0}} k} = \int_0^{\infty} dk \frac{e^{ikx} \sigma^*(k)}{\sqrt{\frac{2\omega+2UV}{v\omega_0}} k} - \int_{\varepsilon^{-(1-a-\beta)}}^{\infty} dk \frac{e^{ikx} \sigma^*(k)}{\sqrt{\frac{2\omega+2UV}{v\omega_0}} k} \quad (155)$$

But by using the previously stated fact that $|kL|^3 \sigma^*(k)$ remains bounded as $k \rightarrow \pm \infty$ it is not difficult to see that the last term in (155) will give a higher order term in (154). We can therefore set the upper integration limit in the second integral in (154) equal to ∞ . Similar arguments can be used for the first integral in (154) to show that we can set the lower integration limit equal to $-\infty$.

By using (45), (46), and the convolution theorem we can now write

$$\begin{aligned} \Phi(x, y, z) \approx & - \frac{e^{vz-i\pi/4}}{\sqrt{\pi}} \int_{-L/2}^x \frac{d\xi \sigma(\xi)}{\sqrt{\frac{2\omega+2UV}{v\omega_0}} |x-\xi|} + vye^{vz} \sigma(x) \\ & - \frac{e^{ik_2 x + vz + i\pi/4}}{\sqrt{\pi}} \int_{-L/2}^x \frac{d\xi \sigma(\xi) e^{-ik_2 \xi}}{\sqrt{\frac{2\omega+2UV}{v\omega_0}} |x-\xi|} \end{aligned} \quad (156)$$

The integral

$$\int_{-L/2}^x \frac{d\xi \sigma(\xi) e^{-ik_2 \xi}}{\sqrt{|x-\xi|}} \quad (157)$$

can be further simplified. It is a Fourier integral. The integrand has a singularity at the upper integration limit, x , and it is zero at the lower

integration limit. The theory for finding asymptotic expansions of such integrals can be found in Erdélyi (1956). We find that (157) can be written as

$$\frac{\Gamma(1/2)}{\sqrt{-k_2}} e^{-ik_2 x - i\pi/4} \sigma(x) + \text{higher order terms}, \quad (158)$$

where Γ is the Gamma function. Further we note that

$$\begin{aligned} \sqrt{\left[\frac{2\omega + 2UV}{v\omega_0} \right] \frac{g}{U^2} \left[\frac{2\omega_0 U}{g} + 1 \right]} &= \sqrt{2} \left[2 + \frac{g}{\omega_0 U} \right] \\ &= 2\sqrt{2} + \text{higher order terms} \end{aligned} \quad (159)$$

So we can write (156) as

$$\begin{aligned} \Phi(x, y, z) &= - \frac{e^{vz - i\pi/4}}{\sqrt{\pi}} \int_{-L/2}^x \frac{d\xi \sigma(\xi)}{\sqrt{\frac{2\omega + 2UV}{v\omega_0} |x - \xi|}} \\ &+ vye^{vz} \sigma(x) - \frac{e^{vz} \sigma(x)}{2\sqrt{2}} \end{aligned} \quad (160)$$

We remember that we have assumed $y > 0$. But we can use (111) together with (109)

$$\phi_D(x, y, z, t) = \Phi(x, y, z) e^{i(\omega t - vx)} \quad (109)$$

so that we can write down a two-term inner expansion of the far-field source solution as

$$\begin{aligned} \phi_D(x, y, z, t) &\sim e^{i(\omega t - vx)} e^{vz} \left[- \frac{e^{-i\pi/4}}{\sqrt{\pi}} \int_{-L/2}^x \frac{d\xi \sigma(\xi)}{\sqrt{\frac{2\omega + 2UV}{v\omega_0} |x - \xi|}} \right. \\ &\left. + v|y| \sigma(x) - \frac{\sigma(x)}{2\sqrt{2}} \right] \end{aligned} \quad (161)$$

We note that (161) does not reduce to (54) when $U = 0$. It should not be expected that (161) reduce to (54) when $U = 0$ since we have assumed $\tau = \frac{\omega U}{g} > 1/4$ and since this assumption has been an important part in our analysis (See the text following (116)). We should note that the last term in (161) represents a disturbance arising from upstream while the last term in (54) represents a disturbance arising from downstream.

3. Comparison with another approach

In the zero-speed problem the inner expansion of the far-field source solution gave two integral terms (see (50)), an integral from $-L/2$ to x and an integral from x to $L/2$. To avoid confusion in the notation, let us now temporarily call the x -axis shown in Fig. 1 for the ξ -axis. Then the integral from $-L/2$ to x represents the integrated effect of sources with local source density $\sigma(\xi)e^{-i\nu\xi}$. Because of our assumptions, the sources are many wave lengths away from x , and so the expression for a source at ξ is the asymptotic expression which is valid for large $\nu(x-\xi)$. A similar interpretation can be given to the integral from x to $L/2$.

One could try to interpret the integral terms in the inner expansion for the forward-speed problem in a similar way as above. One should, however, note an important difference between an oscillating source with zero speed and an oscillating source with great enough forward speed so that $\tau > 1/4$. In the zero-speed case the disturbance will only depend on the distance from the source. For the forward-speed case, however, the main disturbance will be downstream. This means that for the forward-speed problem we should only expect to get an integrated effect from $-L/2$ to x .

Newman (1959) has derived an asymptotic expression for a translating oscillating source valid at large distances. The following asymptotic expression for large positive $\nu(x-\xi)$ for a source located at $(\xi, 0, 0)$ can be obtained from Newman's asymptotic expansion

$$\left[\frac{8\pi}{|x-\xi|} \right]^{1/2} \left[\frac{\nu H_3^2}{1+2\omega_0 U/g} \right]^{1/2} e^{\nu H_3^2 (z+i(\xi-x)) + i\pi/4 + i\omega t}$$

$$- \left[\frac{8\pi}{|x-\xi|} \right]^{1/2} \left[\frac{\nu}{1+2\omega_0 U/g} \right]^{1/2} e^{\nu (z+i(\xi-x)) + i3\pi/4 + i\omega t}$$

(162)

where

$$H_3 = 1 + \frac{g}{\omega_0 U}$$

We multiply (162) by a local source density $\mu(\xi)e^{-i\nu\xi}$ and integrate from $-L/2$ to x . We get

$$- 4\pi e^{i(\omega t - \nu x)} \left[- \frac{e^{\nu z - i\pi/4}}{\sqrt{\pi}} \int_{-L/2}^x \frac{d\xi \mu(\xi)}{\sqrt{\frac{2\omega+2UV}{\nu\omega_0}} |x-\xi|} \right. \\ \left. - \frac{e^{\nu z H_3^2 + ik_2 x + i\pi/4}}{\sqrt{\pi}} \int_{-L/2}^x \frac{d\xi \mu(\xi) H_3 e^{-ik_2 \xi}}{\sqrt{\frac{2\omega+2UV}{\nu\omega_0}} |x-\xi|} \right]$$

where

$$k_2 = - \frac{g}{U^2} (2\omega_0 U/g + 1)$$

Using the fact that $O\left(\frac{g}{\omega_0 U}\right) = O(\epsilon^a)$ (see (144)) this can be written as

$$- 4\pi e^{i(\omega t - \nu x)} \left[- \frac{e^{\nu z - i\pi/4}}{\sqrt{\pi}} \int_{-L/2}^x \frac{d\xi \mu(\xi)}{\sqrt{\frac{2\omega+2UV}{\nu\omega_0}} |x-\xi|} \right. \\ \left. - \frac{e^{ik_2 x + \nu z + i\pi/4}}{\sqrt{\pi}} \int_{-L/2}^x \frac{d\xi \mu(\xi) e^{-ik_2 \xi}}{\sqrt{\frac{2\omega+2UV}{\nu\omega_0}} |x-\xi|} \right] \quad (163)$$

+ higher order terms

(163) should be compared with the integral terms in (156) combined with (109). Taking into account the different normalization of source strength here and in Newman (1959), we see that (163) is the same as the integral terms in (156) combined with (109). This provides a good check on the result we have obtained for the inner expansion of the far-field source solution.

4. The near-field problem and the matching

We now formulate the near-field problem and perform the matching between the near-field and the far-field solutions. A one-term far-field solution is found to be due to a line of sources with source density

$$\sigma_1(x)e^{i(\omega t - \nu x)}$$

spread along the line $y = z = 0$, $-L/2 \leq x \leq L/2$. (See Fig. 1). As in the zero-speed problem, a one-term near-field solution is found to be the negative of the incident wave. The matching of the far-field solution and the near-field solution determines $\sigma_1(x)$ in a similar way as for the zero-speed problem. The two-term near-field solution is given by (193).

It should be noted that "Near-field" means the region near the body where the distance from the body is $O(\epsilon)$. However, we do not expect the near-field approximations to be valid near the bow and stern.

We will express the potential of the diffracted wave as follows:

$$\phi_D = e^{i(\omega t - \nu x)} \psi(x, y, z) \quad (164)$$

Using (103), (99), (102), and the fact that the incident wave potential satisfies the Laplace equation and the free-surface condition (102), we get that ϕ_D will satisfy the Laplace equation and the free-surface condition (102).

Putting (164) into Laplace equation gives

$$\frac{\partial^2 \psi}{\partial y^2} + \frac{\partial^2 \psi}{\partial z^2} - v^2 \psi - 2iv \frac{\partial \psi}{\partial x} + \frac{\partial^2 \psi}{\partial x^2} = 0 \quad (165)$$

in the fluid region.

The free-surface condition is

$$(i\omega + U \frac{\partial}{\partial x})^2 \phi_D + g \frac{\partial \phi_D}{\partial z} = 0 \quad \text{on } z = 0. \quad (166)$$

Putting (164) into (166) gives

$$-\omega_0^2 \psi + g \frac{\partial \psi}{\partial z} + 2iU\omega_0 \frac{\partial \psi}{\partial x} + U^2 \frac{\partial^2 \psi}{\partial x^2} = 0 \quad \text{on } z=0. \quad (167)$$

The body boundary condition (100) together with (103) gives

$$\begin{aligned} & [n_2 \frac{\partial \psi}{\partial y} + n_3 \frac{\partial \psi}{\partial z} - ivn_1 \psi + n_1 \frac{\partial \psi}{\partial x}] \\ & = [ivn_1 - vn_3] \frac{gh}{\omega_0} e^{vz} \quad \text{on } z = h(x,y) \end{aligned} \quad (168)$$

A last condition on ψ is that it must match with the far-field solution.

As in the zero-speed problem, we stretch coordinates

$$y = \epsilon Y, \quad z = \epsilon Z, \quad n_{2D} = \epsilon N, \quad x = X \quad (169)$$

to express that ψ varies very slowly in the x -direction compared with the variation of ψ in the transverse plane.

We assume an asymptotic expansion of ψ of the form

$$\psi \sim \sum_{n=1}^N \psi_n(X, Y, Z; \epsilon) \quad (170)$$

where $\psi_{n+1} = o(\psi_n)$ as $\varepsilon \rightarrow 0$ for fixed X, Y, Z .

By putting (170) in (165), we get

$$\begin{aligned} & \left[\frac{\partial^2}{\partial Y^2} + \frac{\partial^2}{\partial Z^2} - v^2 \varepsilon^2 \right] [\psi_1 + \psi_2 + \dots] \\ & = 2iv\varepsilon^2 \frac{\partial}{\partial X} (\psi_1 + \dots) + \dots \end{aligned} \quad (171)$$

The free-surface condition (167) becomes

$$\begin{aligned} & \frac{\partial}{\partial Z} (\psi_1 + \psi_2 + \dots) - v\varepsilon (\psi_1 + \psi_2 + \dots) \\ & = -2i \frac{U\omega_0}{g} \varepsilon \frac{\partial}{\partial X} (\psi_1 + \dots) + \dots \quad \text{on } Z = 0 \end{aligned} \quad (172)$$

The body boundary condition (168) becomes

$$\begin{aligned} & \frac{\partial}{\partial N} (\psi_1 + \psi_2 + \dots) = (iv\varepsilon n_1 - \varepsilon n_1 \frac{\partial}{\partial X}) (\psi_1 + \dots) \\ & + iv\varepsilon n_1 \frac{gh}{\omega_0} e^{vz} - v\varepsilon n_3 \frac{gh}{\omega_0} e^{vz} \quad \text{on } z = h(x, y) \end{aligned} \quad (173)$$

As in the zero-speed problem, we introduce

$$v\varepsilon = k \quad (174)$$

and

$$\frac{gh}{\omega_0} = c \quad (175)$$

The lowest-order equations become

$$\left[\frac{\partial^2}{\partial Y^2} + \frac{\partial^2}{\partial Z^2} - k^2 \right] \psi_1 = 0 \quad (176)$$

$$\left[\frac{\partial}{\partial Z} - k \right] \psi_1 = 0 \quad \text{on } z = 0 \quad (177)$$

$$\frac{\partial}{\partial N} \psi_1 = - Cn_3 k e^{kZ} \quad \text{on } z = h(x,y) \quad (178)$$

In addition ψ_1 must match with the far-field solution.

A one-term far-field solution is assumed to be the potential associated with a line distribution of sources of density

$$\sigma_1(x) e^{i(\omega t - vx)}$$

spread along the line $y = z = 0$, $-L/2 \leq x \leq L/2$. That solution has been obtained in a previous section, and a one-term inner expansion of the far-field solution can be found from (161). For any fixed x greater than $-L/2$, a one-term inner expansion is

$$e^{i(\omega t - vx)} \left[- \frac{e^{vz - i\pi/4}}{\sqrt{\pi}} \int_{-L/2}^x \frac{d\xi \sigma_1(\xi)}{\sqrt{\frac{2\omega + 2Uv}{v\omega_0} |x - \xi|}} \right] \quad (179)$$

In a similar way as for the zero-speed problem, one sees that the only possibility for a solution satisfying (176), (177), (178), and matching (179) is by requiring that

$$\frac{e^{vz - i\pi/4}}{\sqrt{\pi}} \int_{-L/2}^x \frac{d\xi \sigma_1(\xi)}{\sqrt{\frac{2\omega + 2Uv}{v\omega_0} |x - \xi|}} = C e^{vz} \quad (180)$$

and letting a one-term near-field solution of the diffracted wave be the negative of the incident wave. So

$$\psi_1 = -C e^{vz} \quad (181)$$

We solve (180) for $\sigma_1(x)$ formally by letting it be an equality for all $x \geq -L/2$. We get Abel's integral equation to solve (See Dettman (1965)). The solution is

$$\sigma_1(x) = \sqrt{\frac{2\omega+2UV}{\pi\omega_0 v(x+L/2)}} e^{i\pi/4} C \quad (182)$$

The discussion that followed the expression of $\sigma_1(x)$ for the zero-speed problem (see after equation (80)) can also be applied for the forward-speed problem. The conclusion was that we had to construct a separate expansion for a region in which $x+L/2 = O(\epsilon^\gamma)$, (γ some positive number), and that $\sigma_1(x)$ is not given in that region by (182).

We wish next to find ψ_2 , but first we need to say some more about the far-field.

We expect that a two-term far-field expansion is obtained by a line distribution of sources of density

$$(\sigma_1(x) + \sigma_2(x)) e^{i(\omega t - vx)} \quad (183)$$

spread along the line $y = z = 0$, $-L/2 \leq x \leq L/2$. A two-term inner expansion of this two-term far-field expansion can be obtained from (161). It is

$$e^{i(\omega t - vx)} \left[-\frac{e^{vz}}{\sqrt{\pi}} e^{-i\pi/4} \int_{-L/2}^x \frac{d\xi \sigma_1(\xi)}{\sqrt{\frac{2\omega+2UV}{v\omega_0} |x-\xi|}} - \frac{e^{vz}}{\sqrt{\pi}} e^{-i\pi/4} \int_{-L/2}^x \frac{d\xi \sigma_2(\xi)}{\sqrt{\frac{2\omega+2UV}{v\omega_0} |x-\xi|}} + v|y| e^{vz} \sigma_1(x) - \frac{\sqrt{2}}{4} e^{vz} \sigma_1(x) \right] \quad (184)$$

In the same way as for the zero-speed problem we will find that ψ_2 will satisfy

$$\left[\frac{\partial^2}{\partial y^2} + \frac{\partial^2}{\partial z^2} - k^2 \right] \psi_2 = 0 \quad (185)$$

$$\left[\frac{\partial}{\partial Z} - k \right] \psi_2 = 0 \quad \text{on } Z = 0 \quad (186)$$

$$\frac{\partial \psi_2}{\partial N} = 0 \quad \text{on the submerged part of the body.} \quad (187)$$

In addition ψ_2 must match with the far-field solution.

Ursell (1968a) has derived a solution to (185), (186), and (187). It can be written as

$$\psi_2 = B_2(x) \left[e^{kZ} + \int_{C(+)} k\mu(s;k) \cdot [G(kY,kZ;k\xi(s),k\eta(s)) + G(kY,kZ;-k\xi(s),k\eta(s))] ds \right] \quad (188)$$

For an explanation of (188), see the discussion following equation (87) in the zero-speed problem. $B_2(x)$ in (188) is unknown at the moment now, but will be determined by matching.

The two-term near-field solution,

$$[\psi_1 + \psi_2] e^{i(\omega t - \nu x)}, \quad (189)$$

has the following three-term outer expansion:*

$$e^{i(\omega t - \nu x)} \left[-\frac{e^{\nu Z}}{\sqrt{\pi}} e^{-i\pi/4} \int_{-L/2}^x \frac{d\xi \sigma_1(\xi)}{\sqrt{\frac{2\omega + 2UV}{\nu\omega_0} |x-\xi|}} + B_2(x) e^{kZ} - B_2(x) 4k^2 \pi \frac{|Y|}{\epsilon} e^{kZ} \int_{C(+)} \mu(s,k) e^{k\eta(s)} ds \right]. \quad (190)$$

We see that (190) matches with (184) if we set:

* See (89) and the text in connection with (89).

$$\begin{aligned}
 B_2(x) &= - \frac{\sigma_1(x)}{4k\pi \int_{C(+)} \mu(s,k) e^{k\eta(s)} ds} \\
 &= - \frac{\sqrt{\frac{2\omega+2UV}{\pi\nu\omega_0(x+L/2)}} e^{i\pi/4} C}{4k\pi \int_{C(+)} \mu(s,k) e^{k\eta(s)} ds}
 \end{aligned} \tag{191}$$

and

$$\begin{aligned}
 & - \frac{e^{-i\pi/4}}{\sqrt{\pi}} \int_{-L/2}^x \frac{d\xi \sigma_2(\xi)}{\sqrt{\frac{2\omega+2UV}{\nu\omega_0} |x-\xi|}} \\
 & = B_2(x) + \frac{\sqrt{2}}{4} \sigma_1(x)
 \end{aligned} \tag{192}$$

Equation (192) gives us Abel's integral equation to solve. $B_2(x)$ on the right hand side of (192) has to be numerically determined (see (191)). We are only interested in the fact that the near-field and far-field solutions match, and we are not going to find σ_2 .

It is the near-field solution that has the primary interest and we have found that a two-term near-field solution of the diffraction potential is

$$\begin{aligned}
 [\psi_1 + \psi_2] e^{i(\omega t - \nu x)} &= e^{i(\omega t - \nu x)} \left[-C e^{kZ} \right. \\
 & - \sqrt{\frac{2\omega+2UV}{\pi\nu\omega_0(x+L/2)}} \cdot \frac{e^{i\pi/4} C}{4k\pi \int_{C(+)} \mu(s,k) e^{k\eta(s)} ds} \left[e^{kZ} \right. \\
 & \left. \left. + \int_{C(+)} k\mu(s;k) [G(kY, kZ; k\xi(s), k\eta(s)) + G(kY, kZ; -k\xi(s), k\eta(s))] ds \right] \right]
 \end{aligned} \tag{193}$$

V. NUMERICAL CALCULATIONS

1. Theoretical background

It would be time consuming to evaluate the solutions we have found (see (94) and (193)) for a ship with arbitrary cross-sections. But if the ship had circular cross-sections, there is a faster way to find the solutions. We can use the solution given by Ursell (1968b) for a circular cross-section. Ursell has used a different coordinate system than we have used earlier, and I find it convenient using Ursell's coordinate system when talking about Ursell's solution. The coordinate system is shown in Fig. 8.

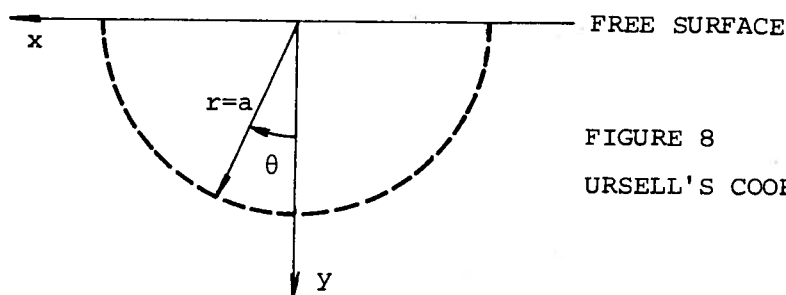


FIGURE 8
URSELL'S COORDINATE SYSTEM

The two-dimensional problem which Ursell solves is given by the Helmholtz equation

$$\left[\frac{\partial^2}{\partial x^2} + \frac{\partial^2}{\partial y^2} - v^2 \right] \phi = 0 \quad (194)$$

in the fluid domain, and the boundary conditions

$$v\phi + \frac{\partial\phi}{\partial y} = 0 \quad \text{when } y = 0, \quad |x| > a \quad (195)$$

and

$$\frac{\partial\phi}{\partial r} = 0 \quad \text{when } r = a, \quad -\pi/2 < \theta < \pi/2 \quad (196)$$

He shows that a solution of (194), (195), and (196) can be written in the form

$$\phi = B_3 \{ A_0 S_0(x,y) + \exp(-vy) + \sum_{m=1}^{\infty} A_m O_m(x,y) \} \quad (197)$$

The functions $S_0(x,y)$ and $O_m(x,y)$ will be discussed presently.

Ursell considered an infinitely long cylinder and there were no appropriate conditions for $x \rightarrow \pm\infty$ that could determine the arbitrary constant B_3 in (197). But we consider a ship, and we have found a condition when $x \rightarrow \pm\infty$ that will determine B_3 . This is similar to what we did in finding the solutions (94) and (193). Then we used an integral equation approach to solve (194), (195), and (196). But for this special case with a circular cross-section it is more convenient to write the solution as (197). We will later come back to the determination of B_3 after we have discussed the terms in (197) some more.

The source term S_0 can be written as

$$S_0(x,y) = 1/2 \left[\int_{-\infty}^{\infty} + \int_{-\infty}^{\infty} \right] \frac{\cosh\mu}{\cosh\mu-1} \exp(-vy \cosh\mu + ivx \sinh\mu) d\mu \quad (198)$$

The paths in the two integrals pass respectively below and above the double pole at $\mu = 0$.

We are going to rewrite (198) so that we can more easily evaluate it numerically. We introduce

$$l = v \sinh\mu \quad (199)$$

as a new integration variable. We can then write (198) as

$$S_0(x,y) = 1/2 \left[\int_{-\infty}^{\infty} + \int_{-\infty}^{\infty} \right] \frac{dl e^{i(lx - y\sqrt{v^2+l^2})}}{\sqrt{v^2+l^2} - v} \quad (200)$$

We will now assume $x \geq 0$. The derivation for $x \leq 0$ will be quite similar, and we are not going to go through that. Since we are operating with a source term, we can later on use the fact that

$$S_0(-x, y) = S_0(x, y) \quad (201)$$

We introduce complex integration paths as shown in Figure 9.

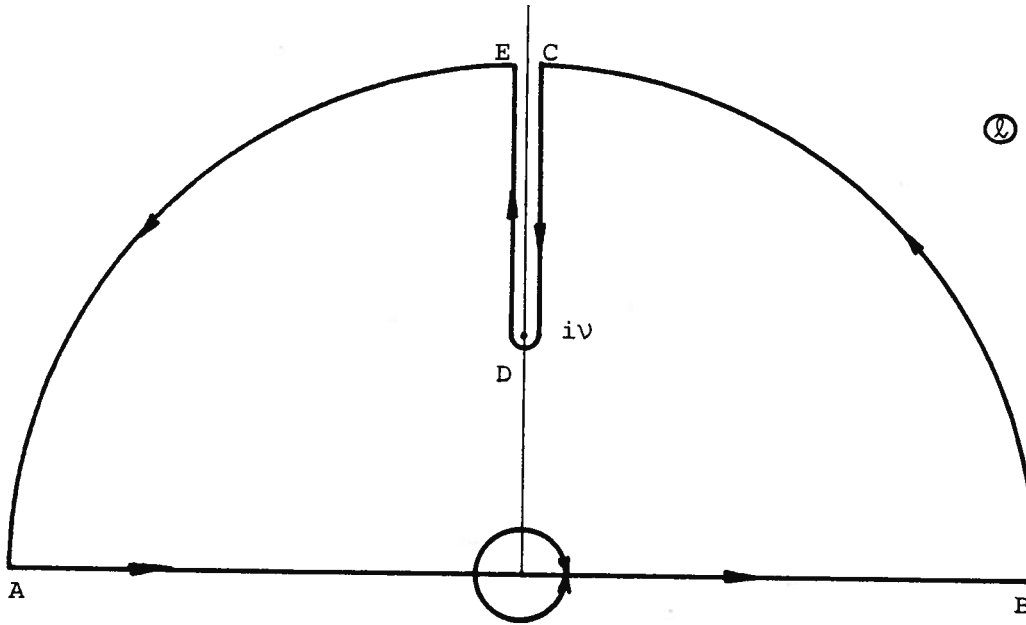


FIGURE 9
COMPLEX INTEGRATION PATHS

We need the residue at $l = 0$. The integrand in (200) has a pole of second order at $l = 0$. The residue is given by

$$\text{Res}(l=0) = \lim_{l \rightarrow 0} \frac{d}{dl} \left[\frac{l^2 e^{ilx - y\sqrt{v^2 + l^2}}}{\sqrt{v^2 + l^2} - v} \right] = 2ivxe^{-vy}$$

By using the residue theorem, letting $B \rightarrow \infty$, $C \rightarrow +i\infty$, $E \rightarrow +i\infty$, $A \rightarrow -\infty$ in Fig. 9, we will get

$$\begin{aligned}
 S_0 &= \int_v^\infty id\eta e^{-x\eta} \left[\frac{e^{-\sqrt{\eta^2-v^2} iy}}{i\sqrt{\eta^2-v^2} - v} + \frac{e^{+\sqrt{\eta^2-v^2} iy}}{i\sqrt{\eta^2-v^2} + v} \right] - 2\pi v x e^{-vy} \\
 &= 2 \int_v^\infty d\eta e^{-x\eta} \left[\frac{\sqrt{\eta^2-v^2} \cos [\sqrt{\eta^2-v^2} y] - v \sin [\sqrt{\eta^2-v^2} y]}{\eta^2} \right] \\
 &\quad - 2\pi v x e^{-vy}
 \end{aligned} \tag{202}$$

We now introduce

$$u = \sqrt{\eta^2 - v^2}$$

as a new integration variable and get

$$\begin{aligned}
 S_0 &= 2 \int_0^\infty \frac{du u}{\sqrt{v^2+u^2}} \left[\frac{u \cos(uy) - v \sin(uy)}{v^2+u^2} \right] e^{-x\sqrt{v^2+u^2}} \\
 &\quad - 2\pi v x e^{-vy}
 \end{aligned}$$

This is true for $x \geq 0$. Using (201) we can write for all x

$$S_0 = 2 \int_0^\infty \frac{du u}{\sqrt{v^2+u^2}} \left[\frac{u \cos(uy) - v \sin(uy)}{v^2+u^2} \right] e^{-|x|\sqrt{v^2+u^2}} - 2\pi v |x| e^{-vy} \tag{203}$$

S_0 has now been written in a form that makes it easy to evaluate it numerically. We will come back to this point later.

The other unexplained terms in (197) are the wave-free potentials O_m . They are given by

$$\begin{aligned}
 O_m(x, y) &= K_{2m-2}(vr) \cos(2m-2)\theta \\
 &\quad + 2K_{2m-1}(vr) \cos(2m-1)\theta + K_{2m}(vr) \cos 2m\theta,
 \end{aligned} \tag{204}$$

$$m = 1, 2, 3, \dots$$

(Ursell denoted these functions by $O_m^{(e)}$.)

K_n are modified Bessel functions as defined by Abramowitz and Stegun (1964).

The coefficients A_0 and A_m in (197) are determined by satisfying the body boundary condition (196). This leads to an equation of the form

$$A_0 \frac{\partial S_0}{\partial r} + \sum_{m=1}^{\infty} A_m \frac{\partial O_m}{\partial r} - v \cos \theta e^{-vr \cos \theta} = 0 \quad \text{on } r = a. \quad (205)$$

We have assumed here that we can differentiate the infinite series in (197) term by term, and we have used the fact that

$$x = r \sin \theta, \quad y = r \cos \theta. \quad (206)$$

$\frac{\partial O_m}{\partial r}$ in (205) is obtained from (204) and by using 9.6.26 in Abramowitz and Stegun (1964). So

$$\begin{aligned} \frac{\partial O_m}{\partial r} &= \left\{ -K_{2m-1}(vr) + \frac{2m-2}{vr} K_{2m-2}(vr) \right\} v \cos(2m-2)\theta \\ &+ 2 \left\{ -K_{2m}(vr) + \frac{2m-1}{vr} K_{2m-1}(vr) \right\} v \cos(2m-1)\theta \\ &+ \left\{ -K_{2m+1}(vr) + \frac{2m}{vr} K_{2m}(vr) \right\} v \cos 2m\theta \end{aligned}$$

We will now describe in more detail how to solve (205) numerically and how numerically to evaluate S_0 in (197) and $\frac{\partial S_0}{\partial r}$ in (205).

Equation (205) is solved by setting up a least-square condition. One assumes that the infinite sums in (197) and (205) converge sufficiently rapidly so that a finite number of terms in the infinite sums gives a satisfactory approximation. One calls this number M and sets up

$$F = \sum_{i=1}^N \left[A_0 \frac{\partial S_0(r, \theta_i)}{\partial r} + \sum_{m=1}^M A_m \frac{\partial O_m(r, \theta_i)}{\partial r} - v \cos \theta_i e^{-v a \cos \theta_i} \right]^2 \quad (207)$$

for $r = a$.

N should be chosen so that $N > 3/2M$.^{*} It is only necessary to choose θ_i in the first quadrant and they have been chosen as follows:

$$\theta_i = \frac{\pi}{4N} + \frac{\pi}{2N} (i-1) \quad , \quad i = 1, 2, \dots, N \quad (208)$$

In accordance with the least-square technique, we apply the condition that

$$\frac{\partial F}{\partial A_n} = 0 \quad , \quad n = 0, 1, \dots, M. \quad (209)$$

This leads to the linear equation system

$$\sum_{m=0}^M A_m \left[\sum_{i=1}^N \frac{\partial O_m(r, \theta_i)}{\partial r} \frac{\partial O_n(r, \theta_i)}{\partial r} \right] = v \sum_{i=1}^N \cos \theta_i e^{-v a \cos \theta_i} \frac{\partial O_n(r, \theta_i)}{\partial r} \quad (210)$$

for $r=a$. n goes from zero to M . We have set $\frac{\partial S_0}{\partial r} = \frac{\partial O_0}{\partial r}$ in (210). (210) can be solved by standard methods.

S_0 in (197) and $\frac{\partial S_0}{\partial r}$ in (210) are numerically evaluated in the following way. We introduce (206) into (203) and write S_0 as

$$\begin{aligned} S_0 = & - 2\pi v r \sin \theta e^{-v r \cos \theta} \\ & + 2 \int_0^A \frac{du u}{\sqrt{v^2 + u^2}} \left[\frac{u \cos(u r \cos \theta) - v \sin(u r \cos \theta)}{v^2 + u^2} \right] e^{-r \sin \theta \sqrt{v^2 + u^2}} \\ & + 2 \int_A^\infty \frac{du u}{\sqrt{v^2 + u^2}} \left[\frac{u \cos(u r \cos \theta) - v \sin(u r \cos \theta)}{v^2 + u^2} \right] e^{-r \sin \theta \sqrt{v^2 + u^2}} \end{aligned} \quad (211)$$

* $N = 10$ was found to give satisfactory results.

We have dropped the absolute value sign, since S_0 and $\frac{\partial S_0}{\partial r}$ will only be evaluated for $0 < \theta < \pi/2$ (See (208)). A in (211) is chosen so that the contribution from the last integral in (211) is sufficiently small. For the last integral we can write

$$\left| \int_A^\infty \frac{du u}{\sqrt{v^2+u^2}} \left[\frac{u \cos(\text{urcos}\theta) - v \sin(\text{urcos}\theta)}{v^2 + u^2} \right] e^{-r \sin\theta \sqrt{v^2+u^2}} \right|$$

$$< \int_A^\infty \frac{du u}{v^2+u^2} e^{-r \sin\theta \sqrt{v^2+u^2}} < \int_A^\infty \frac{du u}{\sqrt{v^2+u^2}} e^{-r \sin\theta \sqrt{v^2+u^2}} = \frac{e^{-r \sin\theta \sqrt{v^2+A^2}}}{r \sin\theta}$$

We note that $\sin\theta \neq 0$, since $0 < \theta < \pi/2$. So we can write (211) as

$$S_0 = -2\pi v r \sin\theta e^{-vr \cos\theta}$$

$$+ 2 \int_0^A \frac{du u^2}{(v^2+u^2)^{3/2}} \cos(\text{urcos}\theta) e^{-r \sin\theta \sqrt{v^2+u^2}}$$

$$- 2 \int_0^A \frac{du uv}{(v^2+u^2)^{3/2}} \sin(\text{urcos}\theta) e^{-r \sin\theta \sqrt{v^2+u^2}} \quad (212)$$

$$+ o(B_1) \quad \text{for } 0 < \theta < \pi/2$$

where $B_1 = \frac{e^{-r \sin\theta \sqrt{v^2+A^2}}}{r \sin\theta}$. For a given small number B_1 the corresponding value of A is given by

$$A = \sqrt{\frac{\left[\log \left[\frac{1}{r \sin\theta B_1} \right] \right]^2}{(r \sin\theta)^2} - v^2} \quad (213)$$

It was found that it was satisfactory to use $B_1 = 0.0001$.

Each integral in (212) was evaluated by first locating the zeroes for the integrand. For the first integrand the zeroes are easily found to be $u = 0$ and $u = \frac{\pi}{2r\cos\theta} (2m+1)$, $m = 0, 1, 2, \dots$, and for the second integrand the zeroes are $u = \frac{\pi}{r\cos\theta} m$, $m = 0, 1, 2, \dots$. Between each zero in an integrand we then used Simpson's formula. As is seen above the length of the interval between each zero depends on θ , and so the number of points used in the Simpson integration should depend on θ . When θ was close to $\pi/2$, as many as 50 points were needed in the Simpson integration. But when θ was close to 0, it was only necessary to use 8 points. If A was less than u at the second zero of an integrand, then Simpson's formula was only used between 0 and A .

We will denote the first integral in (212) by $GI1$ and the second integral by $GI2$, so that

$$S_0 = -2\pi v r \sin\theta e^{-vr\cos\theta} + 2 \cdot GI1 - 2 \cdot GI2 \tag{214}$$

$$+ 0 \left(\frac{e^{-r\sin\theta\sqrt{v^2+A^2}}}{r\sin\theta} \right) \quad \text{for } 0 < \theta < \pi/2$$

Values of $GI1$ and $GI2$ obtained by numerical integration are shown in Figures 10 through 15 as functions of θ for different values of vr .

Let us now define a domain G_0 consisting of all $\theta \in [0, \pi/2]$ and all $r \in [c, M]$. Here $c > 0$ and M is finite. c and M are selected so that $[c, M]$ contains all r -values of interest. It is not difficult to see that the infinite integral which corresponds to $GI2$

$$\int_0^\infty \frac{du \, v u \sin(ur\cos\theta)}{(v^2+u^2)^{3/2}} e^{-r\sin\theta\sqrt{v^2+u^2}} \tag{215}$$

is uniformly convergent on G_0 . Further the integrand of (215) is continuous on $[0, \infty) \times G_0$. It is then known (see Jones (1966)) that

$$\lim_{\theta \rightarrow 0} \int_0^{\infty} \frac{du \, v u \sin(ur \cos \theta)}{(v^2 + u^2)^{3/2}} e^{-r \sin \theta \sqrt{v^2 + u^2}}$$

$$= \int_0^{\infty} \frac{du \, v u \sin(ur)}{(v^2 + u^2)^{3/2}}$$
(216)

By using Gradshteyn and Ryzhik (1965), we can write

$$\int_0^{\infty} \frac{du \, v u \sin ur}{(v^2 + u^2)^{3/2}} = v r K_0(vr)$$
(217)

In this way we can find analytically determined values of GI2 when $\theta = 0$. We can see from Figures 10 through 15 that the agreement between analytically determined values of GI2 and numerically determined values of GI2 is very good.

The infinite integral which corresponds to GI1 is not uniformly convergent on G_0 , so it is not possible to check the numerical values of GI1 in the same way as we did above for GI2.

Let us now consider the numerical evaluation of $\frac{\partial S_0}{\partial r}$. We write S_0 as

$$S_0 = 2 \int_0^{\infty} \frac{du \, u}{\sqrt{v^2 + u^2}} \left[\frac{u \cos(ur \cos \theta) - v \sin(ur \cos \theta)}{v^2 + u^2} \right] e^{-r \sin \theta \sqrt{v^2 + u^2}}$$

$$- 2\pi v r \sin \theta e^{-v r \cos \theta} \quad \text{for } 0 < \theta < \pi/2$$
(218)

(See 203) and (206)). We will only be interested in values of $\frac{\partial S_0}{\partial r}$ for finite values of r and for θ -values satisfying $0 < \theta < \pi/2$. Let us define a domain G_b consisting of all $\theta \in [b, \pi/2]$ and all $r \in [c, M]$. Here $b > 0$, $c > 0$, and M is finite. b is selected so that $[b, \pi/2]$ contains all θ -values of interest, and c and M are selected so that $[c, M]$ contains all r -values of interest. Further, let us denote the integrand in (218) by f . It is easily seen that

$\int_0^{\infty} \frac{\partial f}{\partial r} du$ is uniformly convergent on G_b , and that $\frac{\partial f}{\partial r}$ is continuous on $[0, \infty) \times G_b$. It is then known that $\frac{\partial}{\partial r} \int_0^{\infty} f du = \int_0^{\infty} \frac{\partial f}{\partial r} du$ (See Jones (1966)).

So we can write

$$\begin{aligned} \frac{\partial S_0}{\partial r} &= 2 \int_0^{\infty} \frac{du u}{\sqrt{v^2+u^2}} \left[\frac{-u^2 \cos \theta \sin(ur \cos \theta) - v u \cos \theta \cos(ur \cos \theta)}{v^2+u^2} \right] e^{-r \sin \theta \sqrt{v^2+u^2}} \\ &+ 2 \int_0^{\infty} \frac{du u}{\sqrt{v^2+u^2}} \left[\frac{u \cos(ur \cos \theta) - v \sin(ur \cos \theta)}{v^2+u^2} \right] \left[-\sin \theta \sqrt{v^2+u^2} \right] e^{-r \sin \theta \sqrt{v^2+u^2}} \\ &- 2\pi v \sin \theta e^{-vr \cos \theta} + 2\pi v^2 r \sin \theta \cos \theta e^{-vr \cos \theta} \end{aligned} \quad (219)$$

By rearranging the terms in (219) we can write

$$\begin{aligned} \frac{\partial S_0}{\partial r} &= 2 \int_0^{\infty} \frac{du u^2}{(u^2+v^2)^{3/2}} \left[-v \cos \theta - \sin \theta \sqrt{v^2+u^2} \right] \cos(ur \cos \theta) e^{-r \sin \theta \sqrt{v^2+u^2}} \\ &+ 2 \int_0^{\infty} \frac{du u}{(u^2+v^2)^{3/2}} \left[-u^2 \cos \theta + v \sin \theta \sqrt{v^2+u^2} \right] \sin(ur \cos \theta) e^{-r \sin \theta \sqrt{v^2+u^2}} \\ &- 2\pi v \sin \theta e^{-vr \cos \theta} + 2\pi v^2 r \sin \theta \cos \theta e^{-vr \cos \theta} \end{aligned} \quad (220)$$

The integrals in $\frac{\partial S_0}{\partial r}$ were numerically evaluated in a way similar to that used for the integrals in S_0 . The approximation to the first integral in (220) multiplied with r is called DGI1 and the approximation to the second integral multiplied by r is called DGI2.

The values of DGI1 and DGI2 as functions of θ for different values of vr are shown in Figures 16 through 21.

We have now explained how to obtain numerically the terms in the brackets of (197). We will refer to these terms as "Ursell's solution" and denote them by ϕ_u . So

$$\phi = B_3 \phi_u \quad (221)$$

(See 197). ϕ_u has been plotted in Fig. 22 as a function of νr for different values of θ and in Fig. 23 as a function of θ for different values of νr .

We now have to find B_3 in (221). B_3 will of course be determined in the same way as we did in the previous chapters where we solved the zero- and the forward-speed problem. We prefer now to use the coordinate system shown in Fig. 1.

If we take an outer expansion of (221), the term which is linear in y will be

$$-B_3 A_0 2\pi\nu |y| e^{\nu z} \quad (222)$$

(See (197) and (203)). In accordance with what has been done in the previous chapters, (222) should (for both the zero-speed and forward-speed cases) match with

$$\nu |y| e^{\nu z} \sigma_1(x) e^{i(\omega t - \nu x)}, \quad (223)$$

where $\sigma_1(x)$ can be written for both cases as

$$\sigma_1(x) = \sqrt{\frac{(2\omega + 2U\nu)}{\pi\omega_0 \nu (x+L/2)}} e^{i\pi/4} \frac{gh}{\omega_0} \quad (224)$$

By equating (222) and (223) and putting the expression for B_3 into (221), we can write the potential

$$\phi = -\frac{e^{i\pi/4}}{2\pi A_0} \sqrt{\frac{(2\omega + 2U\nu)}{\pi\omega_0 \nu (x+L/2)}} \frac{gh}{\omega_0} e^{i(\omega t - \nu x)} \phi_u \quad (225)$$

Using Bernoulli's equation, it is now easy to find the pressure. To the leading order the pressure will be

$$\frac{p}{\rho gh} = \frac{e^{i3\pi/4}}{2\pi A_0} \sqrt{\frac{2\omega + 2Uv}{\pi\omega_0 v(x+L/2)}} \phi_u e^{i(\omega t - vx)} \quad (226)$$

The force and moment on a part of the ship or on the total ship can easily be found from the pressure.

One should note the simple forward-speed dependence in (226). ϕ_u and A_0 will only depend on the wave length. So for a given wave length the amplitudes of the pressure, force and moment for a given forward speed can be obtained from the corresponding values at zero speed by multiplying the zero-speed results by a constant factor.

2. Numerical example

The "ship-like" form that we applied the theory to is shown in Fig. 24. It shows the water plane of the ship. The ship has fore and aft symmetry

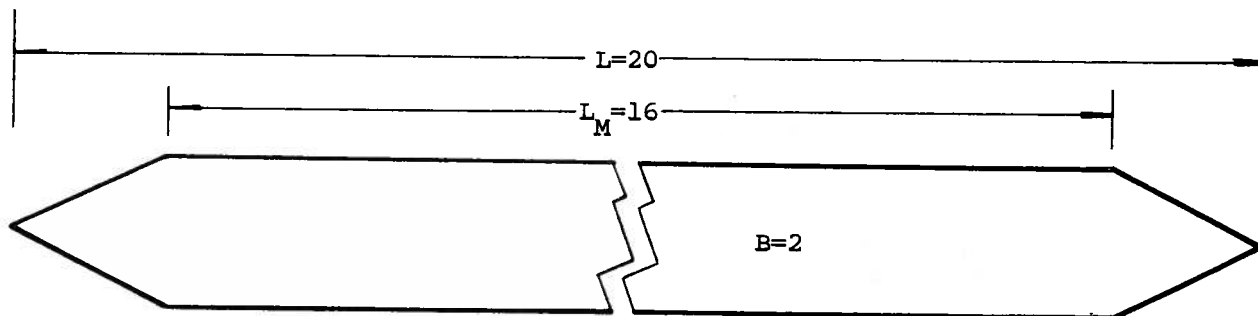


FIGURE 24

SHIP MODEL USED IN THE NUMERICAL EXAMPLE

and circular cross-sections, with radius equal to one half of the beam at the water plane. Further, $L/B = 10$ and $L_M/B = 8$, where L is the total length, B is the beam midships at the water plane, and L_M is the length of the parallel midbody of the ship.

We applied the theory for $\lambda/L = 0.25, 0.3, 0.35, 0.4, 0.45, 0.5, 0.55, 0.6$, and Froude numbers $0.0, 0.1, 0.2, 0.3$. To stop using the theory at

$\lambda/L = 0.6$ was in a way arbitrary. We cannot predict how large the wave length should be for the theory to fail. Experience is going to tell us that.

The chosen wave length range is important in the determination of the dynamic loads on a ship. (See Faltinsen (1970)).

We have plotted the pressure amplitude^{*} distribution along the ship for $\theta = 0.0785$ ($\approx 4.5^\circ$) for different wave lengths (See Fig. 25 through 32). The pressure amplitude due to the incident wave potential has also been plotted; this is called the "Froude-Kriloff pressure". Even where the "theoretical" values of the pressure near the bow and stern have been plotted, one should note that they are not assumed to be valid (See the chapters about the zero-speed and forward-speed problems.). The very high "theoretical" values at station 1 are mainly due to the factor $(x+L/2)^{-1/2}$ (See (226)).

The pressure has a decaying factor $(x+L/2)^{-1/2}$ along the parallel mid-body. This predicted trend seems to be confirmed by experiments of Abels (1959) and Lee (1964).

Multiplication factors to multiply the zero-speed result to make them valid at a given forward speed (see the text following (226)), have been given in the figures.

The cross-sectional variation of the pressure amplitude at station 10 for different wave lengths is shown in Figures 33 through 40. The Froude-Kriloff pressure amplitudes have been plotted too. In Figure 38 there are shown some experimental values. The experimental model has nearly the same L/T - ratio as the model we calculate for. (See Fig. 24). T denotes the draft at midships, and the B is the beam midships. The B/T -ratio for our model is 2.0 but the B/T -ratio for the experimental model is 2.74.

* The pressure amplitude is non-dimensionalized with respect to ρgh , where ρ is the density of water, g is the acceleration of gravity, and h is the amplitude of the incoming wave.

The experimental model does not have circular cross-sections (See Abels (1959)). The experiments seem to agree with our theoretical prediction but it is, of course, very difficult to conclude anything as long as our model and the experimental model are different.

We have also calculated the vertical force over different parts of the ship. The parts of the ship are from forward perpendicular to different stations. So the amplitudes of these forces are shown as a function of station number for different wave lengths in Figures 41 through 48. The Froude number is zero.

When calculating the vertical forces according to our theory, we have used the "theoretical" values also in the bow region. This is not in accordance with our assumptions. Due to the unrealistically high pressures calculated in the bow region, our theory will surely predict too-large forces. The forces have been compared with values computed by the procedure described in Salvesen, Tuck and Faltinsen (1970). One should note that Salvesen, Tuck, and Faltinsen (1970) did not show that their procedure to calculate exciting force over parts of the ship was correct. But recent work of Ogilvie (1971) seems to indicate that it is a correct procedure. By comparing the values obtained by our new theory and by the Salvesen-Tuck-Faltinsen procedure and taking into account that the forces over the bow region have to be reduced, one can conclude that there is a good agreement between the two procedures.

The total force on the ship has also been calculated for different wave lengths in the zero-speed case. See Fig. 49. We have compared our theoretical values with the Khaskind formula (Newman (1962)). But note that we have used strip-theory approximation for the heaving potential in the Khaskind formula. Strictly speaking this can only be justified for parts of the ship away from the bow and stern regions, and when the wave length is short compared with the length of the ship and of the order of magnitude of the transverse dimensions of the ship. But due to the oscillating factor $e^{-i\nu x}$ in the Khaskind formula, the potential at the ends of the ship will not be unimportant in the Khaskind formula when the wave length is short compared with the length of the ship.

Thus, strictly speaking, the Khaskind formula with strip-theory approximation cannot be rationally justified for any wave length. But, for lack of anything better, it has been common to use the strip-theory approximation in the Khaskind formula, and one must admit that the results have been good.

For the same reason given with respect to the forces over parts of the ship, one must conclude that our theory will predict too-large forces. Taking this into account, one can see that the agreement between our theory and Khaskind formula with strip-theory approximation is good except in the vicinity of $\lambda/L = 0.45$.

3. Comparison with experiments

C.M. Lee has measured the pressure-distribution along a restrained, semi-submerged, prolate spheroid which was towed at a constant speed in regular head-sea waves. He used the experimental pressure values to calculate a longitudinal force distribution along the spheroid (C.M. Lee (1964)). He did not publish the data for the pressure distribution along the spheroid, but he was kind and gave us those data.

The surface of the prolate spheroid that C.M. Lee used can be described by the equation:

$$\frac{x^2}{\ell^2} + \frac{y^2+z^2}{b_0^2} = 1 \quad ,$$

where $\ell = 19.8''$ and $b_0 = 3.3''$. x, y, z are defined by Figure 1. He measured the pressure at cross-sections located at $x = -16''$ (called C_F), $x = -12.5''$ (called B_F), $x = -7''$ (called A_F), $x = 0$ (called \emptyset), $x = 7''$ (called A_A), $x = 12.5''$ (called B_A), $x = 16''$ (called C_A) . He did the experiments for $\lambda/L = 0.5, 0.75, 1.0, 1.25, 1.5, \text{ and } 2.0$ where λ is the wave length and L is the length of the model. The Froude numbers of the model were $F_n = 0.082, 0.123, 0.164, 0.205, 0.246, 0.328$.

Because we have assumed that the wave length should be short compared with the length of the ship, we have only compared experiments and theory for $\lambda/L = 0.5$. Further there were evidently some irregularities in the experiments for $Fn = 0.328$, and so we did not compare experiments and theory for that Froude-number. We decided to present the comparisons between experiments and theory for Froude-numbers 0.082 and 0.205, but the agreement between theory and experiments was just as good for Froude-numbers 0.123, 0.164, and 0.246.

In Figures 50 through 55 are shown the comparisons of the pressure amplitudes for Froude-number 0.085. Figure 50 shows the longitudinal distribution of the pressure amplitude along the keel of the spheroid. It is seen that the experiments confirm the theoretically predicted longitudinal deformation of the wave along the ship. Figure 51 shows the pressure-variation along the cross-section B_F . (The index F indicates that the cross-section is on the forward part of the model.) The variable θ , the abscissa in the figure, is $\pi/2$ for a point in the undisturbed free-surface and 0 for a point located on the center plane of the model. It is seen that the agreement between theory and experiments is reasonably good. Similar comparisons are made for cross-section A_F in Fig. 52, cross-section \emptyset in Fig. 53, cross-section A_A in Fig. 54, cross-section B_A in Fig. 55. (The index A indicates that the cross-section is on the after part of the model.) It is seen that the agreement is good, especially for the after cross-sections.

In Figures 56 through 61 are shown the comparisons of the pressure amplitudes for Froude-number 0.205. Fig. 56 shows the longitudinal distribution of the pressure along the keel of the spheroid. Figures 57-61 show the pressure variation on the cross-sections B_F , A_F , \emptyset , A_A , and B_A , respectively. It is seen that the agreement between experiments and theory is at least as good as in the case of the smaller Froude-number. Since the theory is not assumed to be valid near the bow or stern, no comparisons have been made for cross-sections C_F and C_A .

In Fig. 62 is shown the comparison between theory and experiments for the longitudinal distribution of the phase angle of the pressure. The theory predicts that for all Froude-numbers the phase-angle of the pressure is $\pi/4$

before the phase-angle of the Froude-Kriloff pressure. For a given cross-section, the experimental value of the phase angle varied somewhat. So the presented data are averages. The variation is, roughly speaking, not more than $\pm 10^\circ$. It is seen that the agreement between experiments and theory is good.

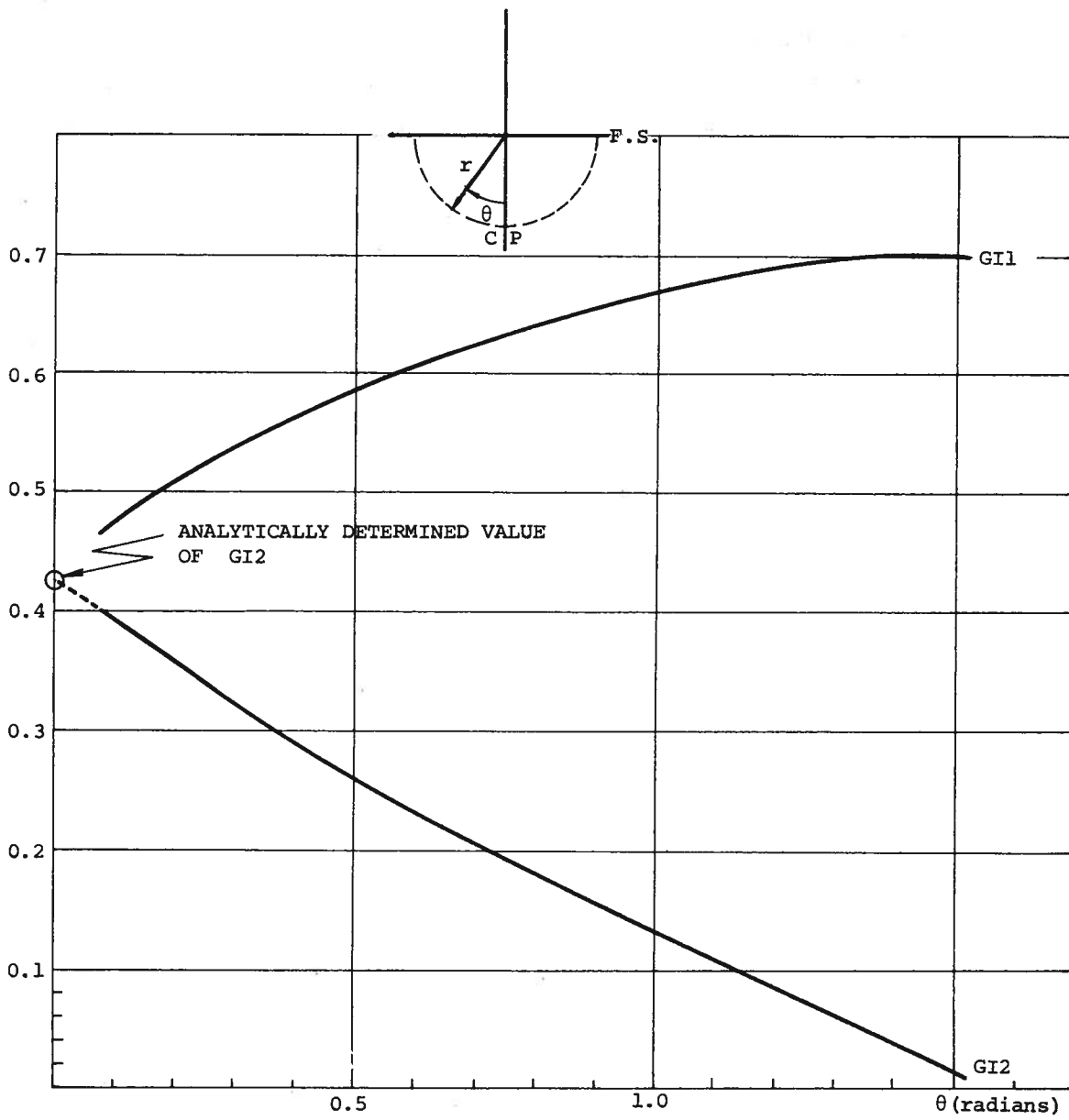


FIGURE 10
INTEGRALS IN THE SOURCE FUNCTION AS A FUNCTION OF θ
FOR $\nu r = 0.3142$

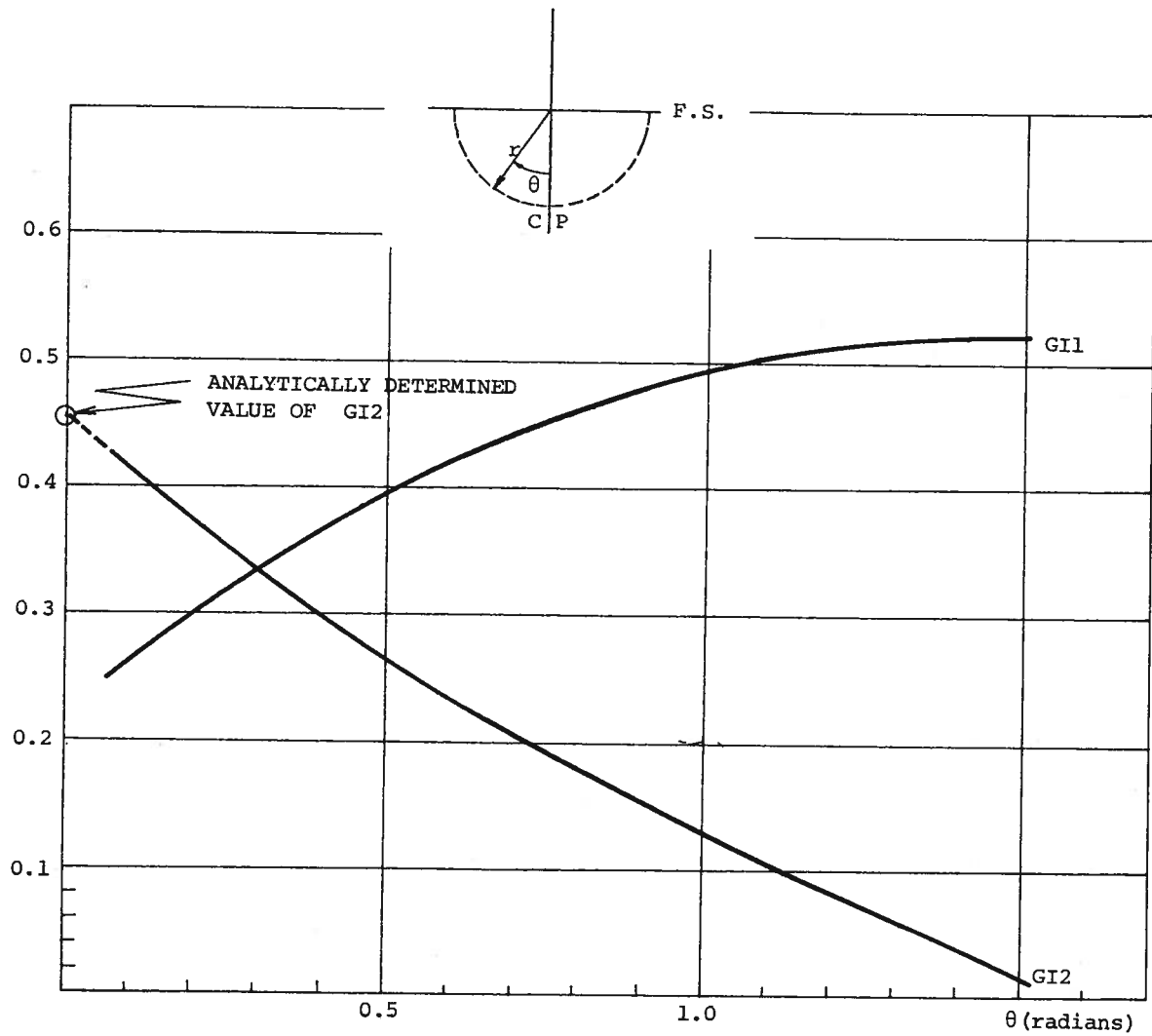


FIGURE 11
INTEGRALS IN THE SOURCE FUNCTION AS A FUNCTION OF θ
FOR $\nu_r = 0.4189$

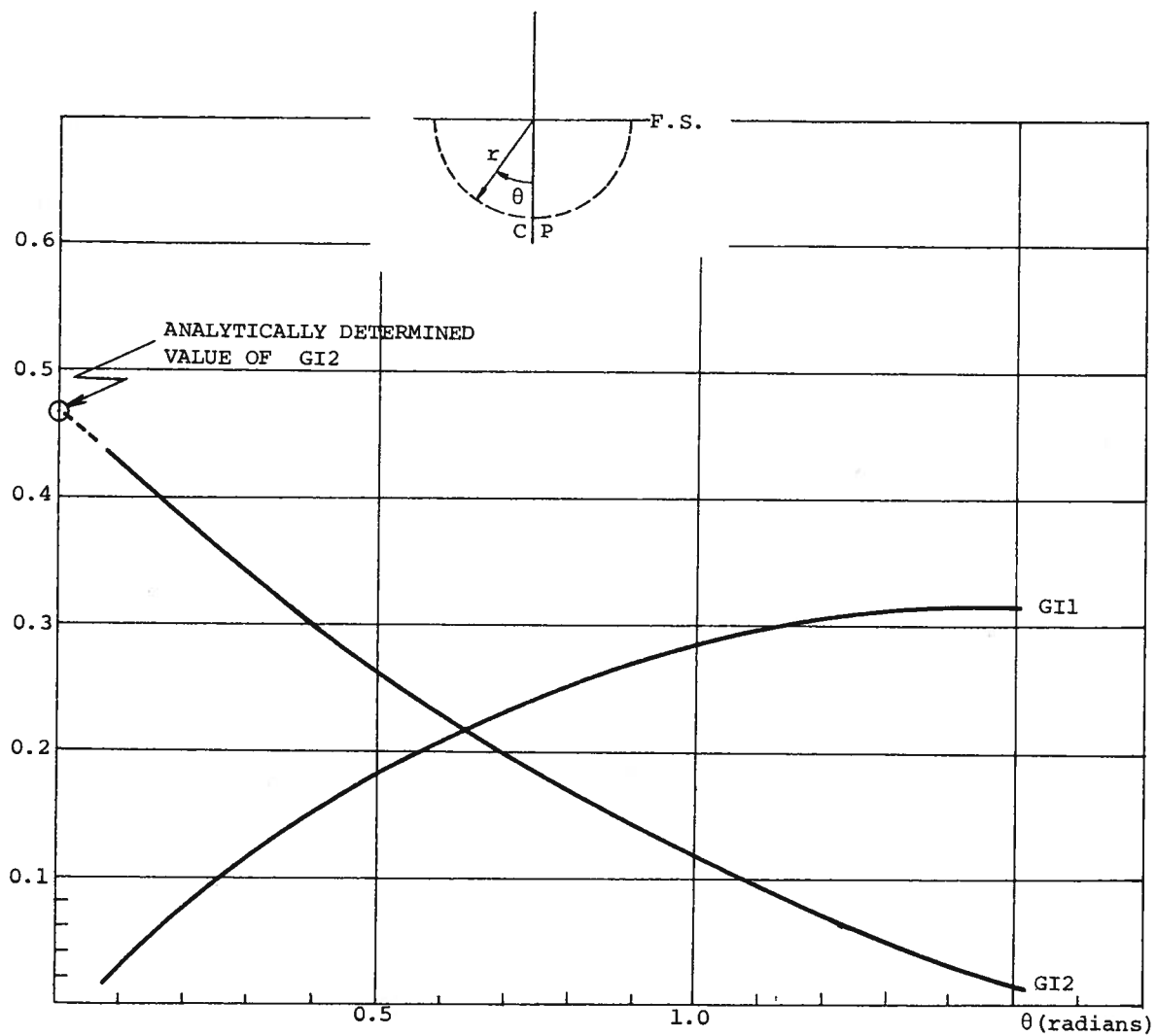


FIGURE 12
INTEGRALS IN THE SOURCE FUNCTION AS A FUNCTION OF θ
FOR $v_r = 0.6283$

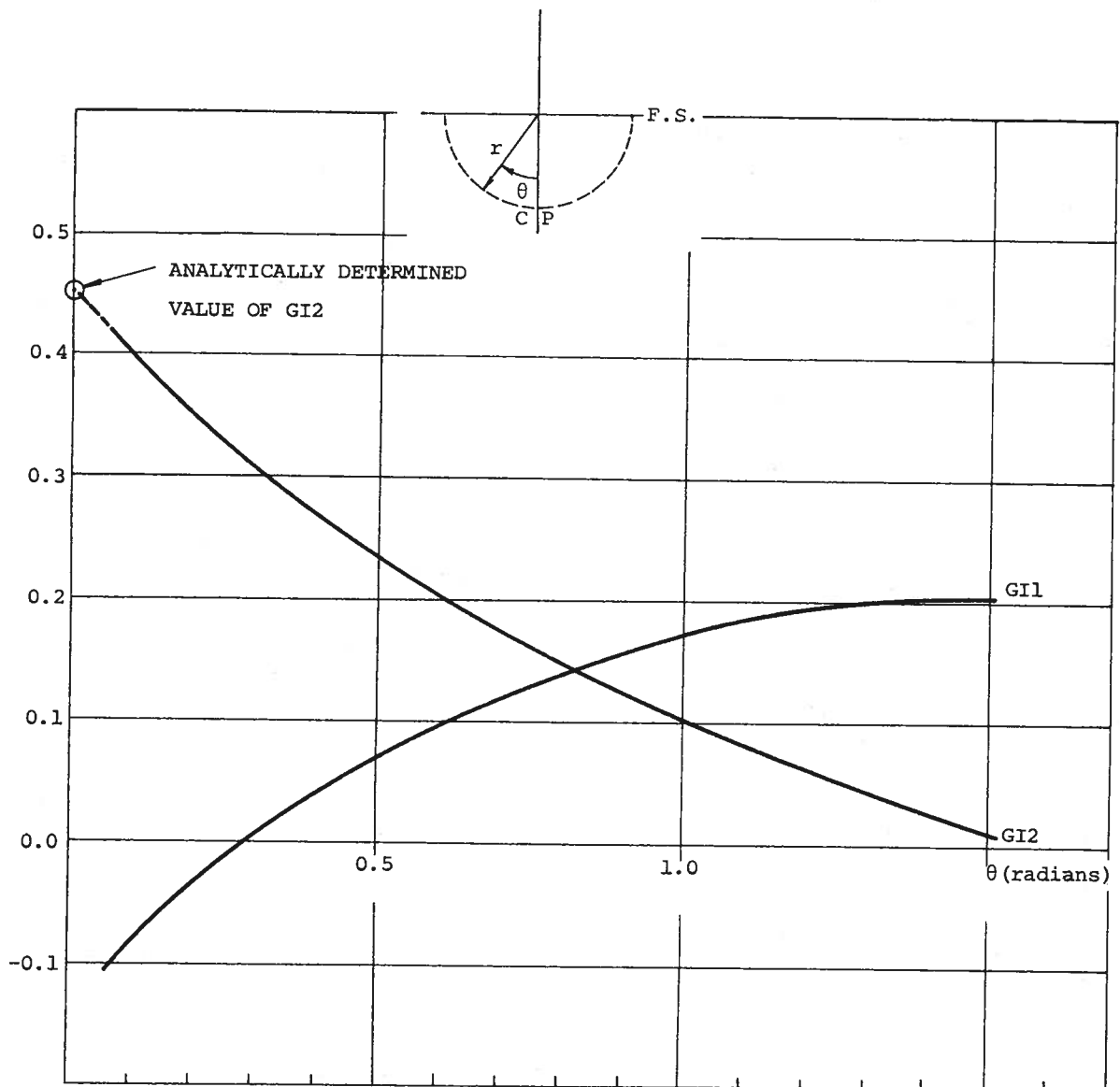


FIGURE 13

INTEGRALS IN THE SOURCE FUNCTION AS A FUNCTION OF θ
FOR $\nu_r = 0.8378$

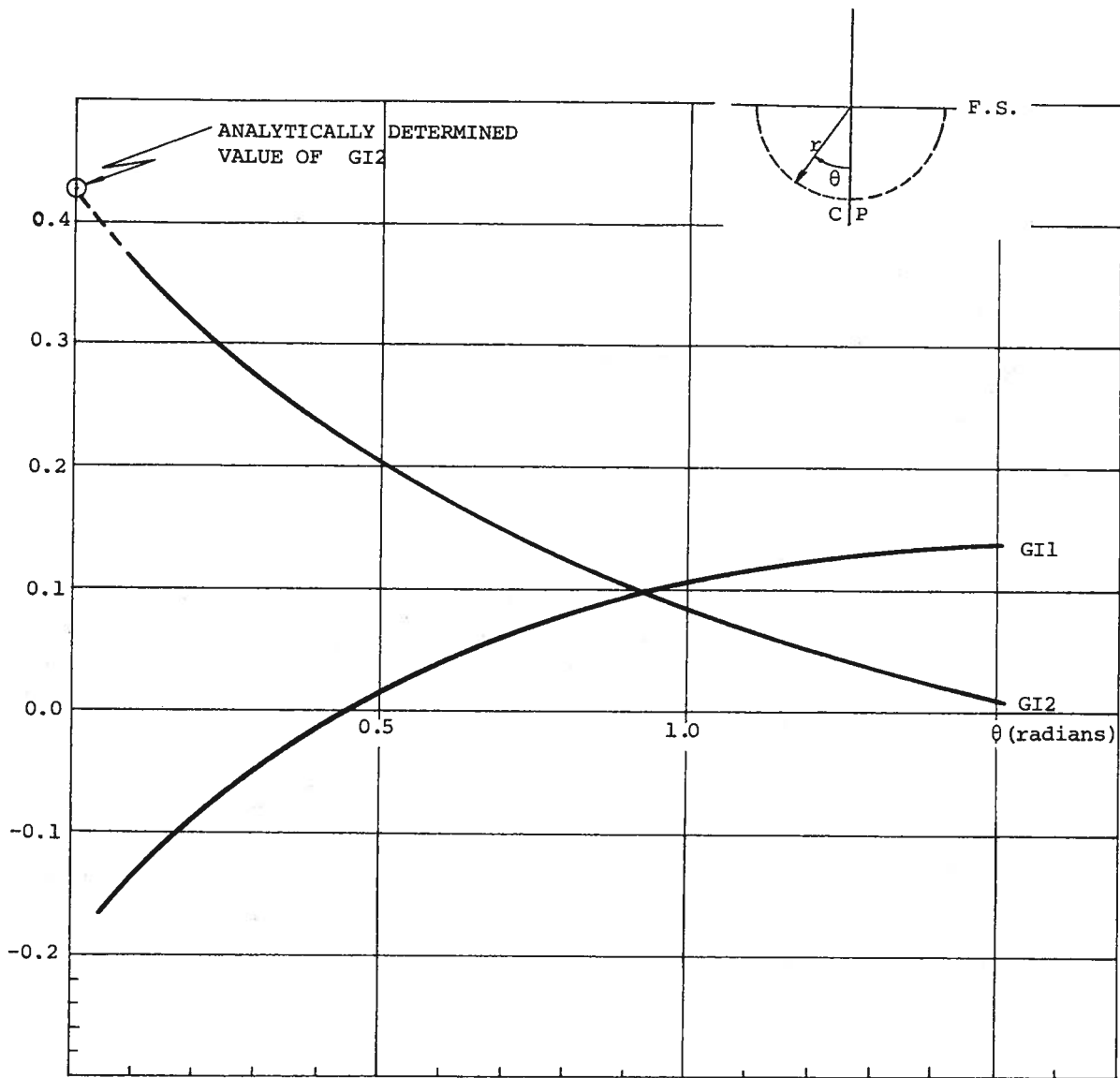


FIGURE 14

INTEGRALS IN THE SOURCE FUNCTION AS A FUNCTION OF θ

FOR $v_r = 1.0472$

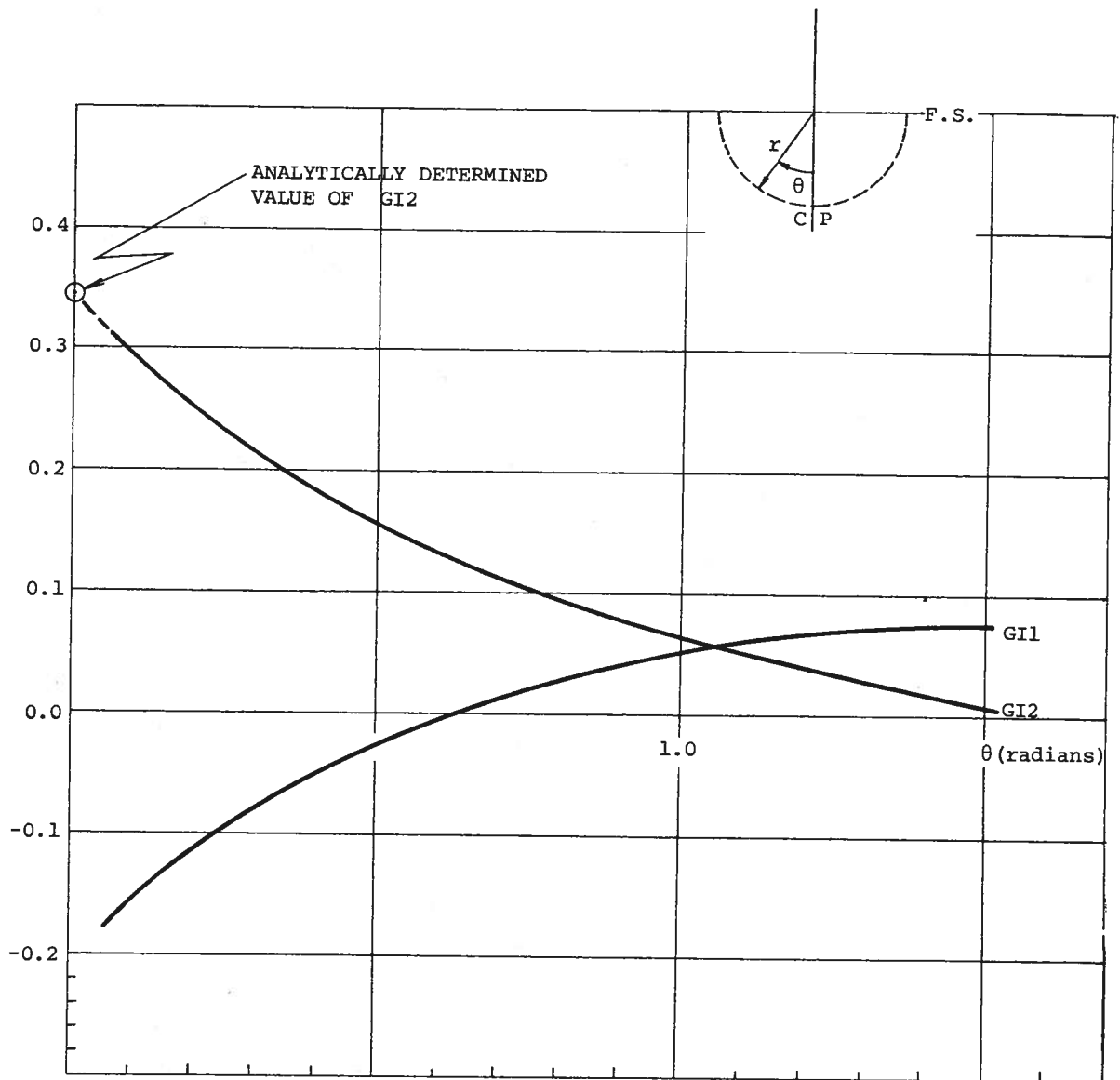


FIGURE 15
INTEGRALS IN THE SOURCE FUNCTION AS A FUNCTION OF θ
FOR $v_r = 1.3963$

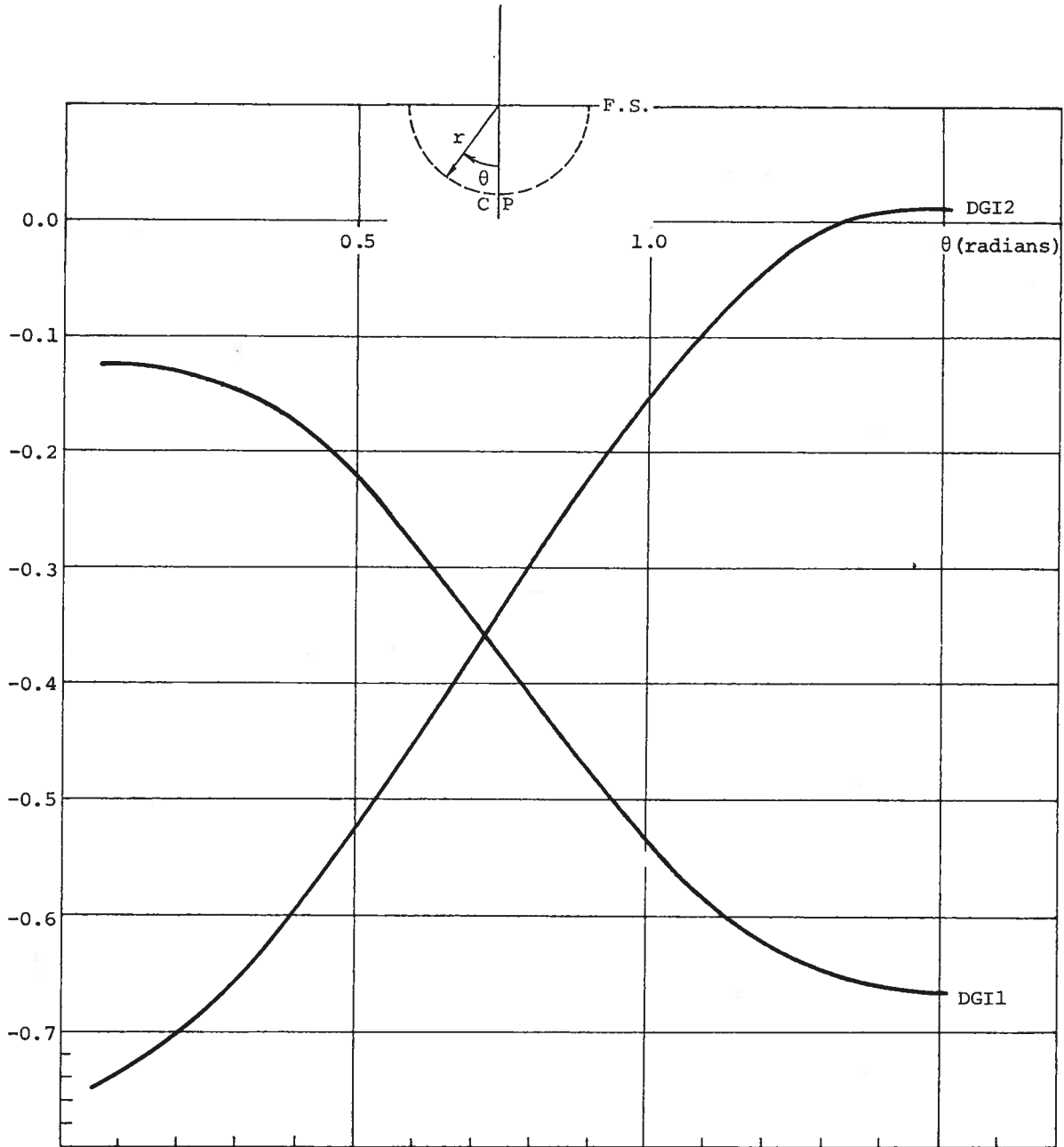


FIGURE 16
INTEGRALS IN THE DERIVATIVE OF THE SOURCE FUNCTION AS
A FUNCTION OF θ FOR $\nu r = 0.3142$

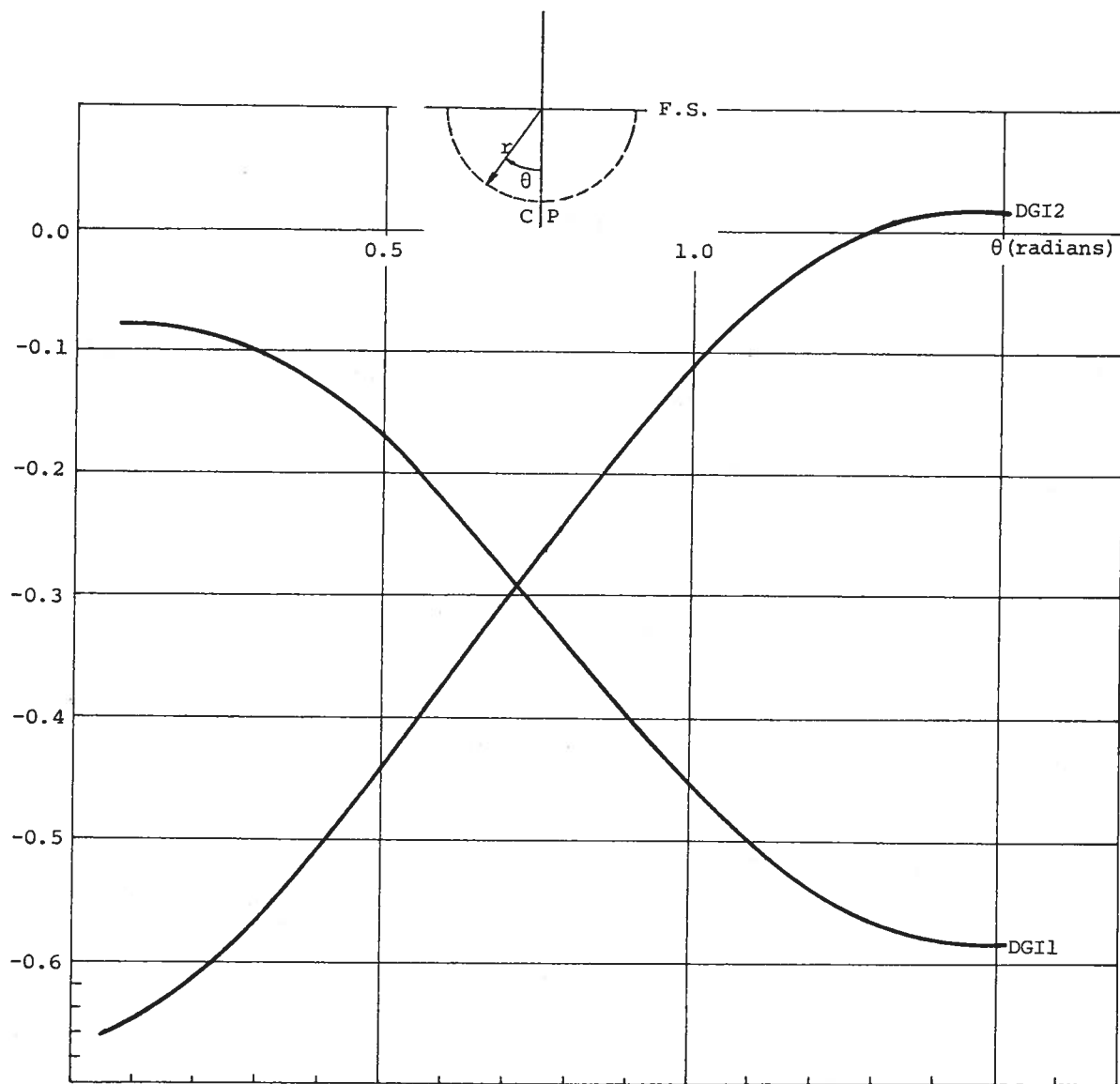


FIGURE 17
INTEGRALS IN THE DERIVATIVE OF THE SOURCE FUNCTION AS
A FUNCTION OF θ FOR $v_r = 0.4189$

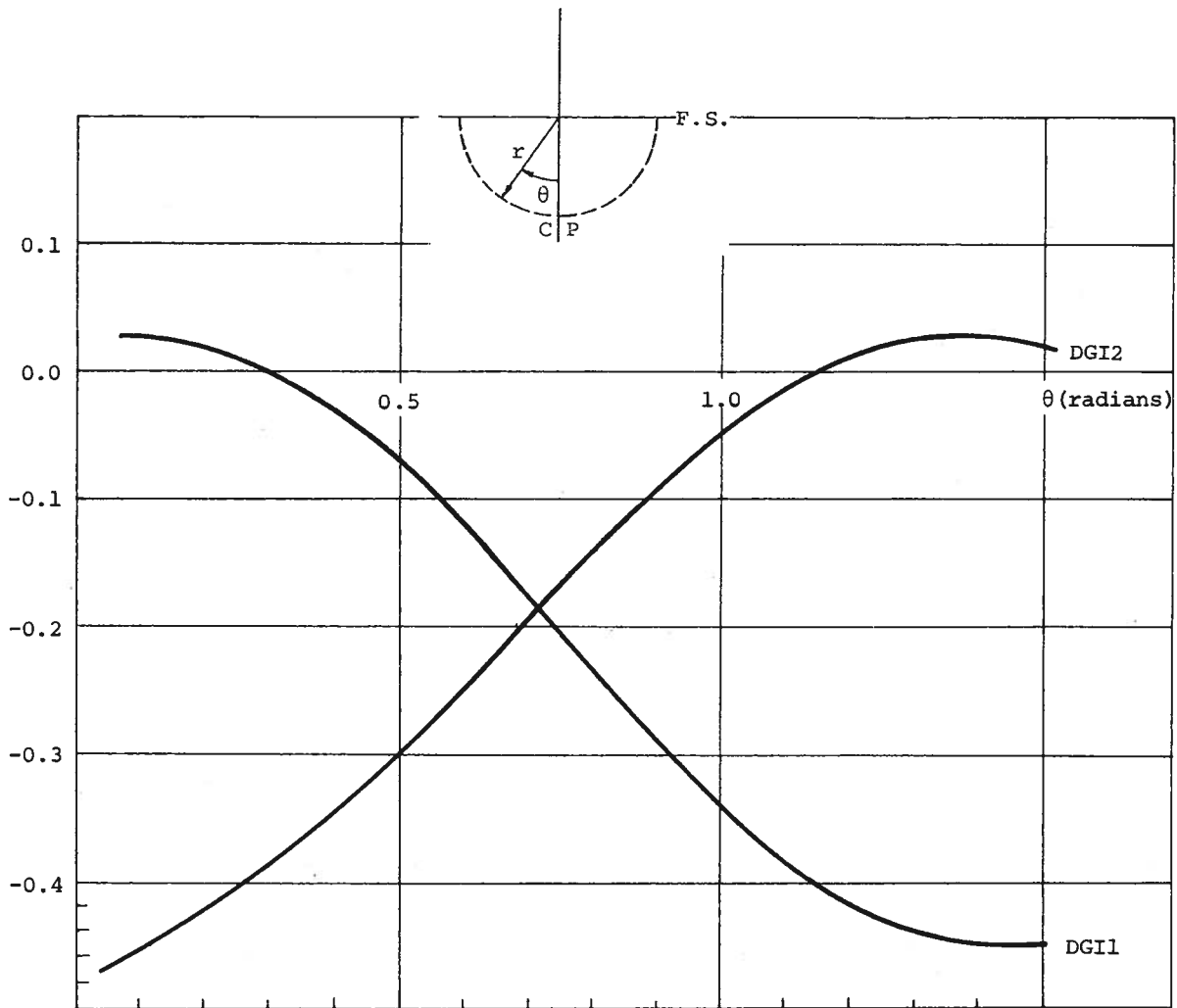


FIGURE 18
INTEGRALS IN THE DERIVATIVE OF THE SOURCE FUNCTION AS
A FUNCTION OF θ FOR $v_r = 0.6283$

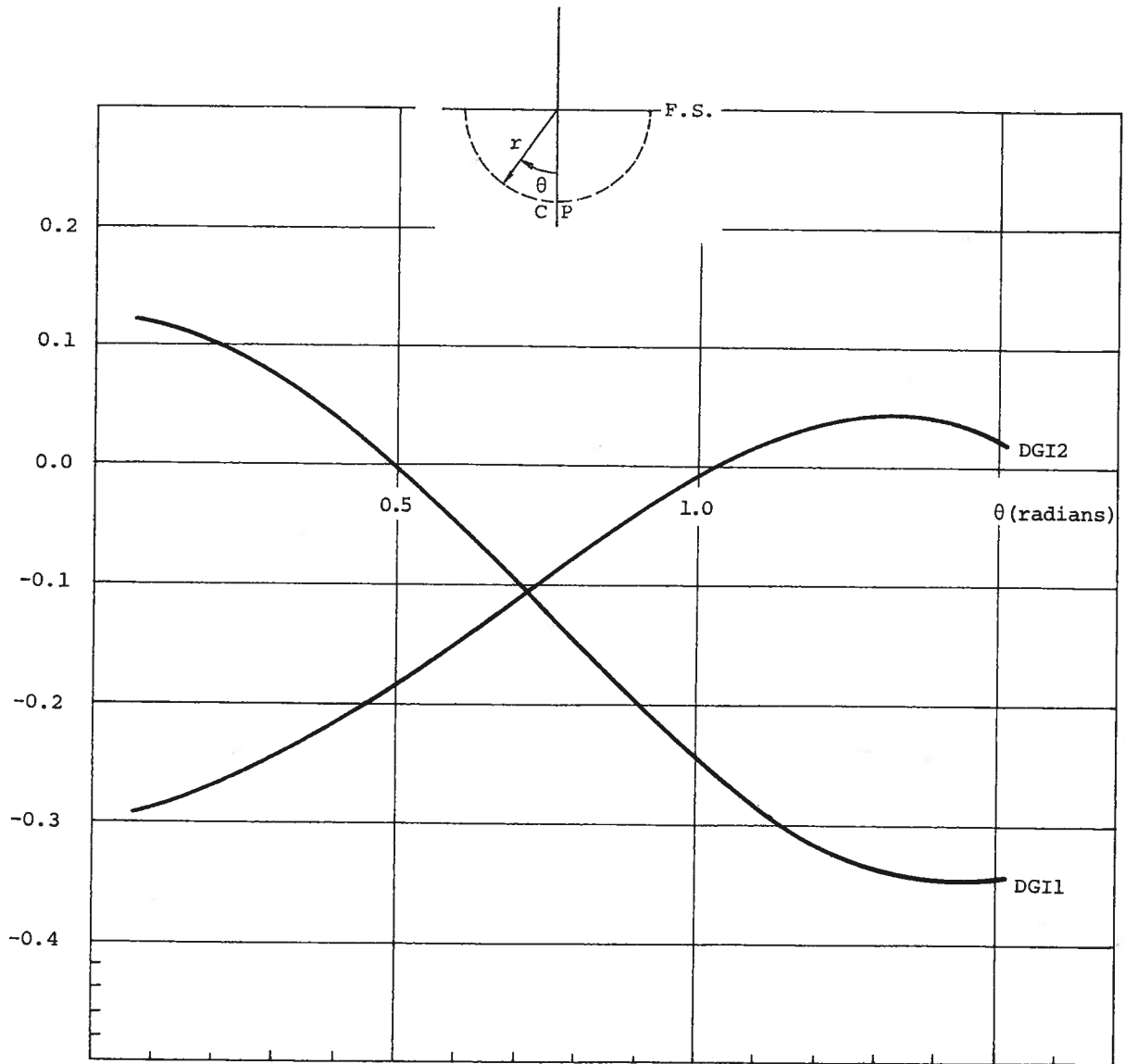


FIGURE 19

INTEGRALS IN THE DERIVATIVE OF THE SOURCE FUNCTION AS
A FUNCTION OF θ FOR $v_r = 0.8378$

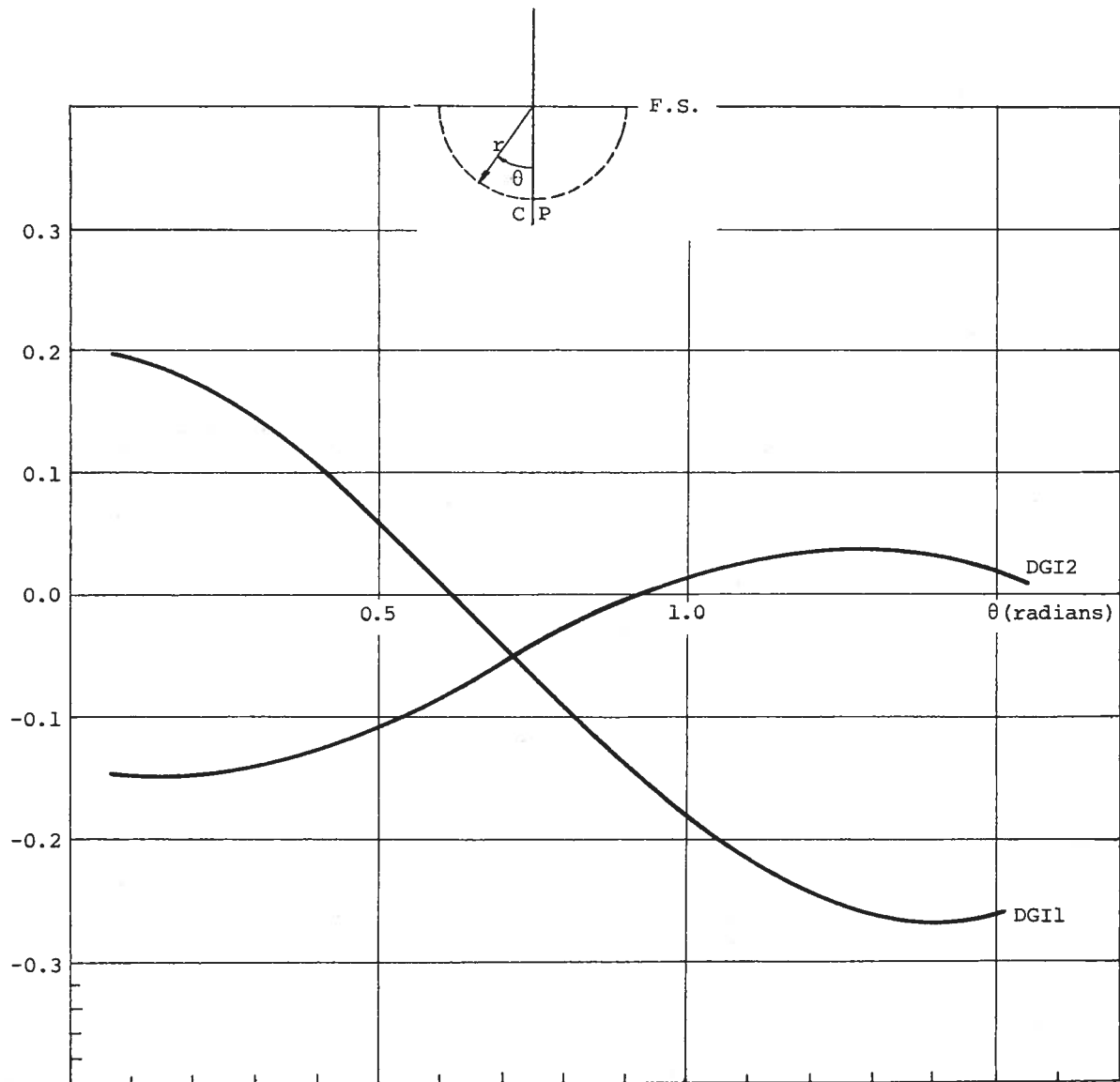


FIGURE 20
INTEGRALS IN THE DERIVATIVE OF THE SOURCE FUNCTION AS
A FUNCTION OF θ FOR $\nu r = 1.0472$

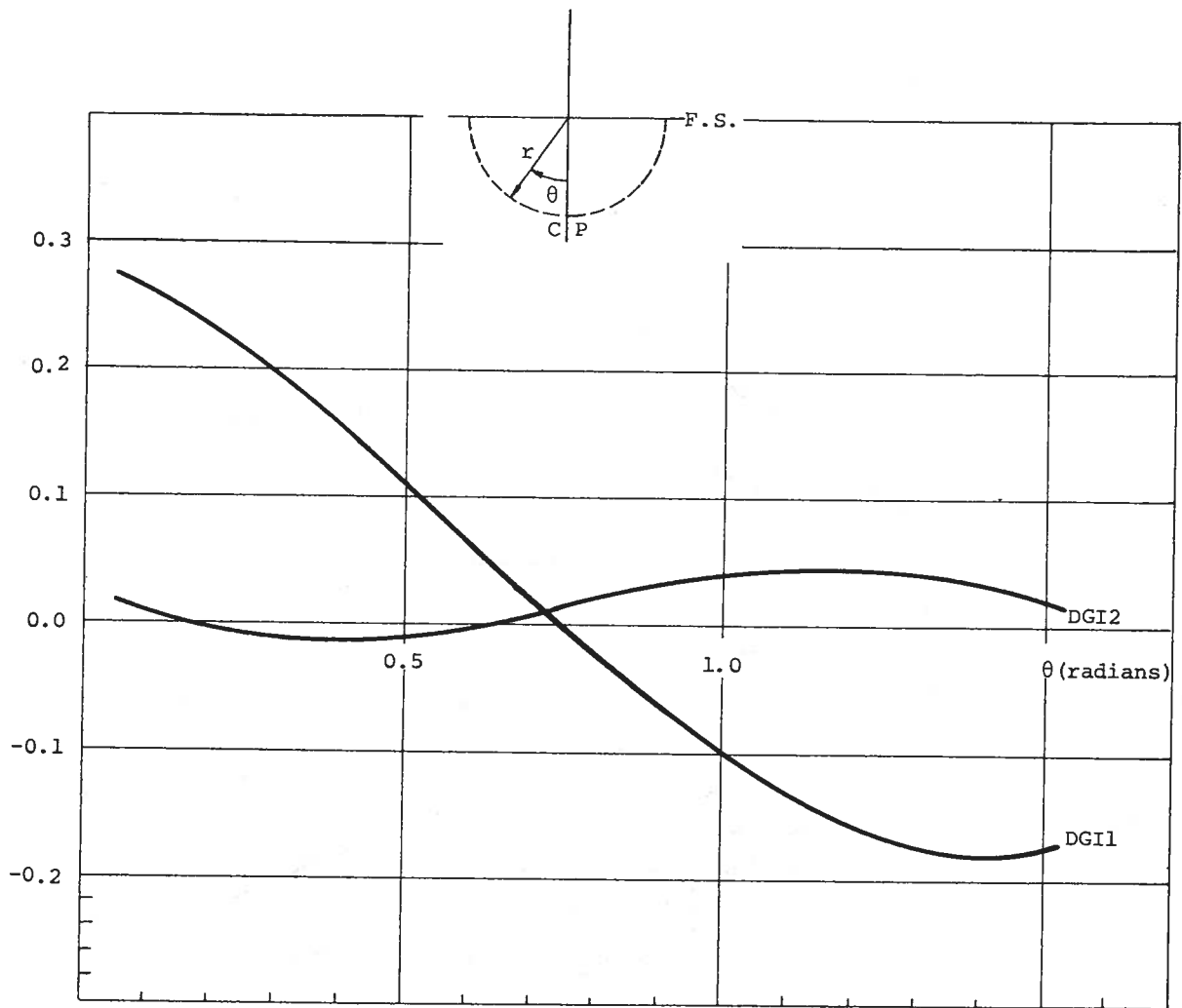


FIGURE 21

INTEGRALS IN THE DERIVATIVE OF THE SOURCE FUNCTION AS
A FUNCTION OF θ FOR $\nu r = 1.3962$

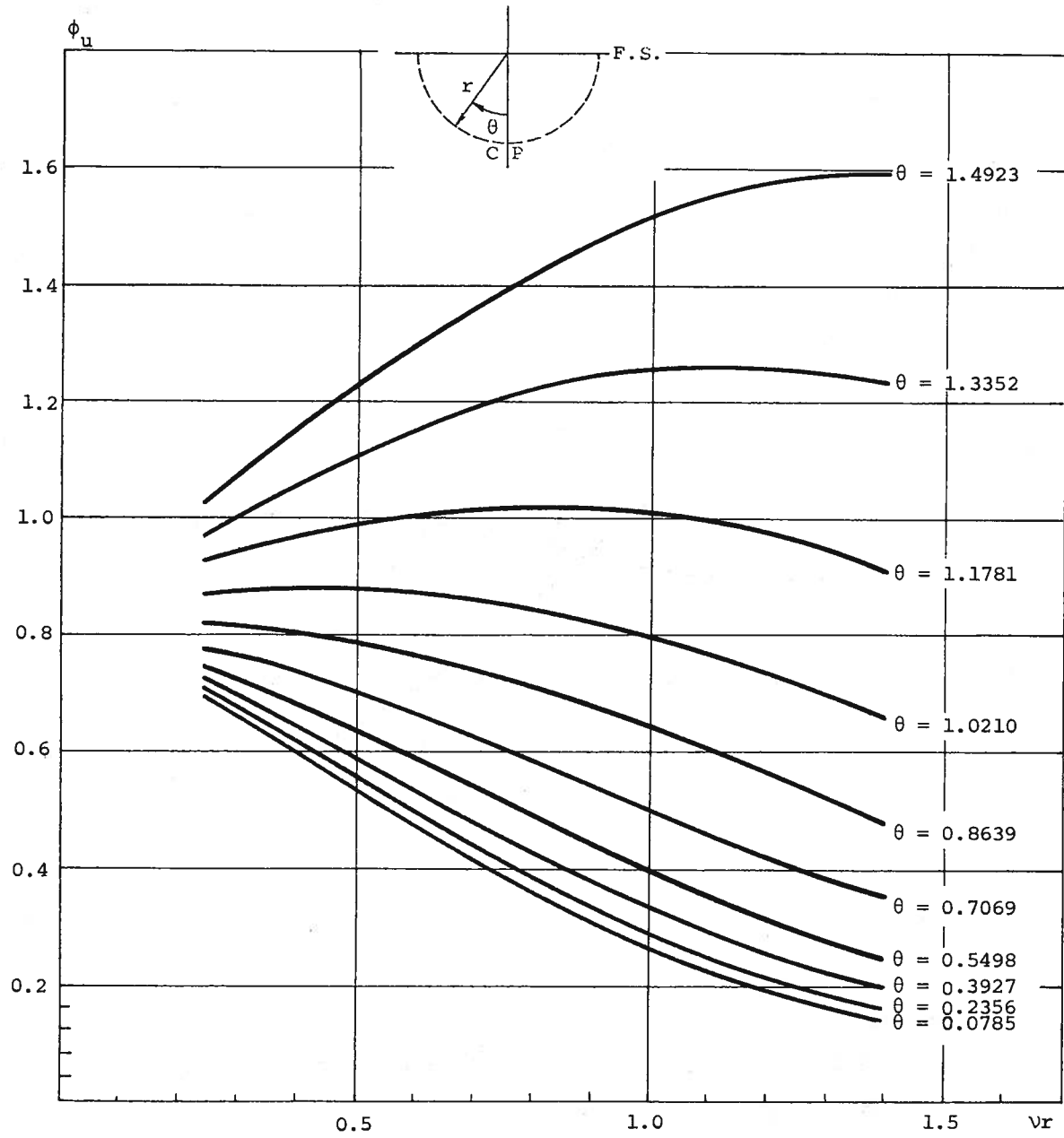


FIGURE 22
URSELL'S SOLUTION AS A FUNCTION OF vr FOR A GIVEN
VALUE OF θ

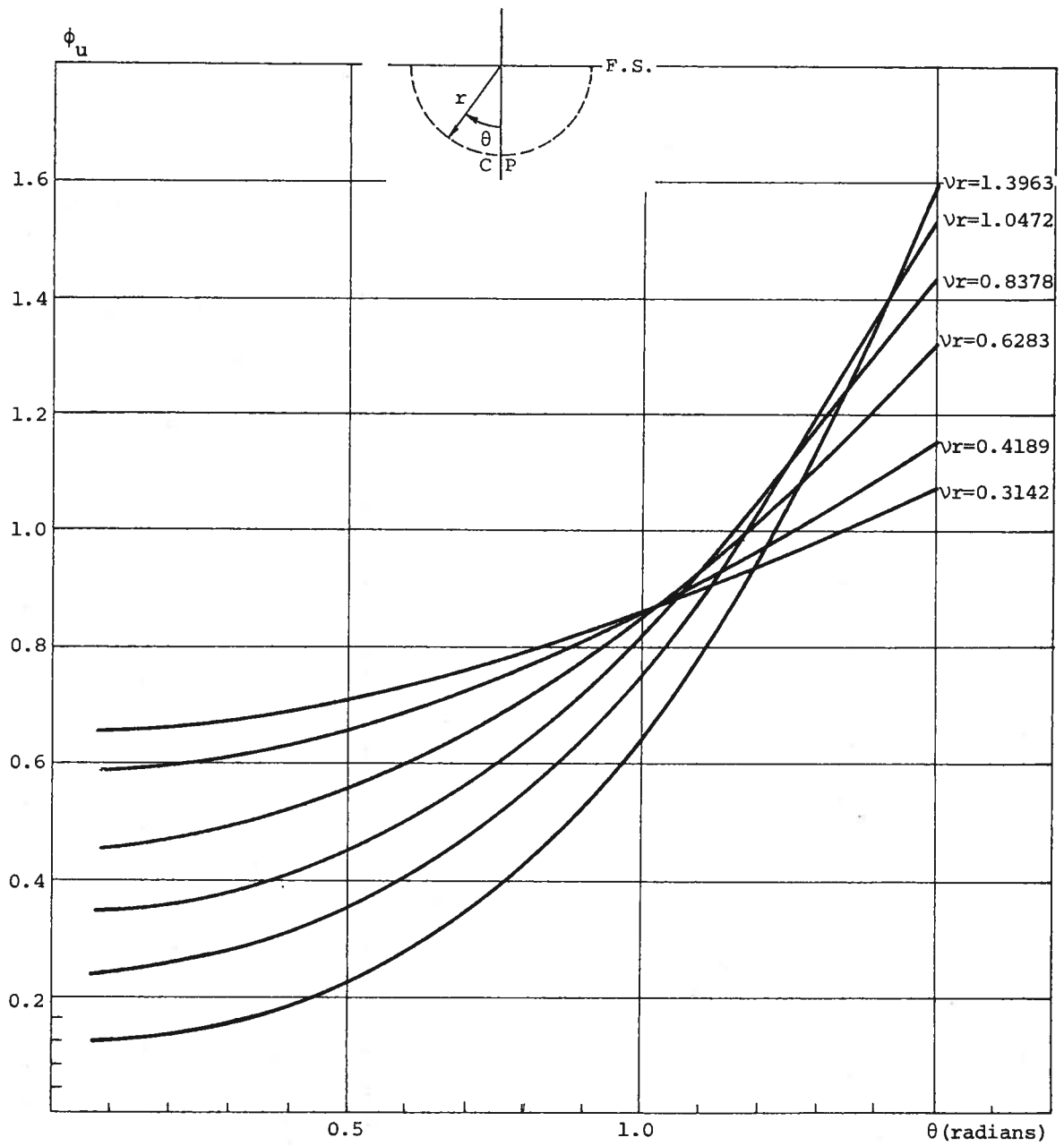


FIGURE 23
URSELL'S SOLUTION AS A FUNCTION OF θ FOR GIVEN
VALUE OF ν_r

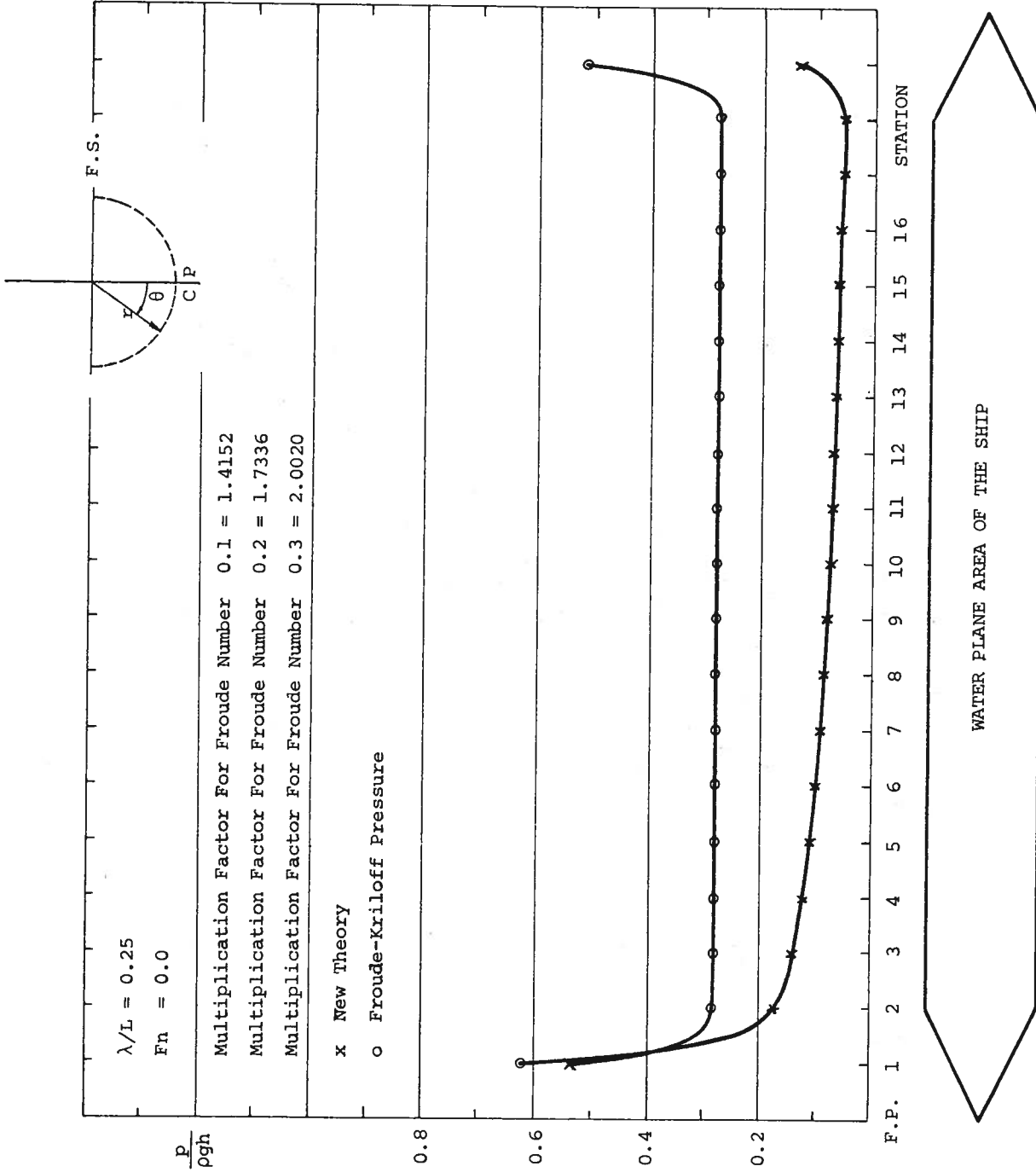


FIGURE 25 LONGITUDINAL DISTRIBUTION OF THE PRESSURE FOR $\theta = 0.0785$

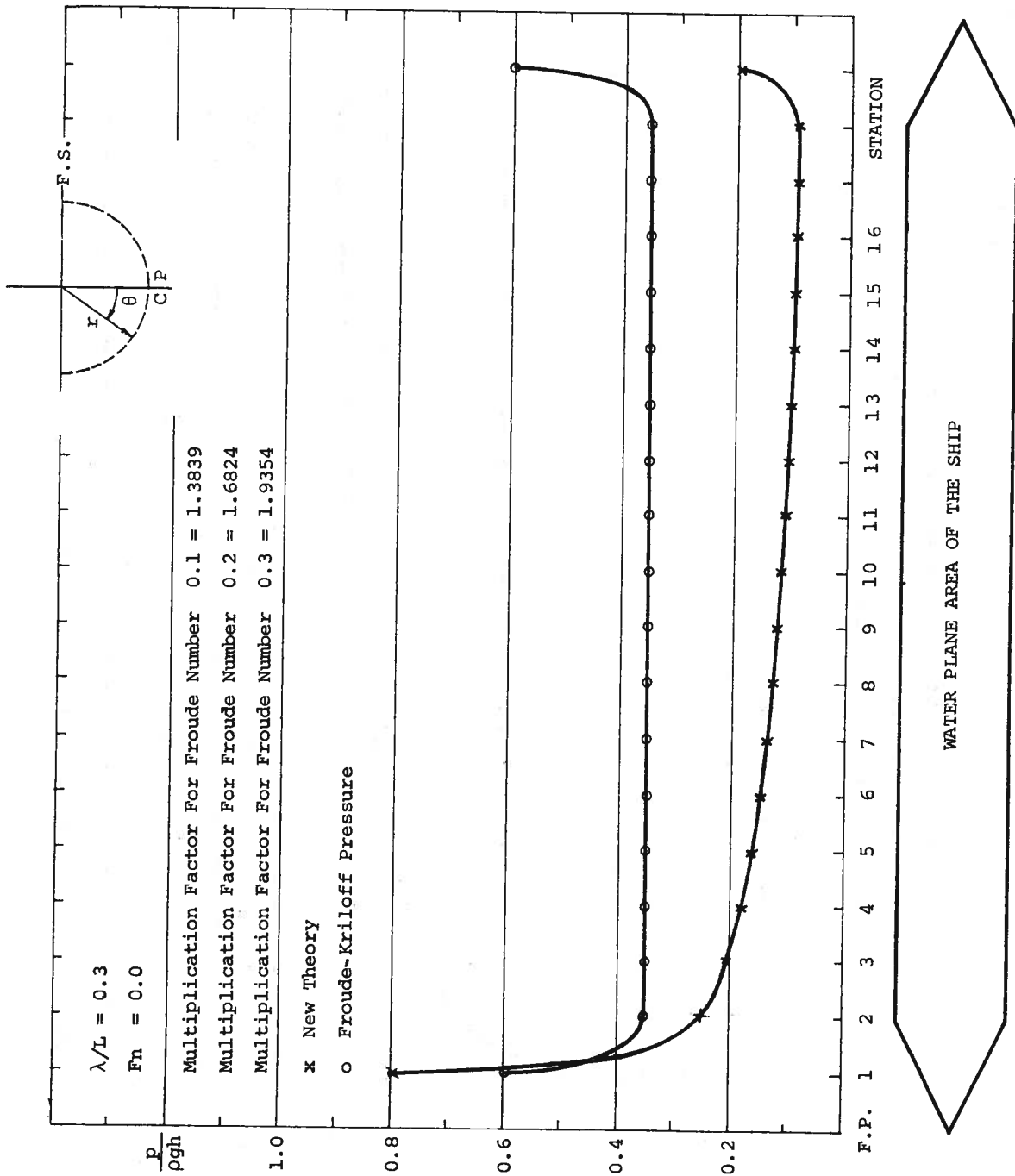


FIGURE 26 LONGITUDINAL DISTRIBUTION OF THE PRESSURE FOR $\theta = 0.0785$

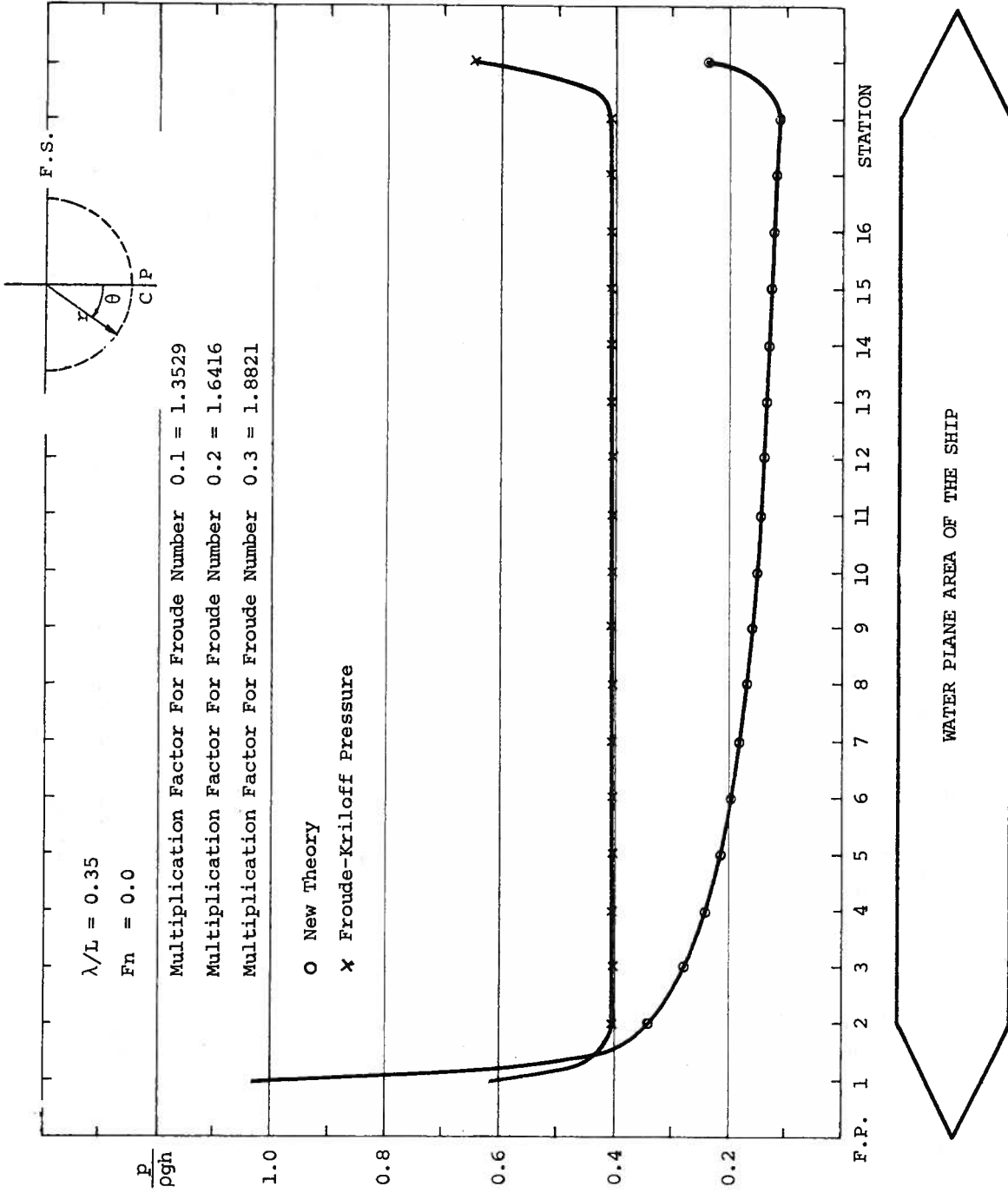


FIGURE 27 LONGITUDINAL DISTRIBUTION OF THE PRESSURE FOR $\theta = 0.0785$

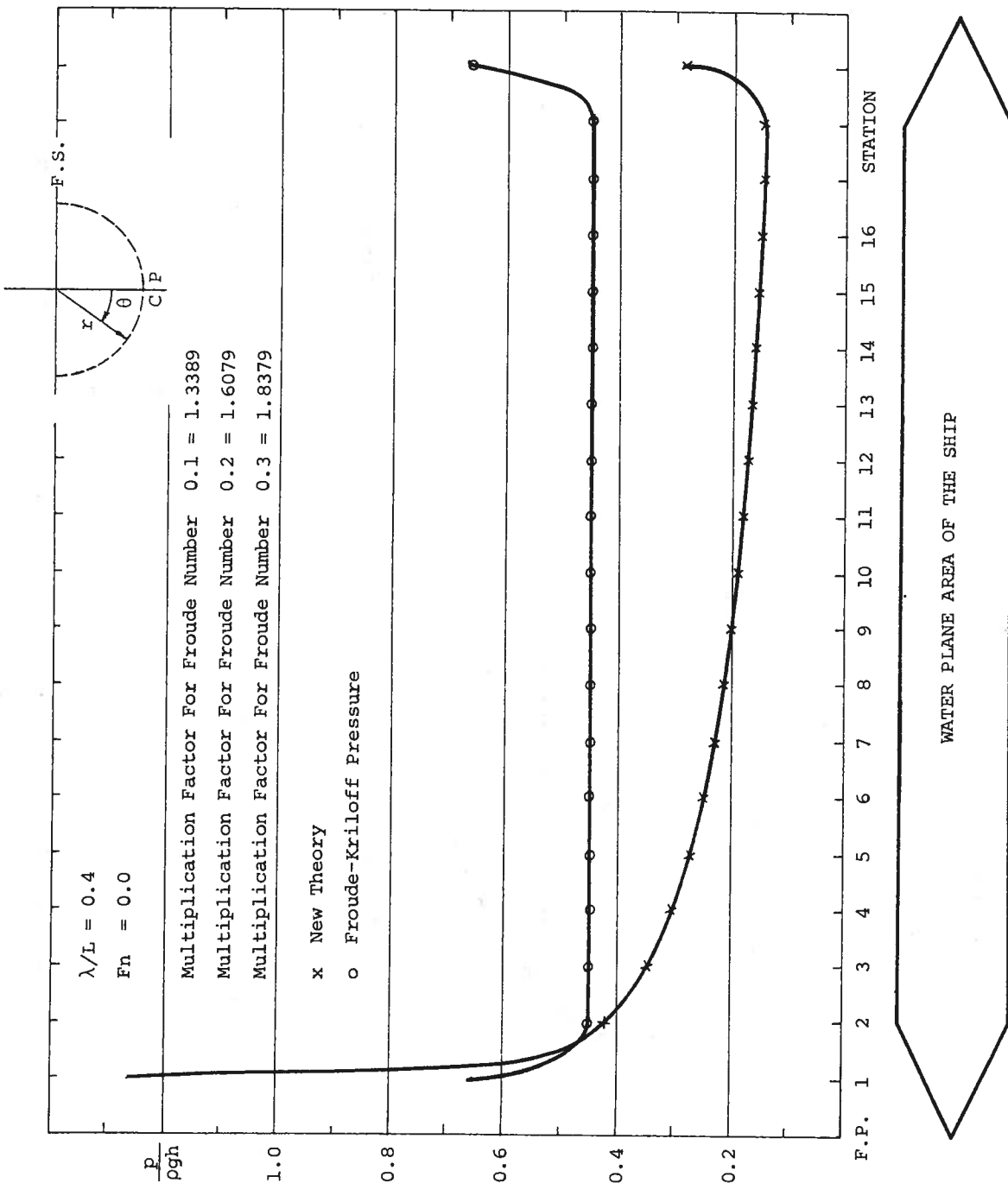


FIGURE 28 LONGITUDINAL DISTRIBUTION OF THE PRESSURE FOR $\theta = 0.0785$

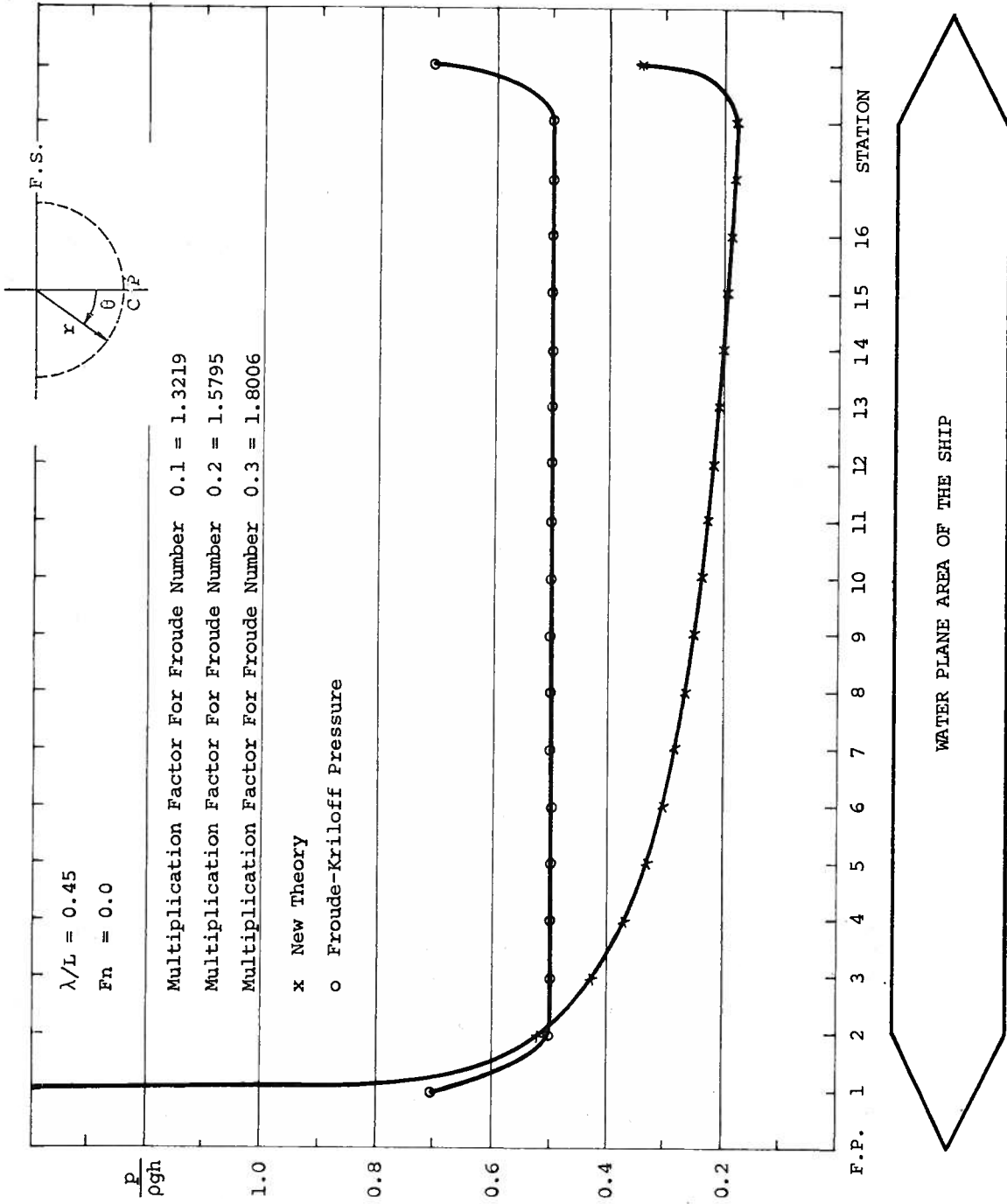


FIGURE 29 LONGITUDINAL DISTRIBUTION OF THE PRESSURE FOR $\theta = 0.0785$

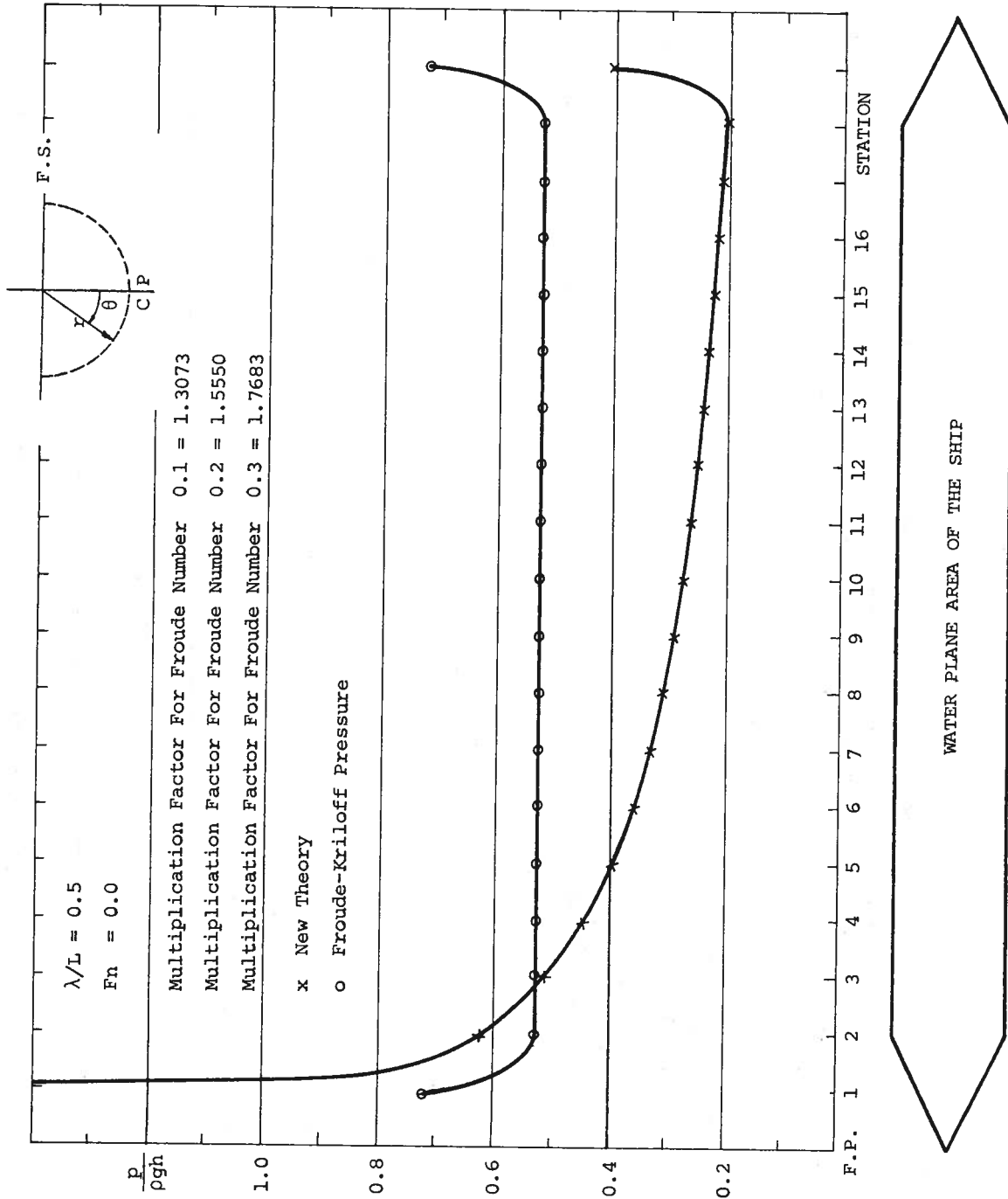


FIGURE 30 LONGITUDINAL DISTRIBUTION OF THE PRESSURE FOR $\theta = 0.0785$

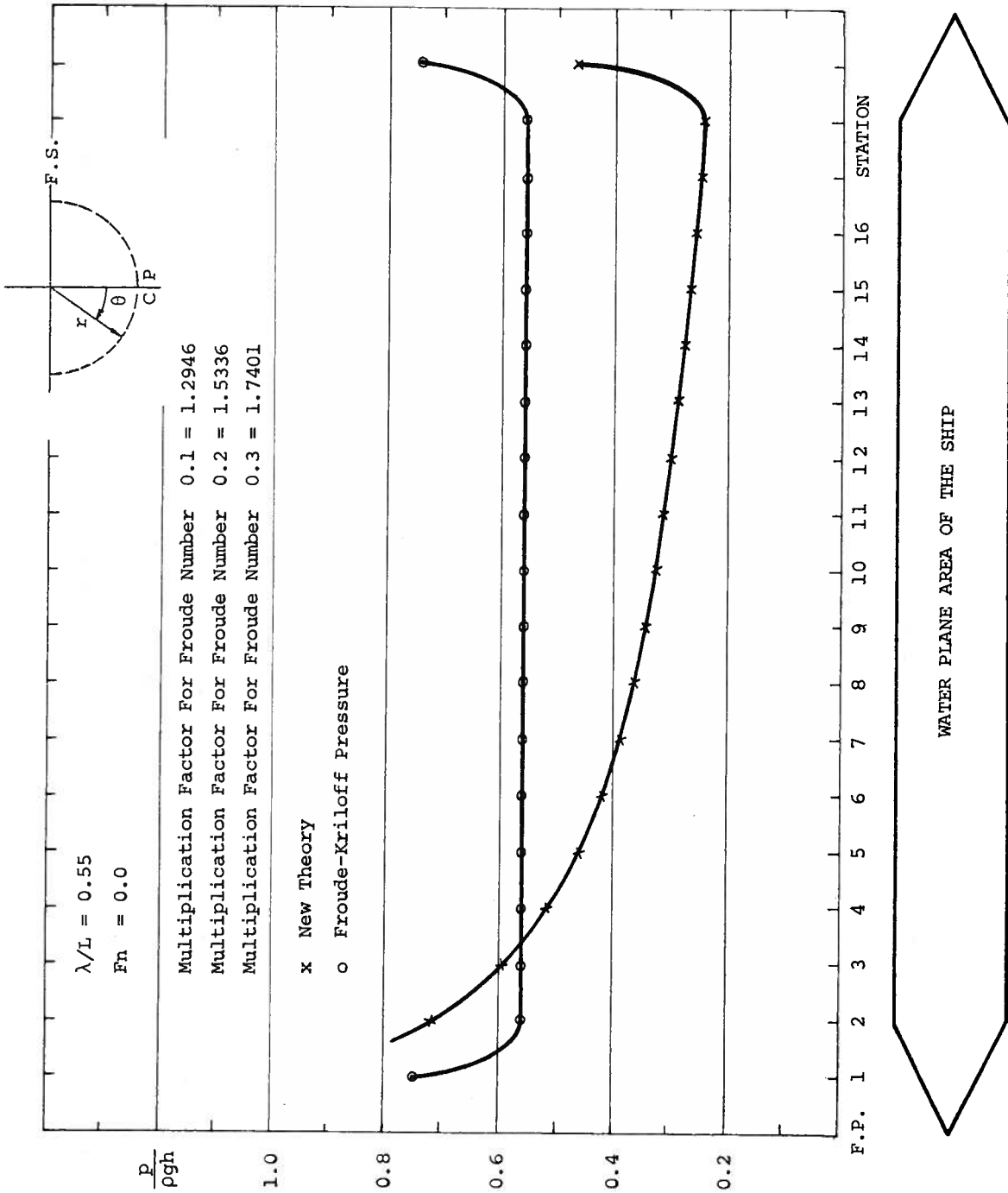


FIGURE 31 LONGITUDINAL DISTRIBUTION OF THE PRESSURE FOR $\theta = 0.0785$

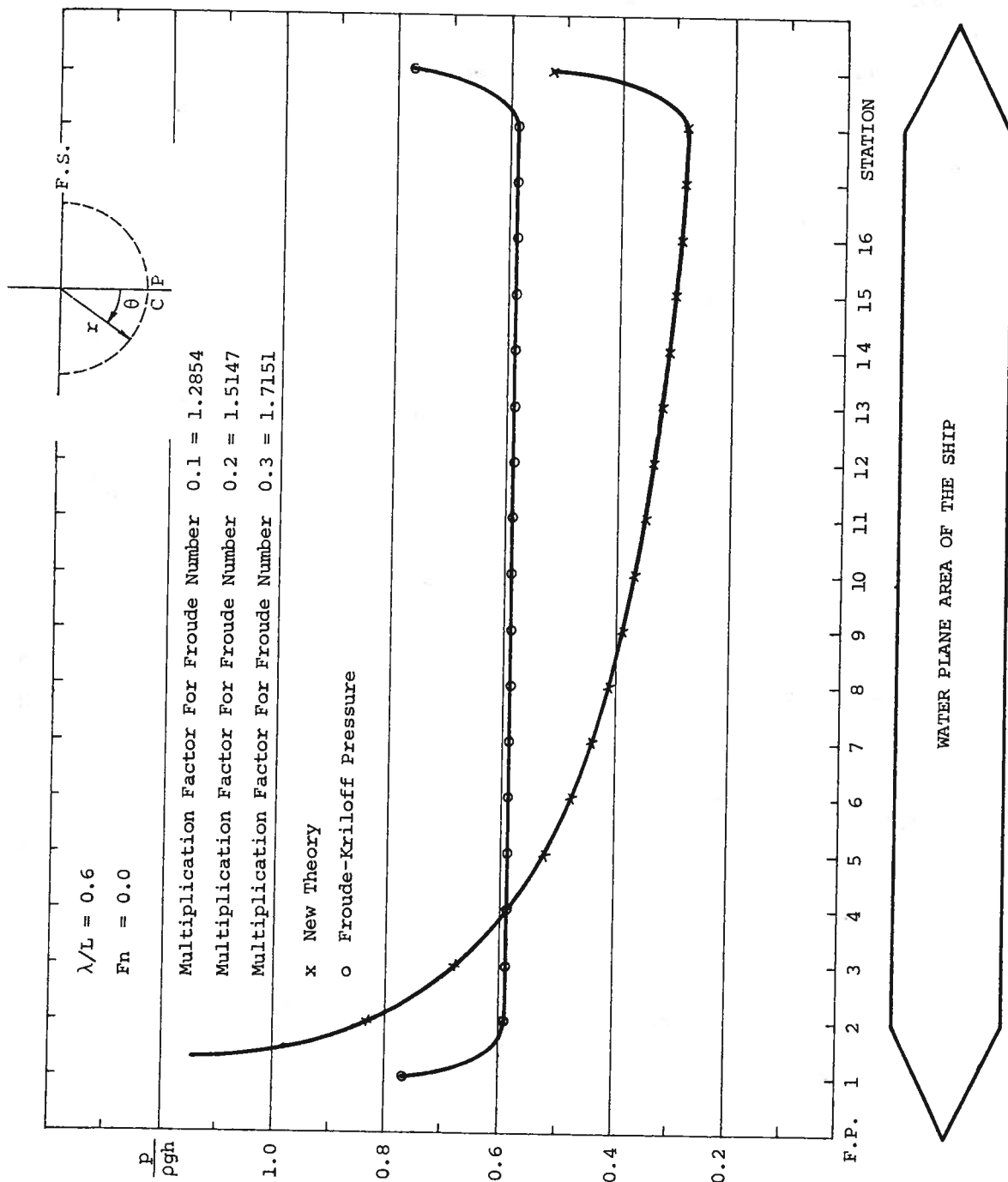


FIGURE 32 LONGITUDINAL DISTRIBUTION OF THE PRESSURE FOR $\theta = 0.0785$

$\lambda/L = 0.25$

$Fn = 0.0$

Multiplication Factor For Froude Number 0.1 = 1.4152

Multiplication Factor For Froude Number 0.2 = 1.7336

Multiplication Factor For Froude Number 0.3 = 2.0020

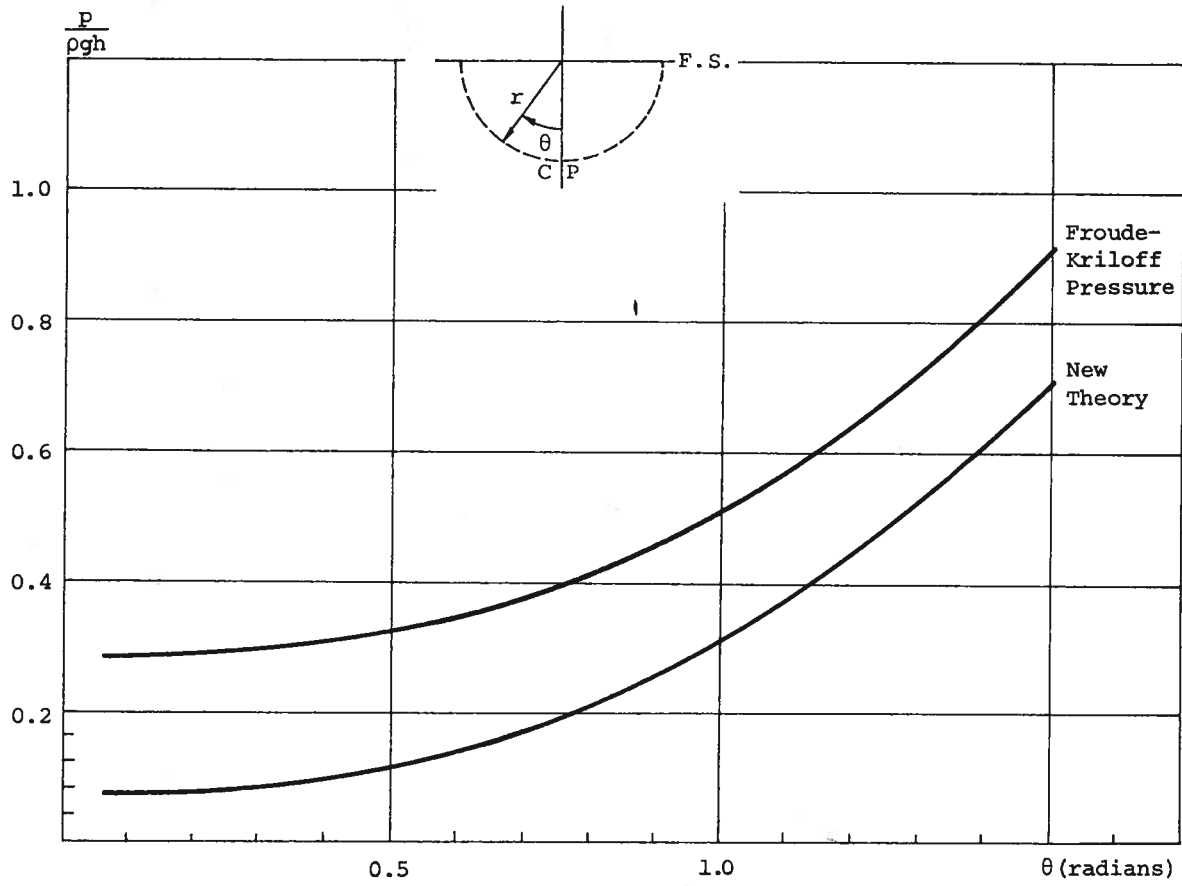


FIGURE 33

PRESSURE DISTRIBUTION AT STATION 10

$\lambda/L = 0.3$

$Fn = 0.0$

Multiplication Factor For Froude Number 0.1 = 1.3839

Multiplication Factor For Froude Number 0.2 = 1.6824

Multiplication Factor For Froude Number 0.3 = 1.9354

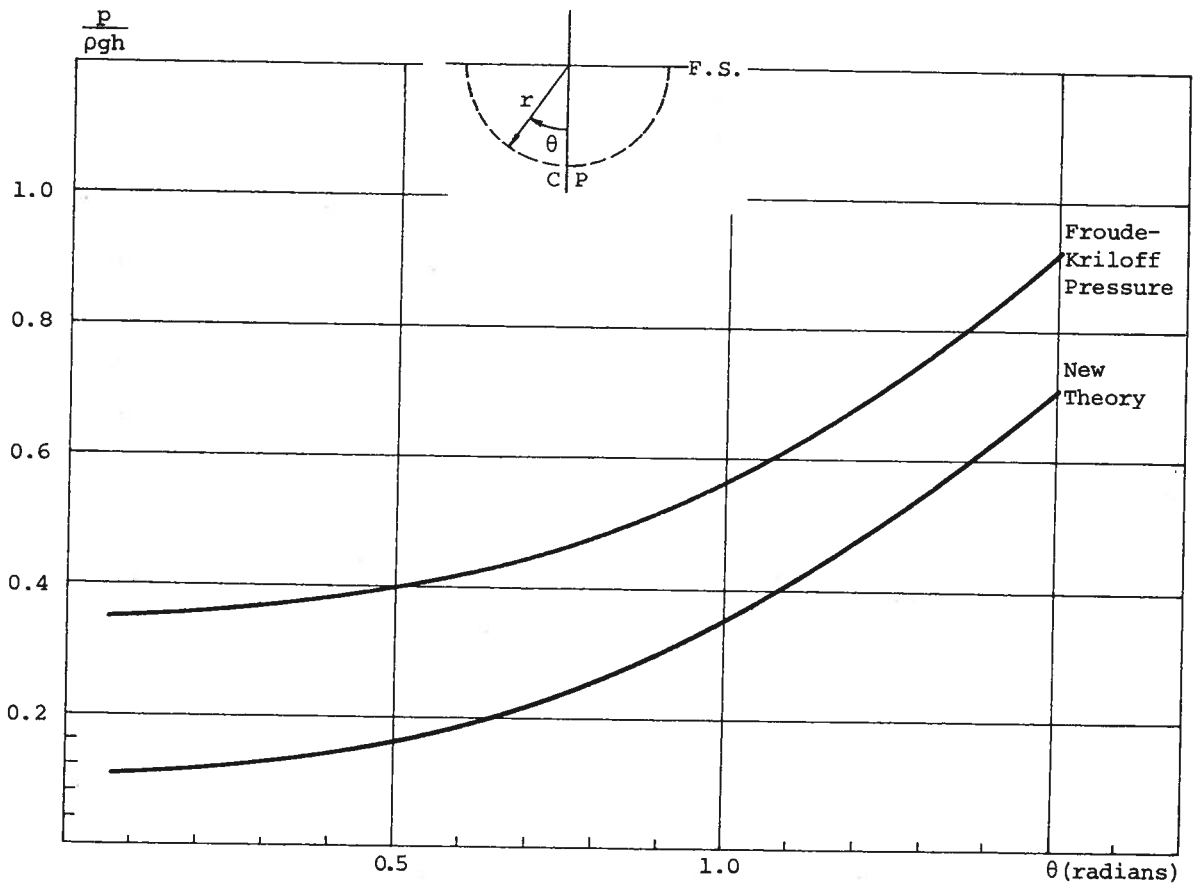


FIGURE 34

PRESSURE DISTRIBUTION AT STATION 10

$\lambda/L = 0.35$

$Fn = 0.0$

Multiplication Factor For Froude Number 0.1 = 1.3592

Multiplication Factor For Froude Number 0.2 = 1.6416

Multiplication Factor For Froude Number 0.3 = 1.8821

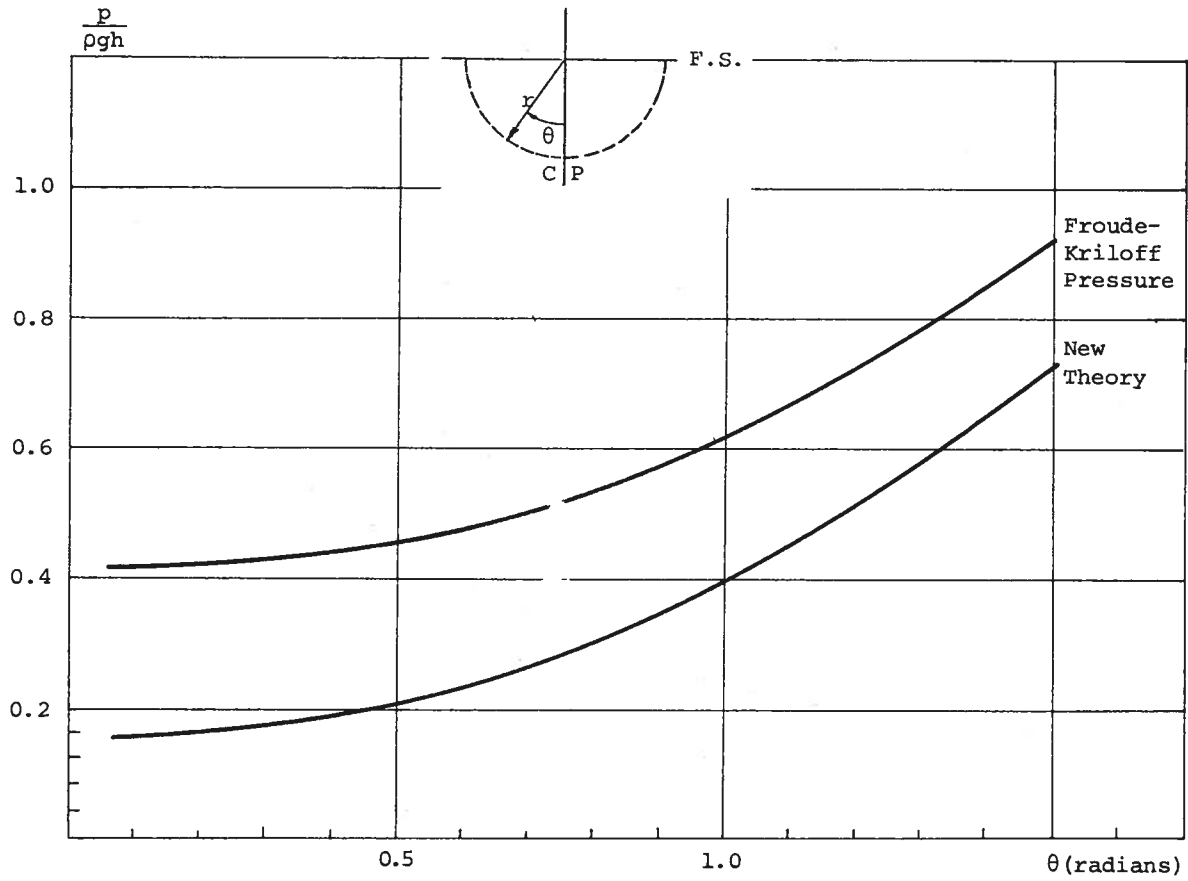


FIGURE 35
PRESSURE DISTRIBUTION AT STATION 10

$\lambda/L = 0.4$

$Fn = 0.0$

Multiplication Factor For Froude Number 0.1 = 1.3389

Multiplication Factor For Froude Number 0.2 = 1.6079

Multiplication Factor For Froude Number 0.3 = 1.8379

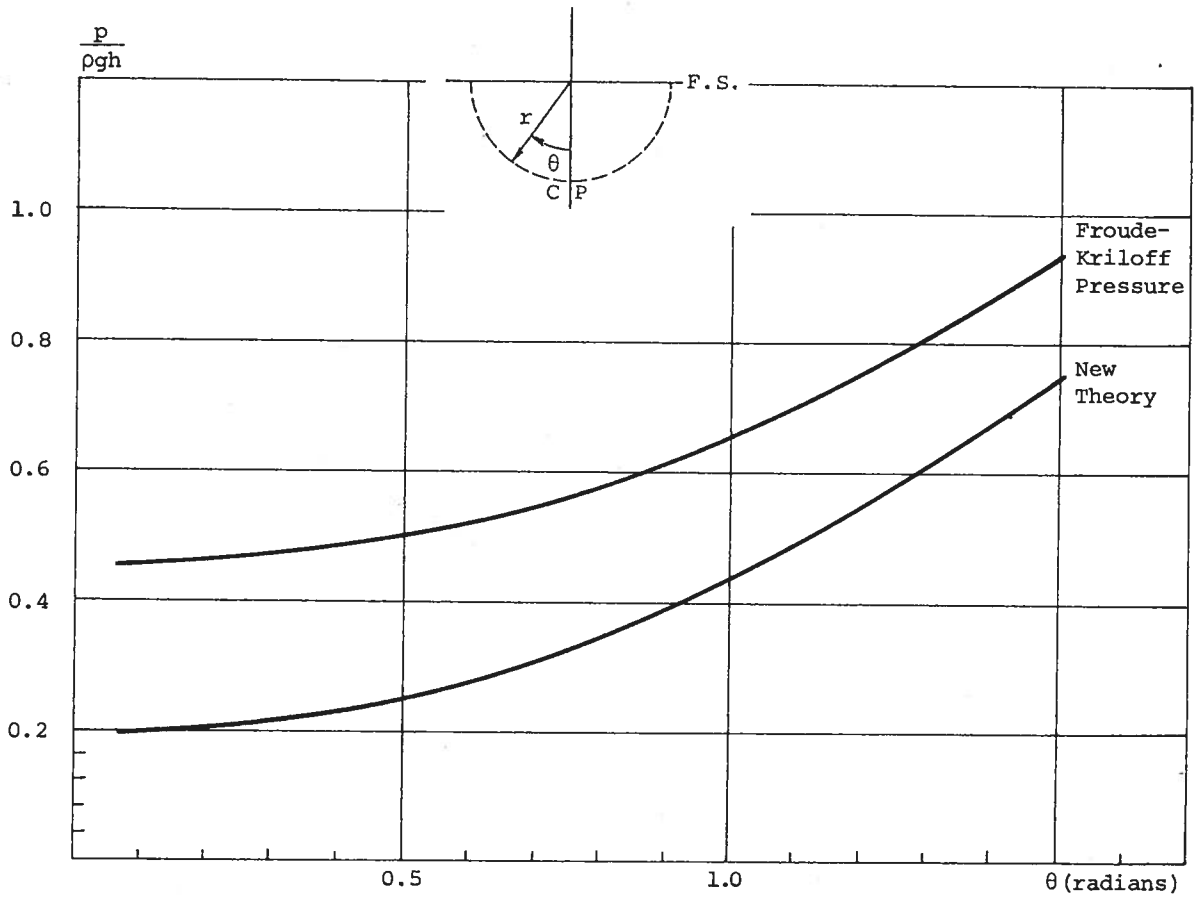


FIGURE 36

PRESSURE DISTRIBUTION AT STATION 10

$\lambda/L = 0.45$

$Fn = 0.0$

Multiplication Factor For Froude Number 0.1 = 1.3219

Multiplication Factor For Froude Number 0.2 = 1.5795

Multiplication Factor For Froude Number 0.3 = 1.8006

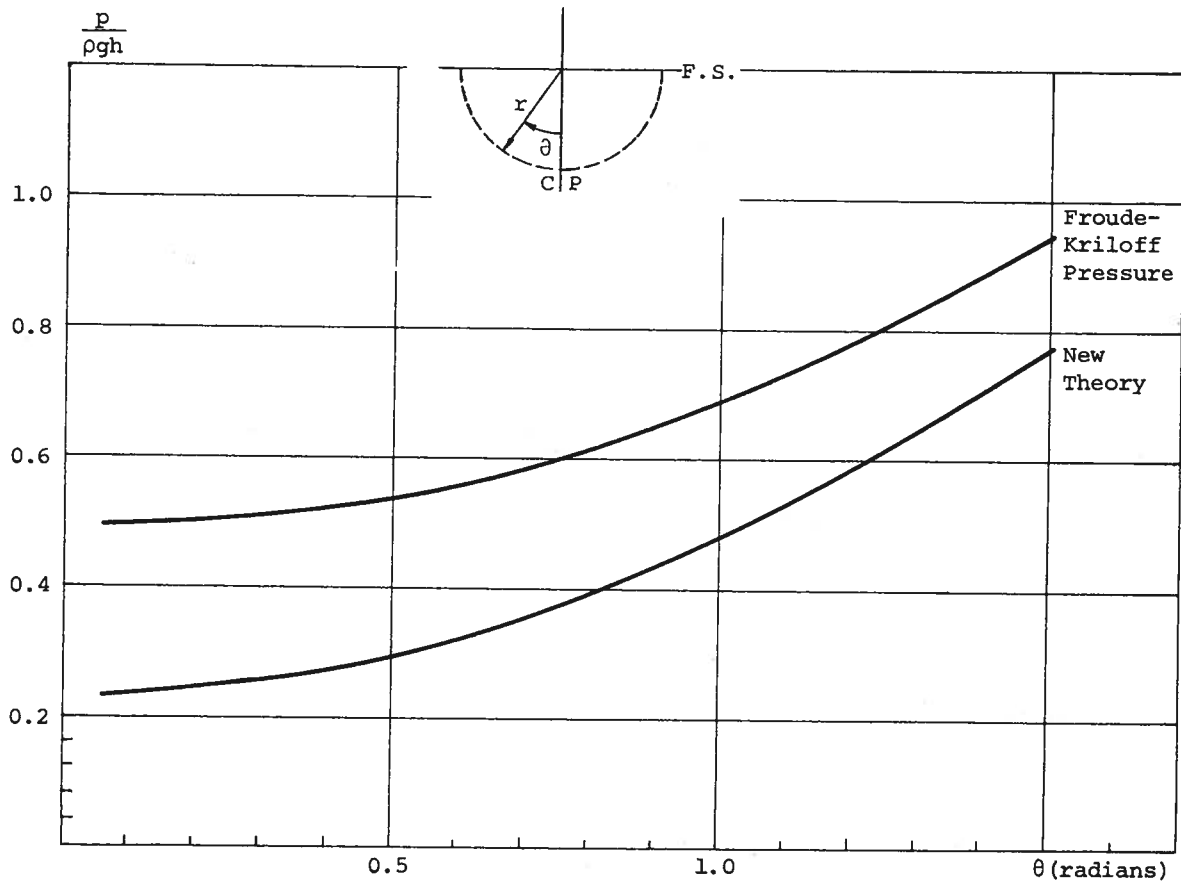


FIGURE 37
PRESSURE DISTRIBUTION AT STATION 10

$\lambda/L = 0.5$

$Fn = 0.0$

Multiplication Factor For Froude Number 0.1 = 1.3073

Multiplication Factor For Froude Number 0.2 = 1.5550

Multiplication Factor For Froude Number 0.3 = 1.7683

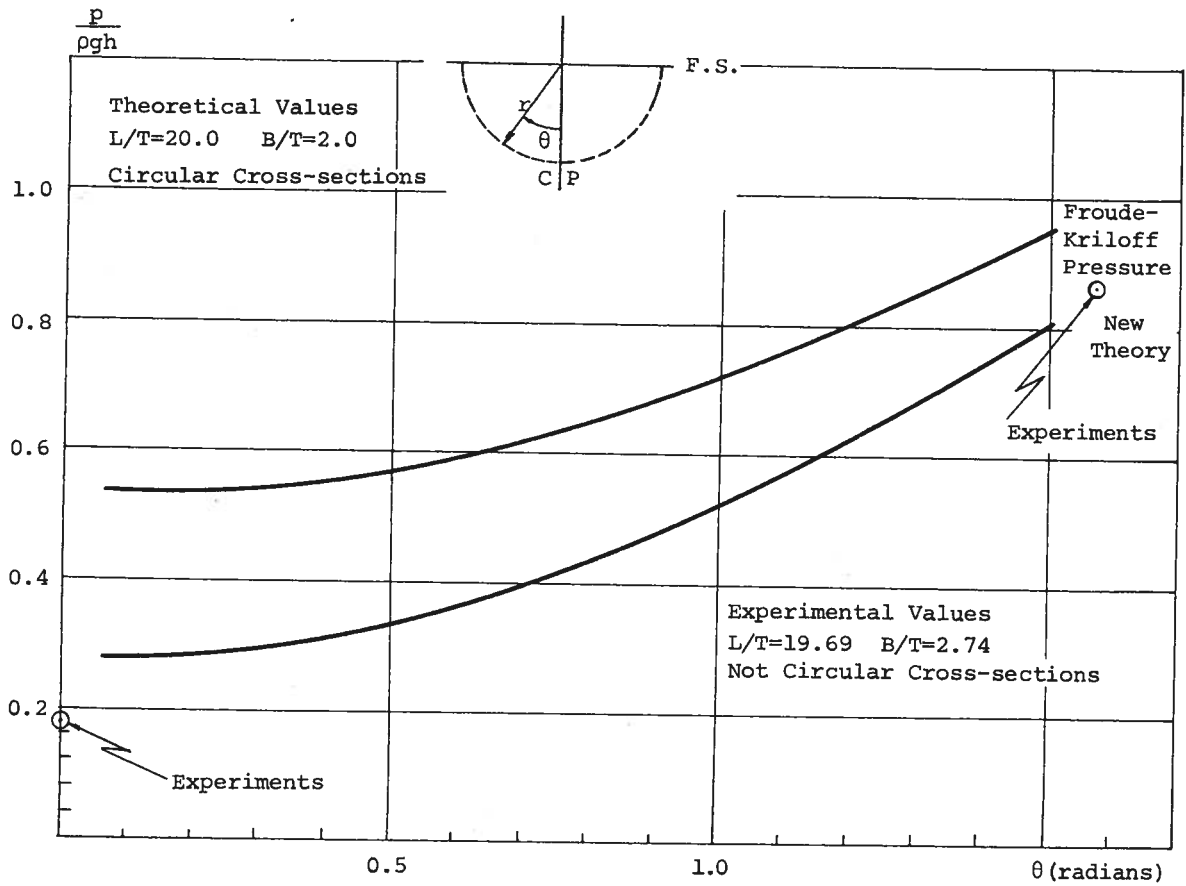


FIGURE 38

PRESSURE DISTRIBUTION AT STATION 10

$\lambda/L = 0.55$

$F_n = 0.0$

Multiplication Factor For Froude Number 0.1 = 1.2946

Multiplication Factor For Froude Number 0.2 = 1.5336

Multiplication Factor For Froude Number 0.3 = 1.7401

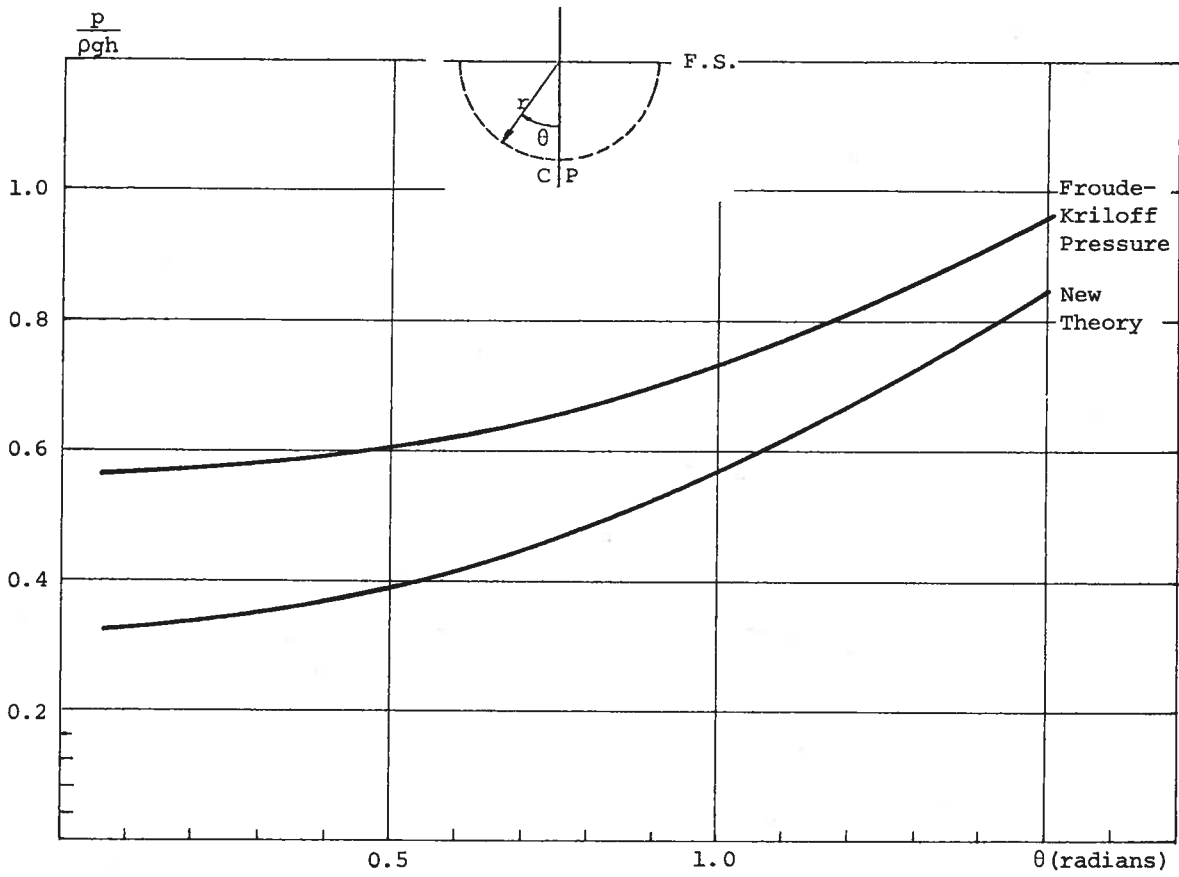


FIGURE 39

PRESSURE DISTRIBUTION AT STATION 10

$\lambda/L = 0.6$

$Fn = 0.0$

Multiplication Factor For Froude Number 0.1 = 1.2854

Multiplication Factor For Froude Number 0.2 = 1.5147

Multiplication Factor For Froude Number 0.3 = 1.7151

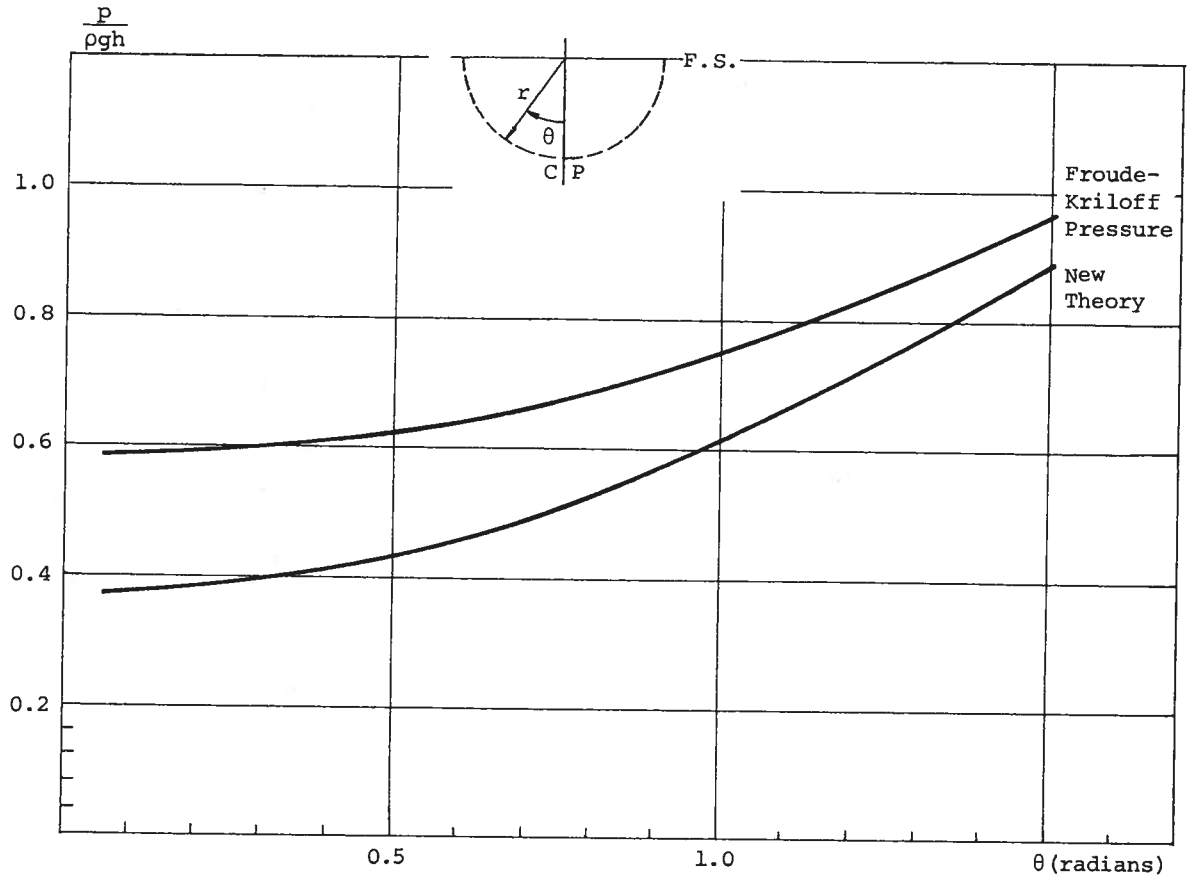


FIGURE 40

PRESSURE DISTRIBUTION AT STATION 10

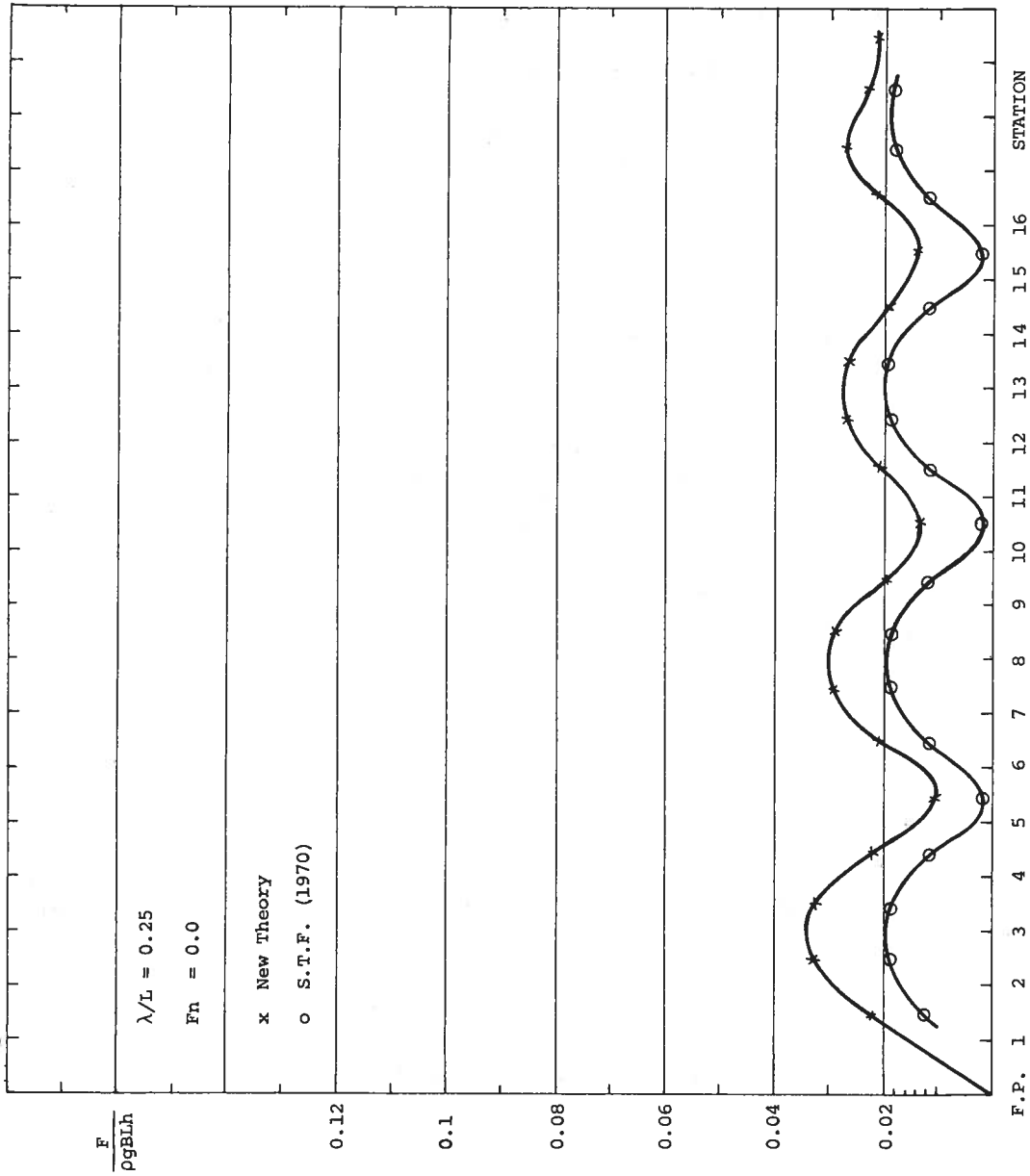


FIGURE 41 FORCE SUMMED UP FROM FORWARD PERPENDICULAR TO STATION K AS A FUNCTION OF STATION K

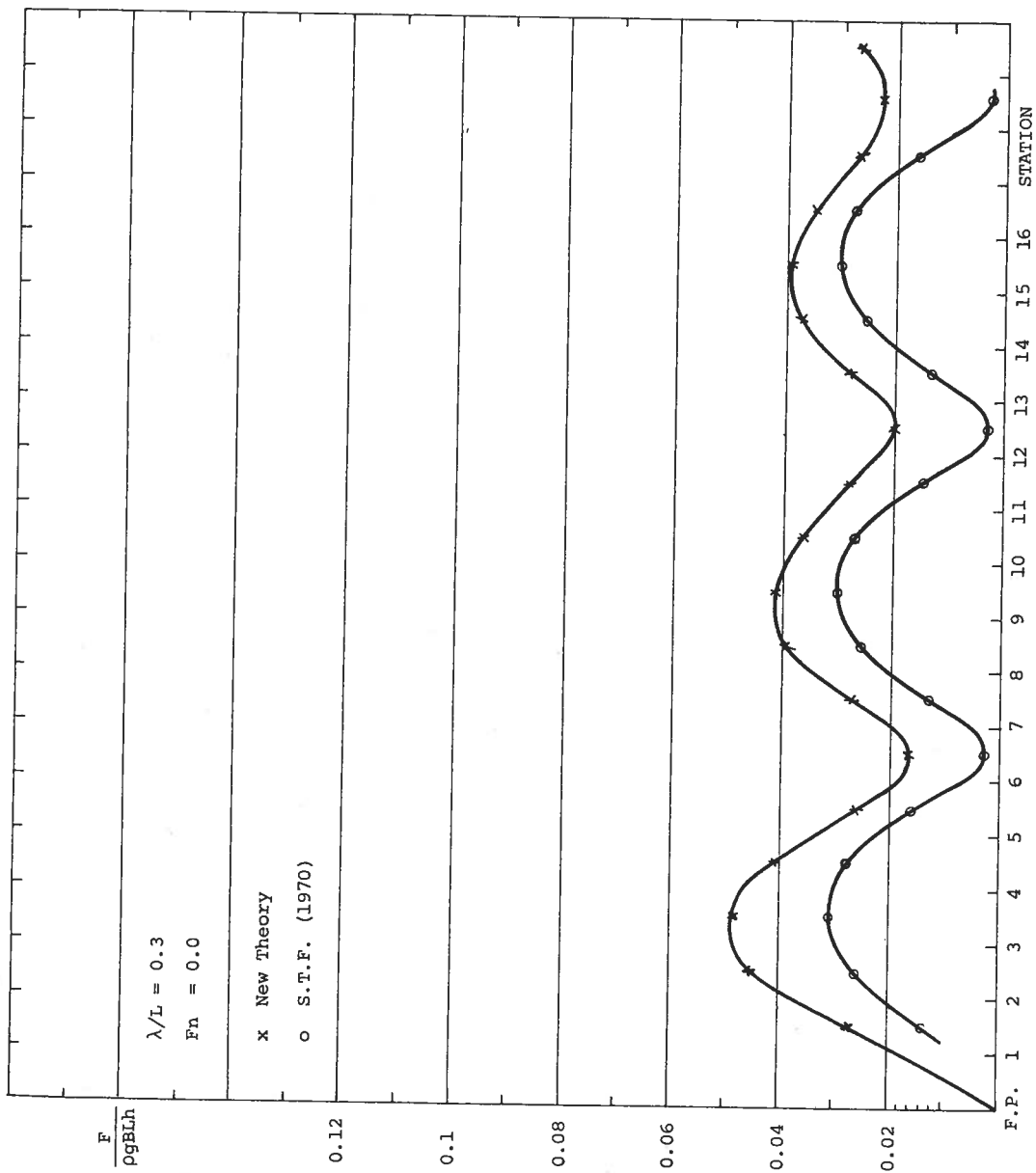


FIGURE 42 FORCE SUMMED UP FROM FORWARD PERPENDICULAR TO STATION K AS A FUNCTION OF STATION K

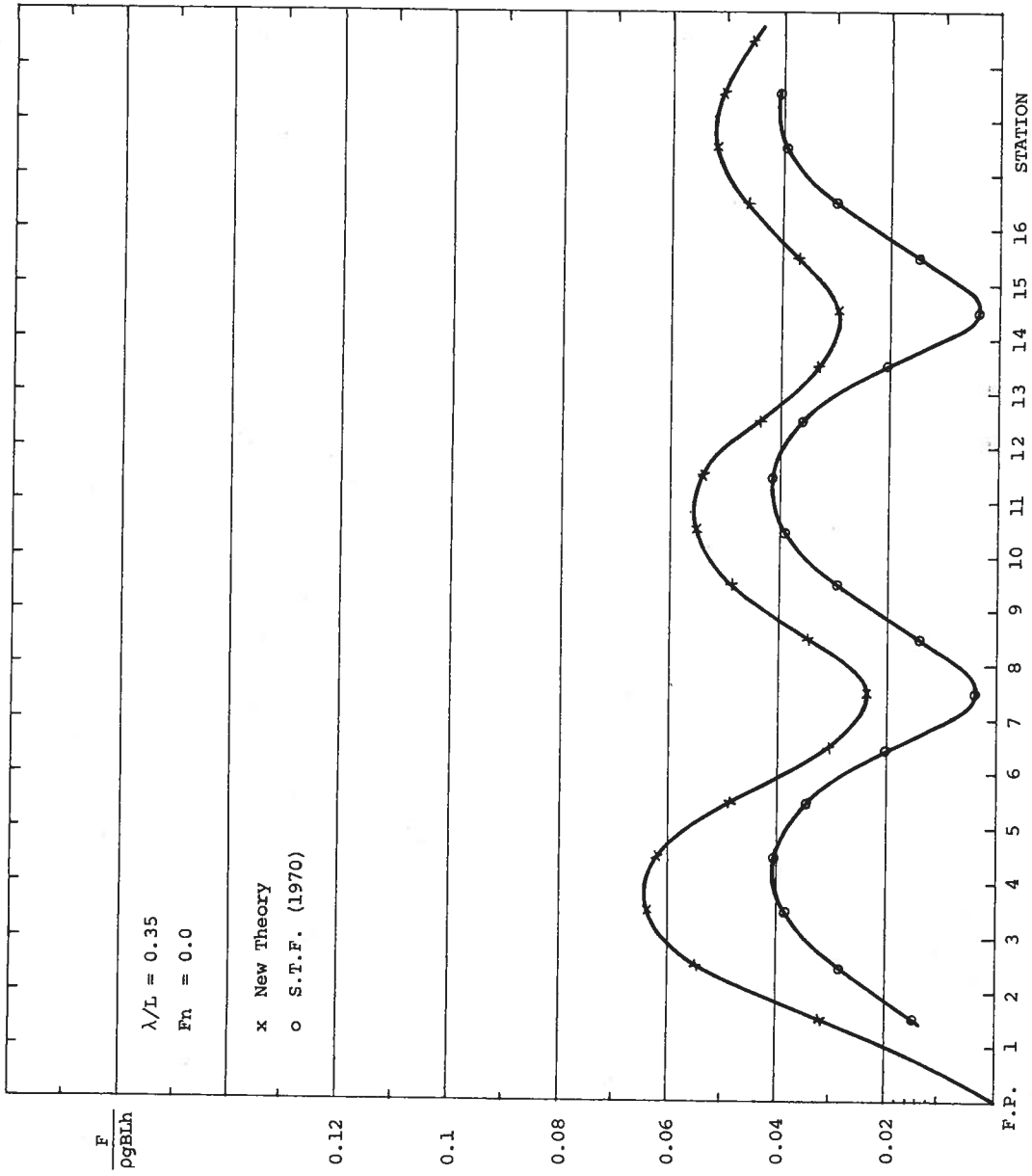


FIGURE 43 FORCE SUMMED UP FROM FORWARD PERPENDICULAR TO STATION K AS A FUNCTION OF STATION K

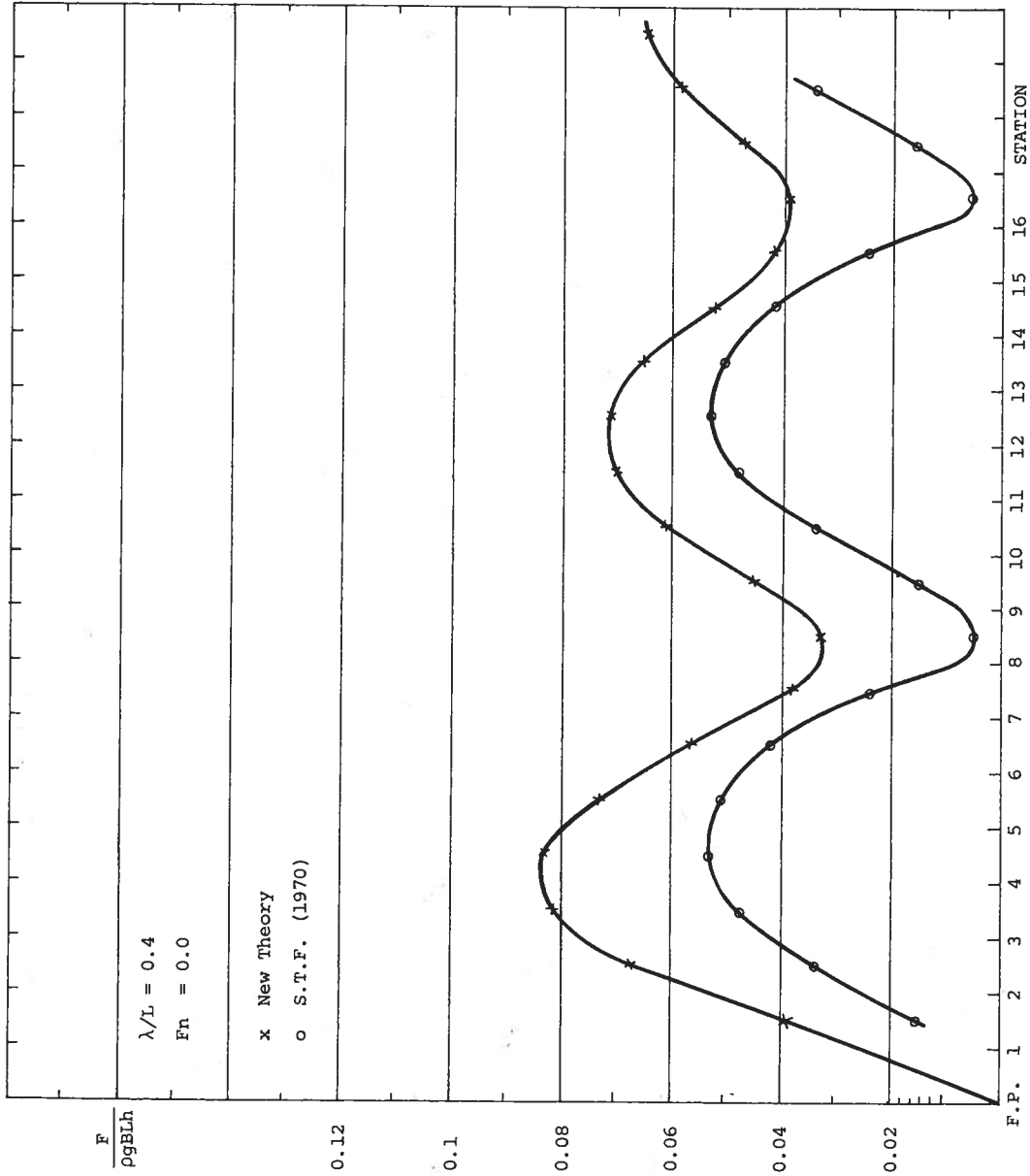


FIGURE 44 FORCE SUMMED UP FROM FORWARD PERPENDICULAR TO STATION K AS A FUNCTION OF STATION K

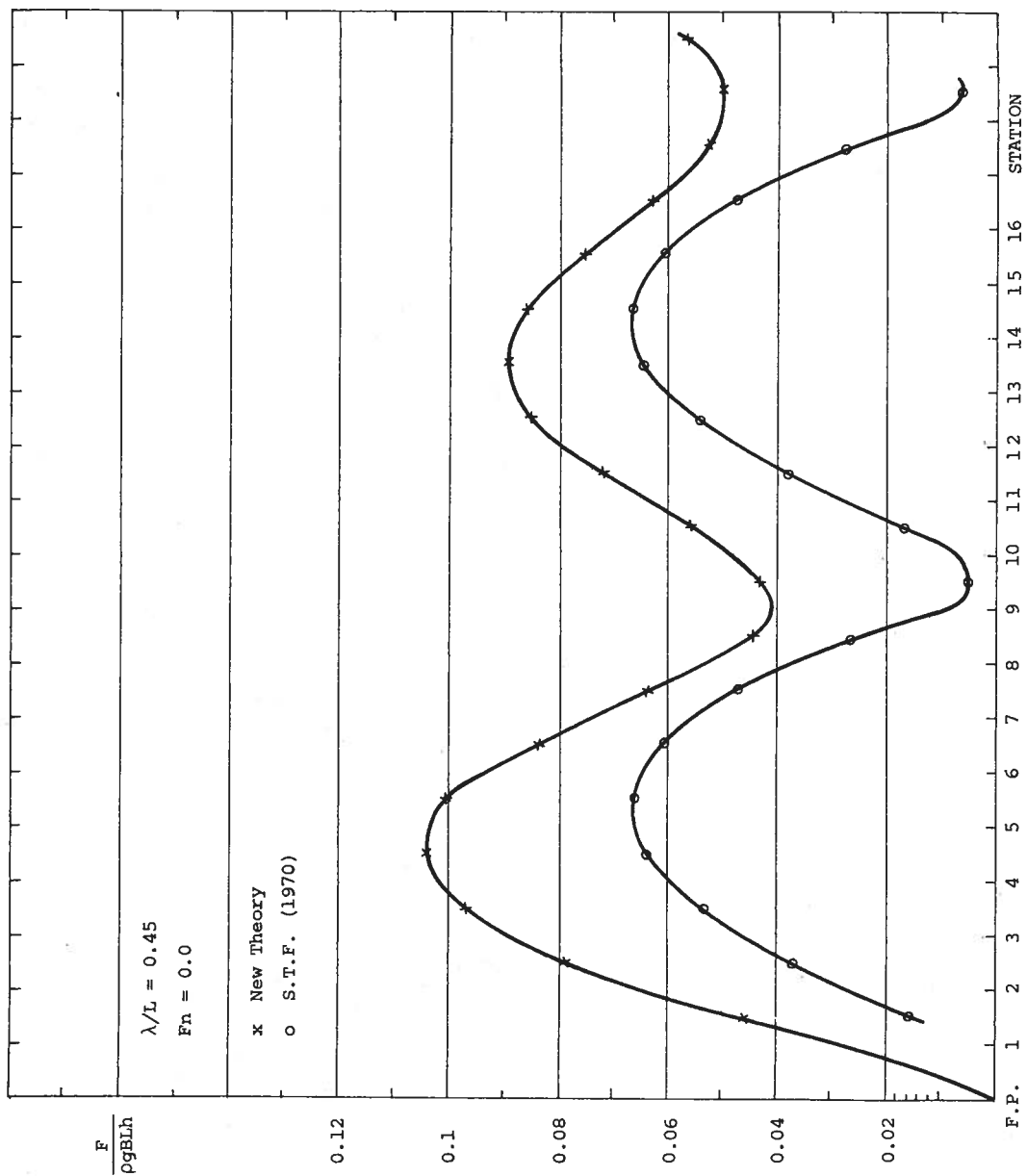


FIGURE 45 FORCE SUMMED UP FROM FORWARD PERPENDICULAR TO STATION K AS A FUNCTION OF STATION K

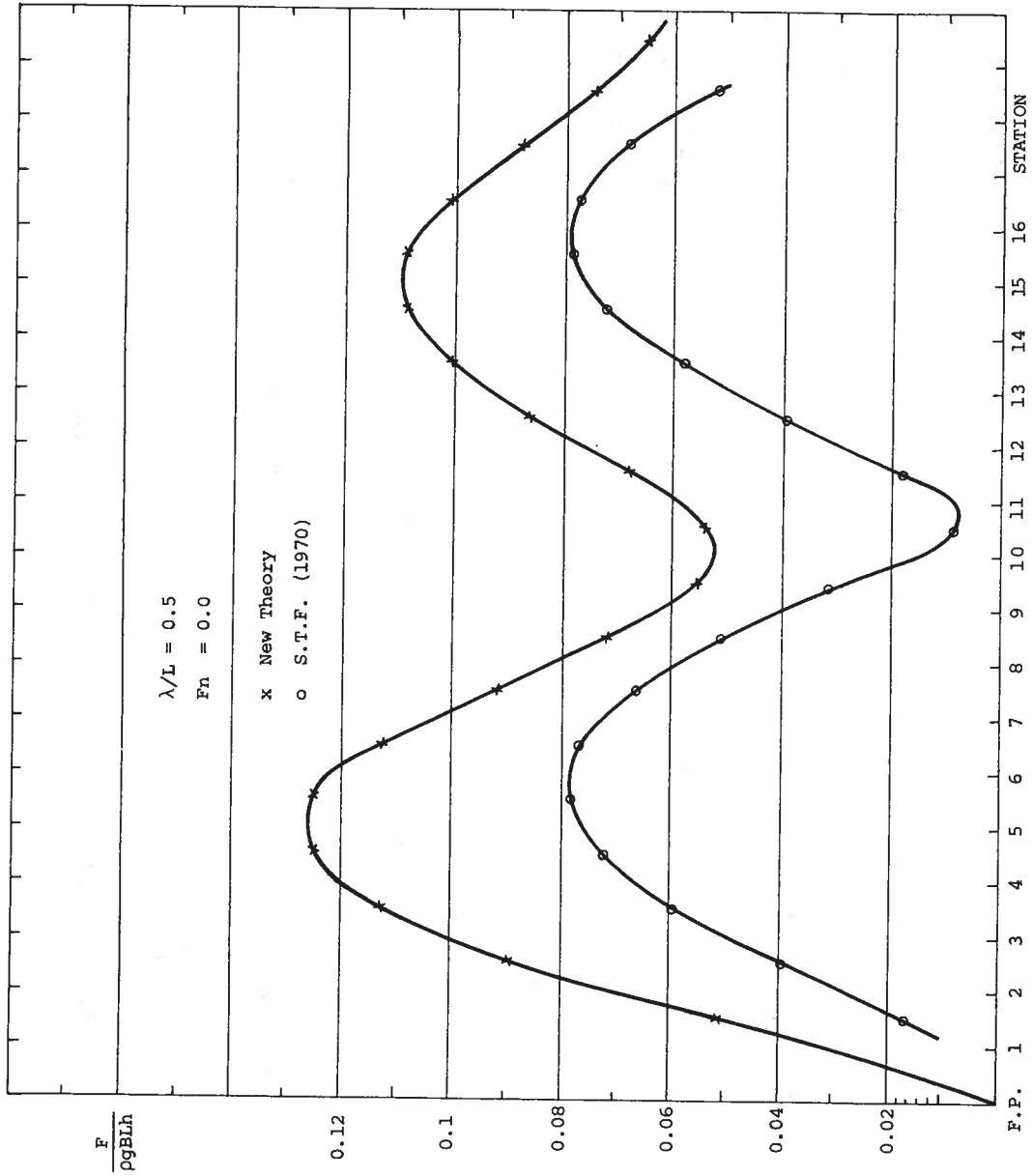


FIGURE 46 FORCE SUMMED UP FROM FORWARD PERPENDICULAR TO STATION K AS A FUNCTION OF STATION K

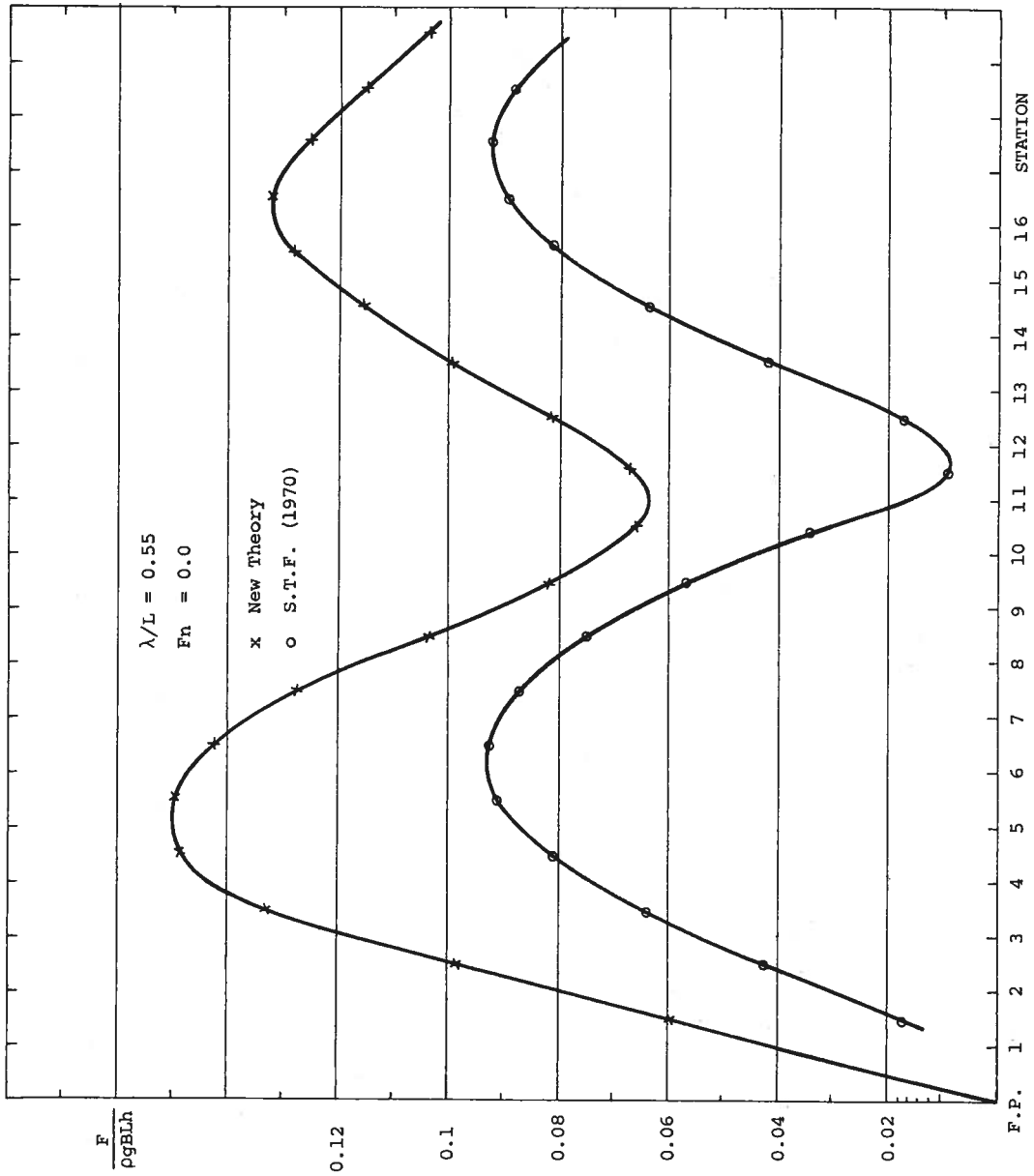


FIGURE 47 FORCE SUMMED UP FROM FORWARD PERPENDICULAR TO STATION K AS A FUNCTION OF STATION K

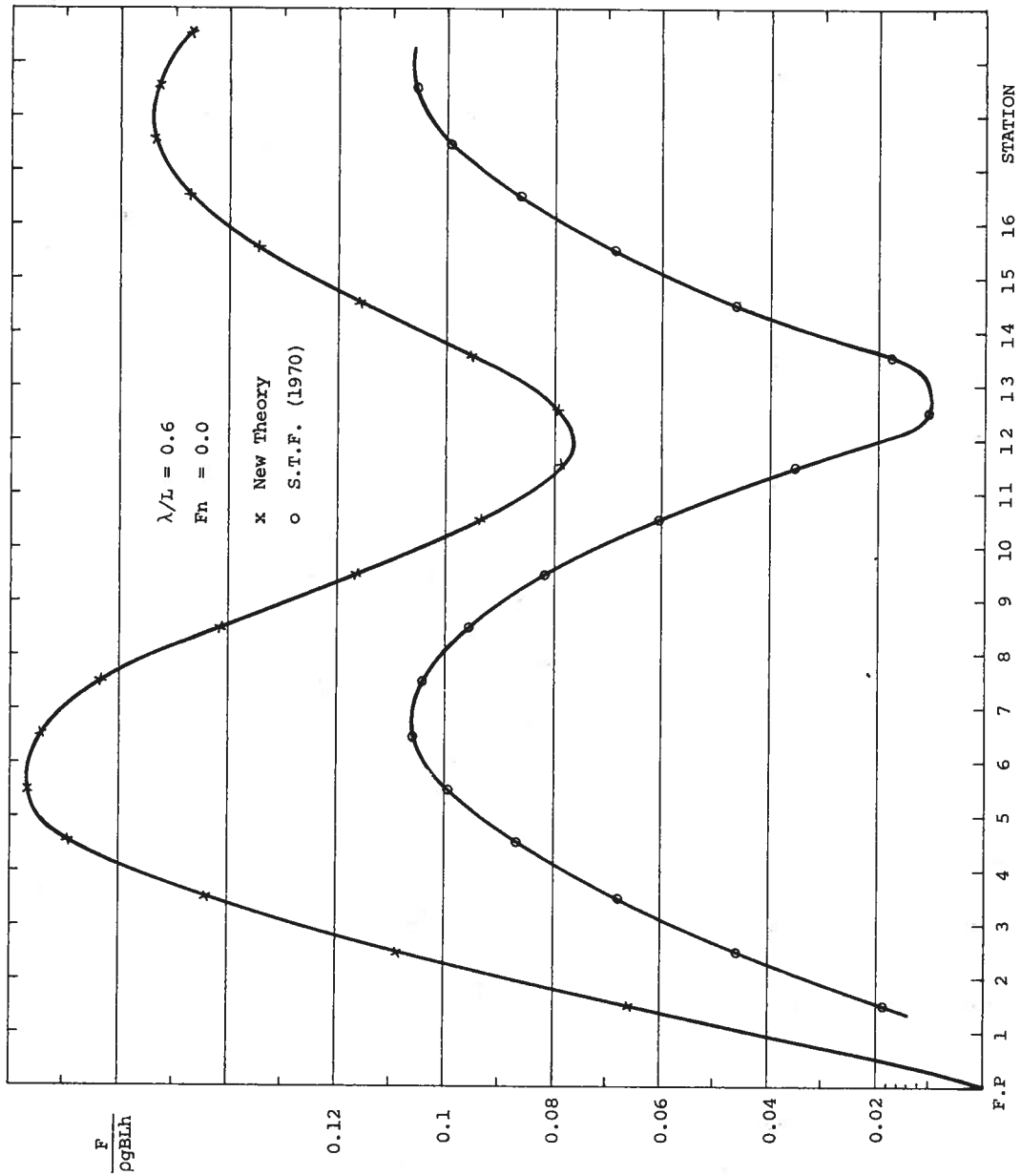


FIGURE 48 FORCE SUMMED UP FROM FORWARD PERPENDICULAR TO STATION K AS A FUNCTION OF STATION K

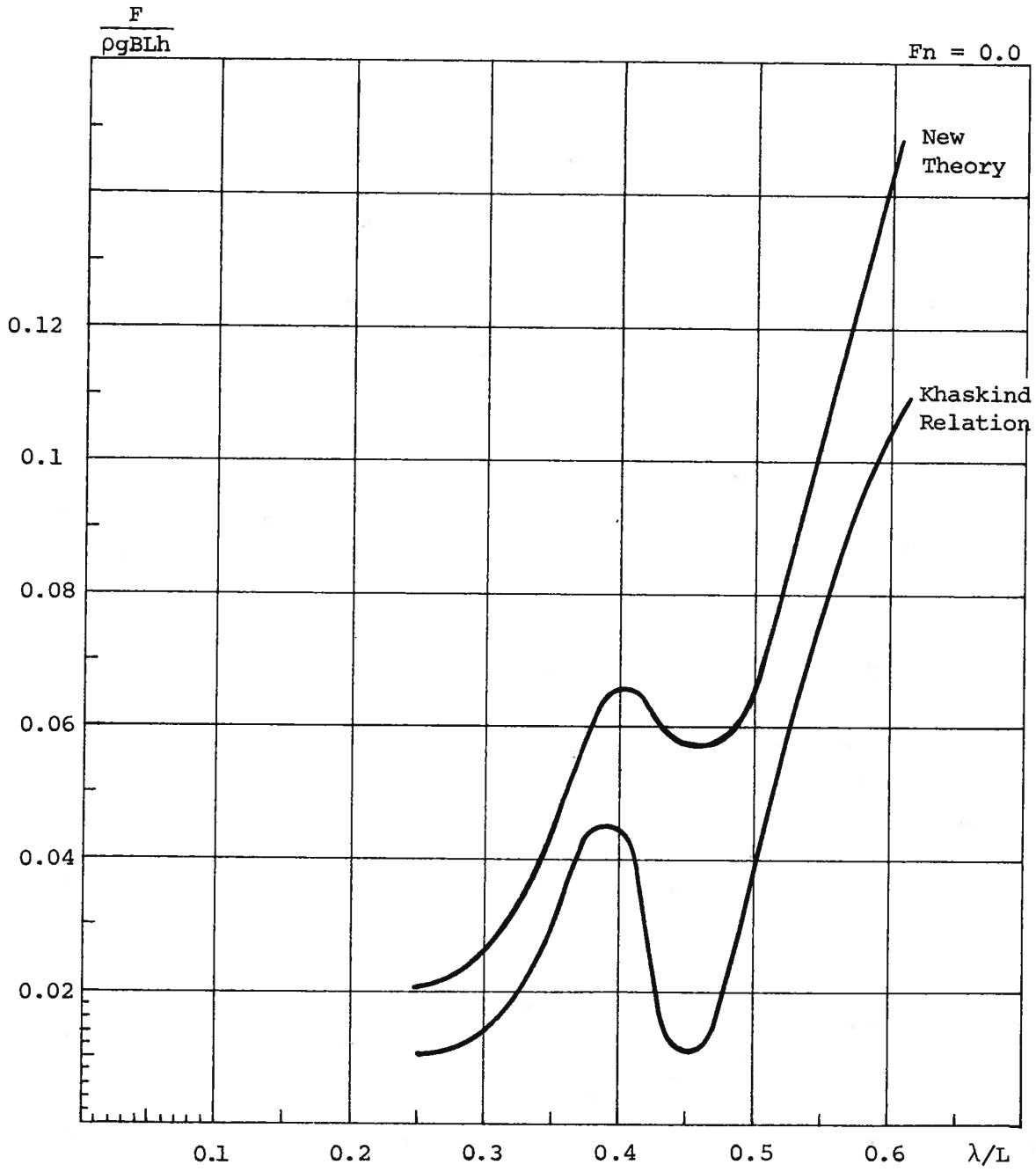


FIGURE 49
TOTAL FORCE ON THE SHIP AS A FUNCTION
OF WAVE LENGTH

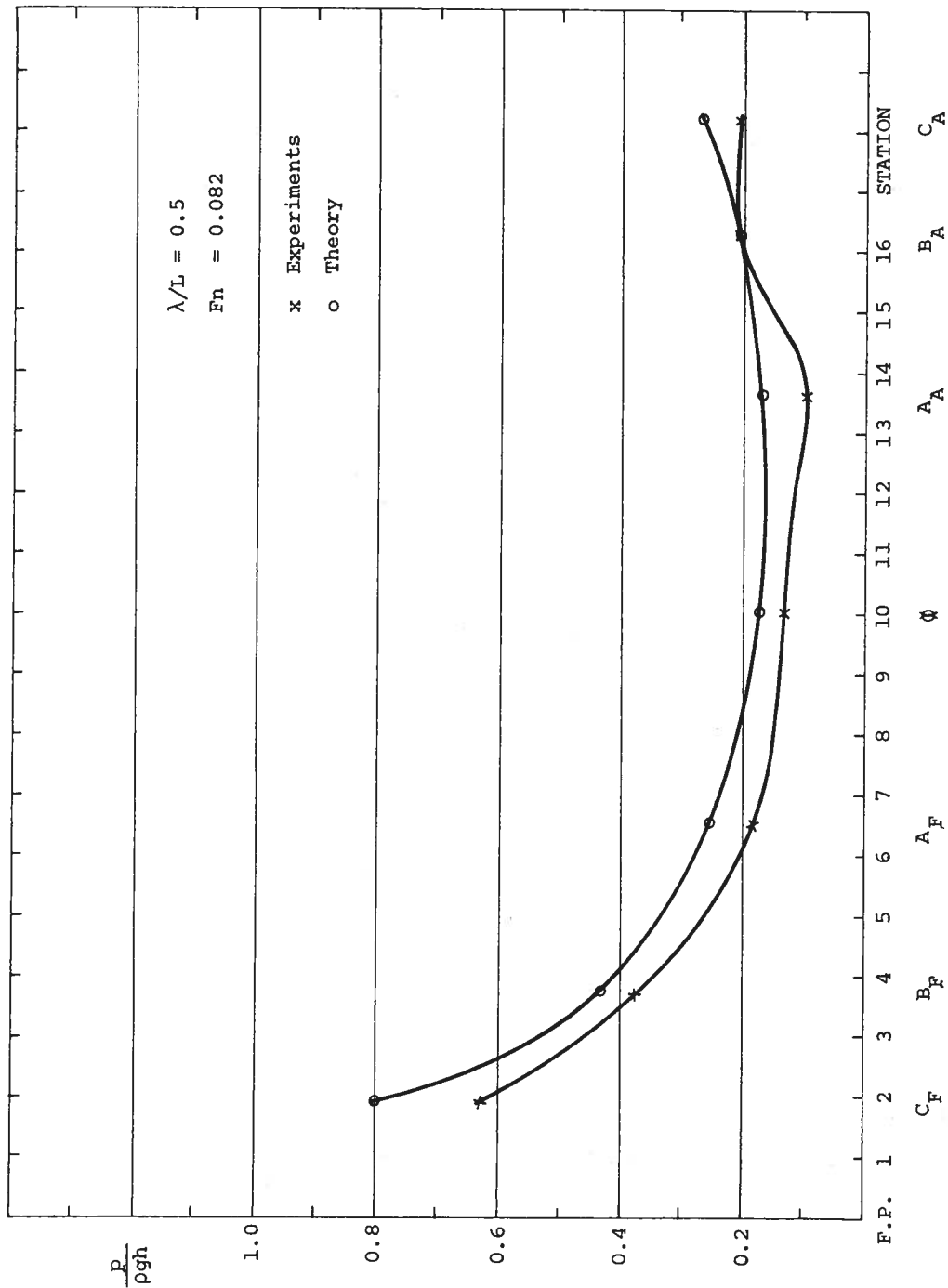


FIGURE 50
LONGITUDINAL DISTRIBUTION OF THE PRESSURE ALONG THE KEEL OF THE SPHEROID

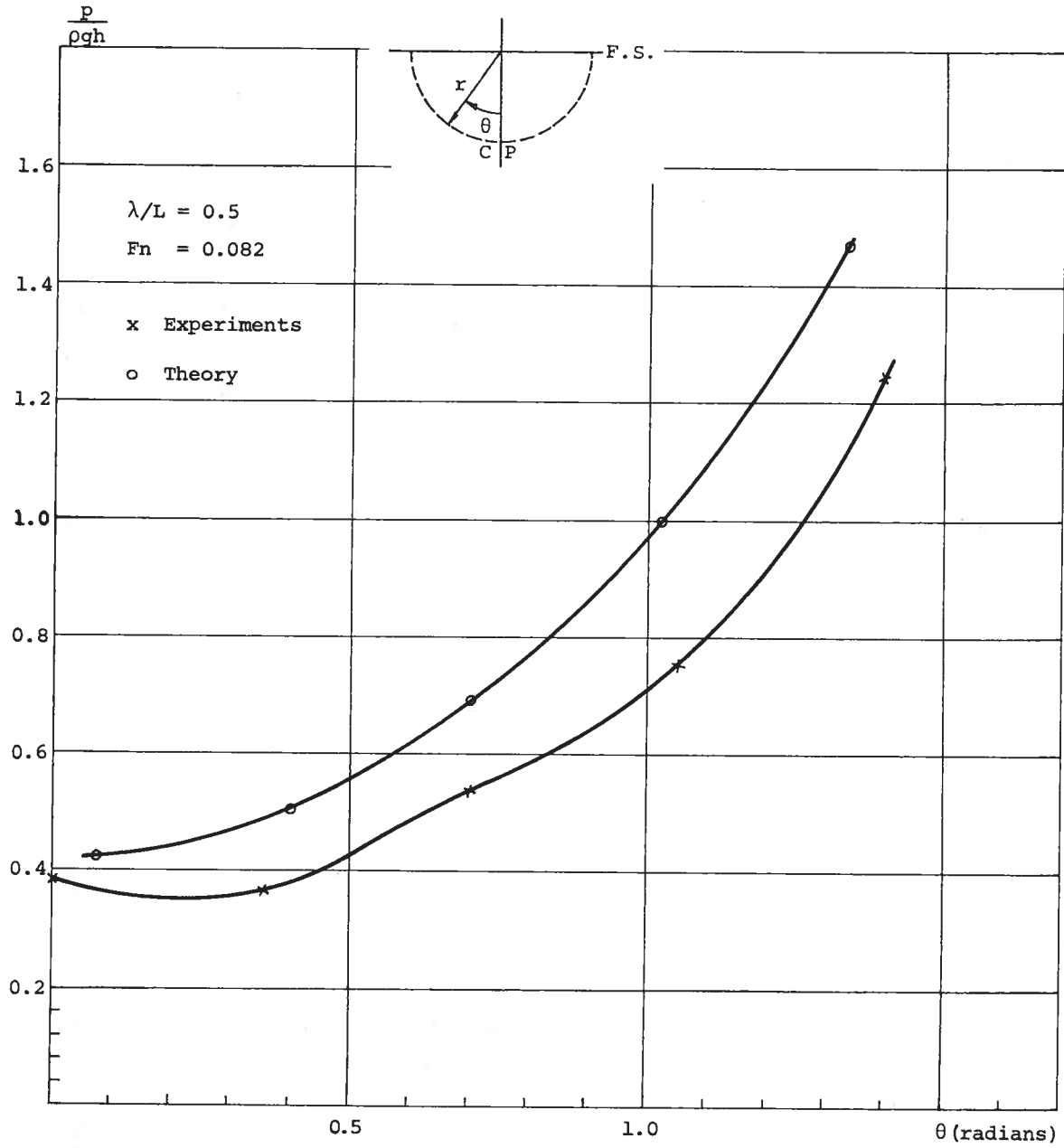


FIGURE 51

PRESSURE VARIATION ALONG THE CROSS-SECTION B_F

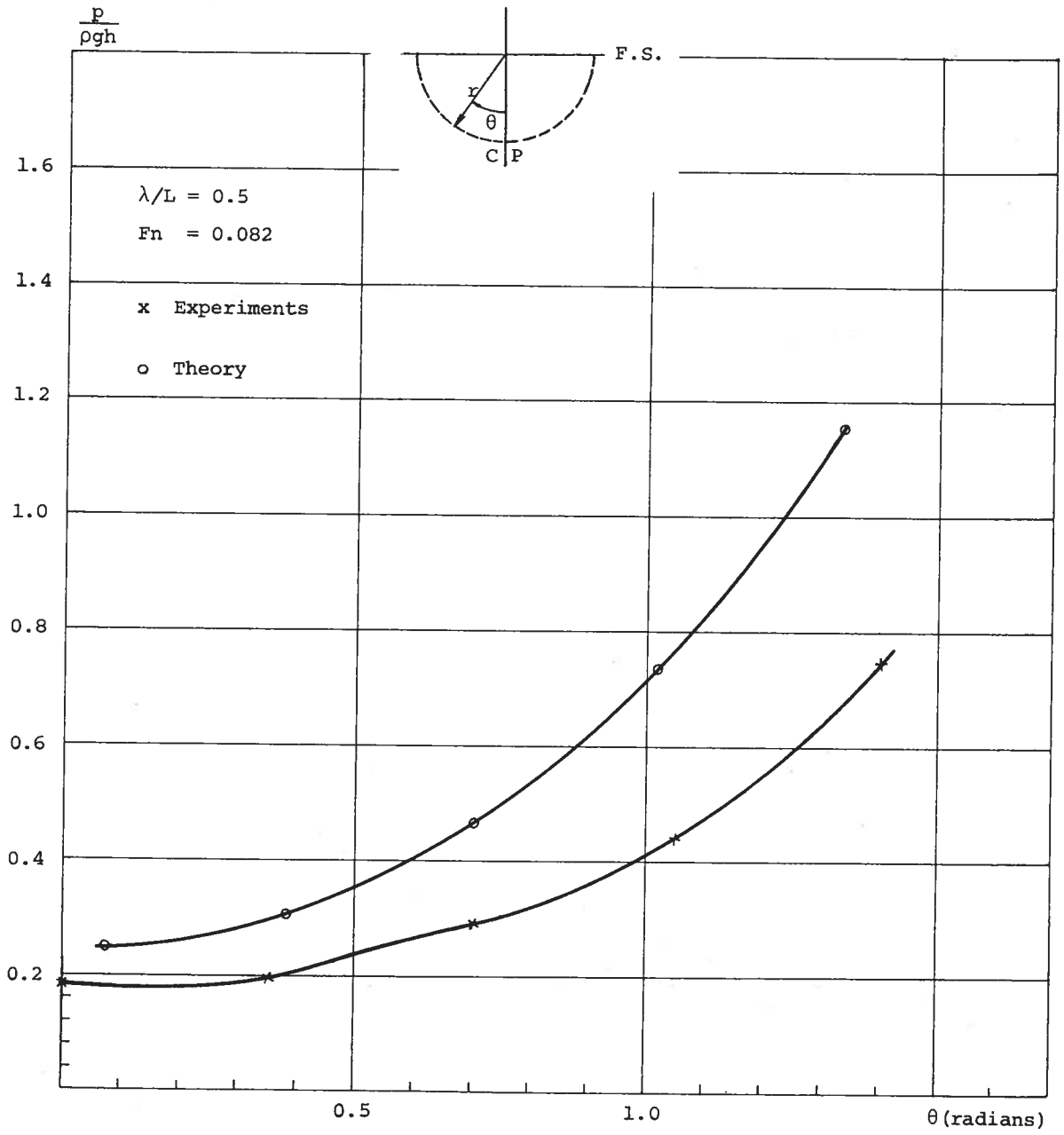


FIGURE 52

PRESSURE VARIATION ALONG THE CROSS-SECTION A_F

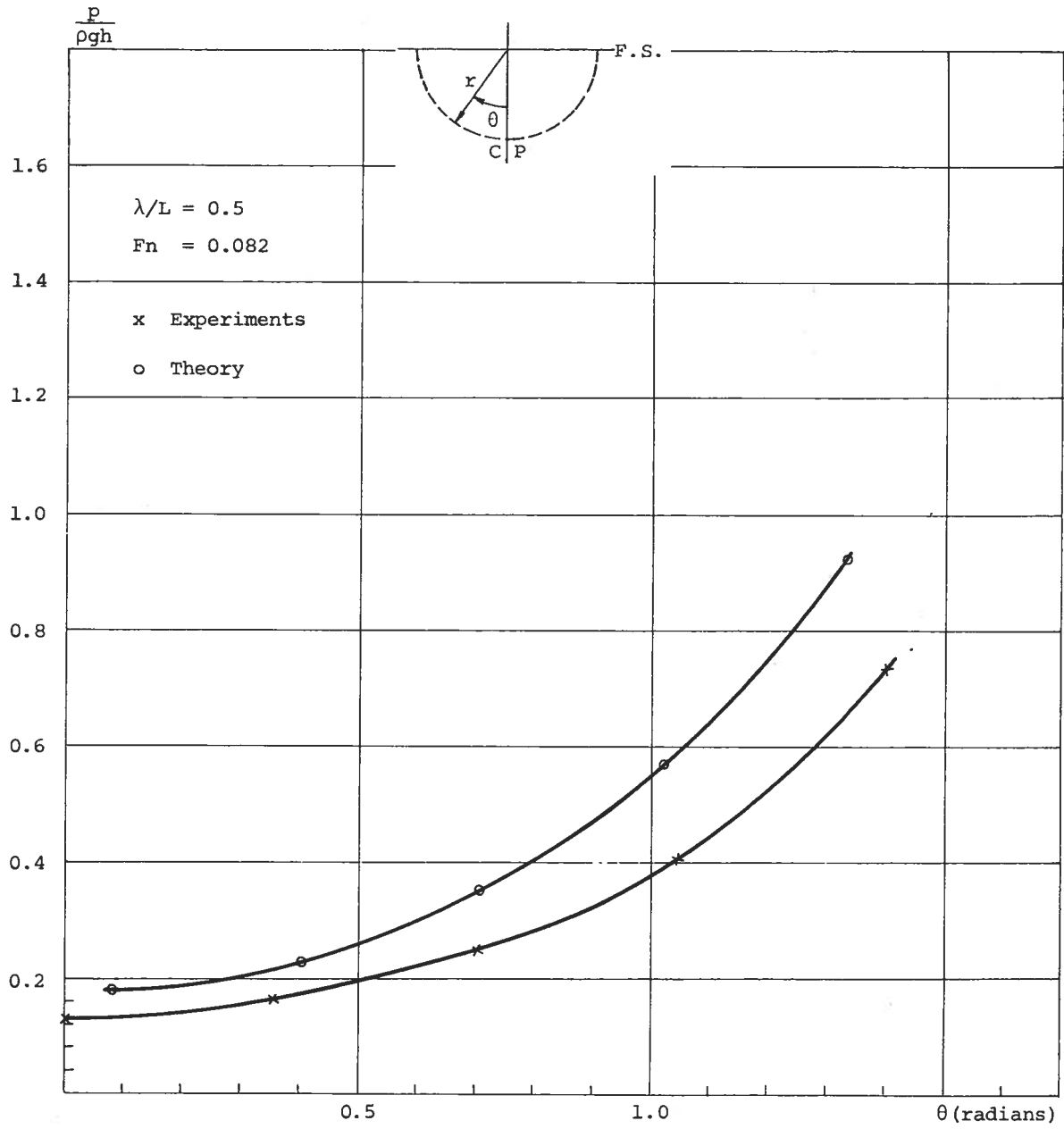


FIGURE 53

PRESSURE VARIATION ALONG THE CROSS-SECTION 

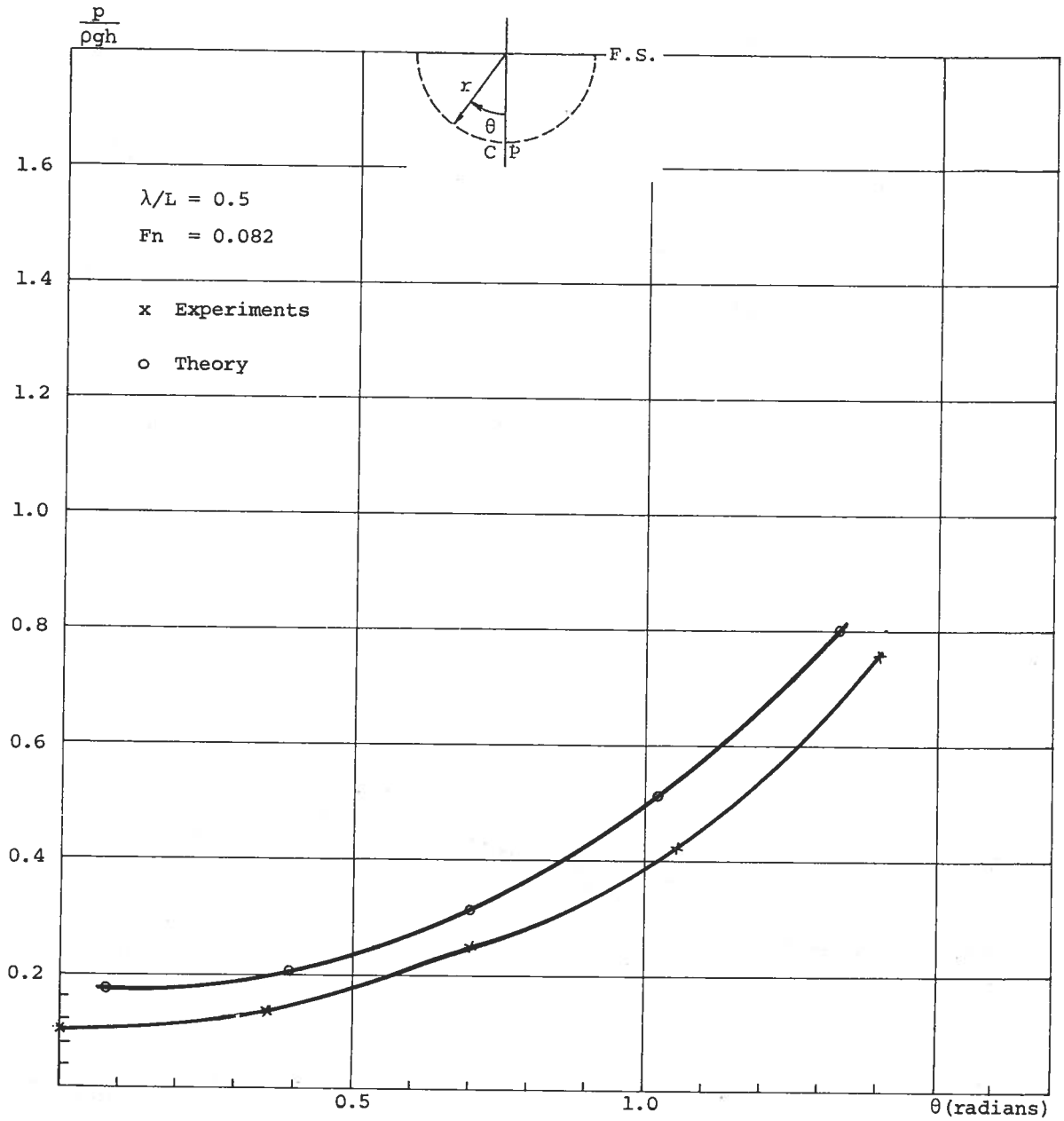


FIGURE 54

PRESSURE VARIATION ALONG THE CROSS-SECTION A_A

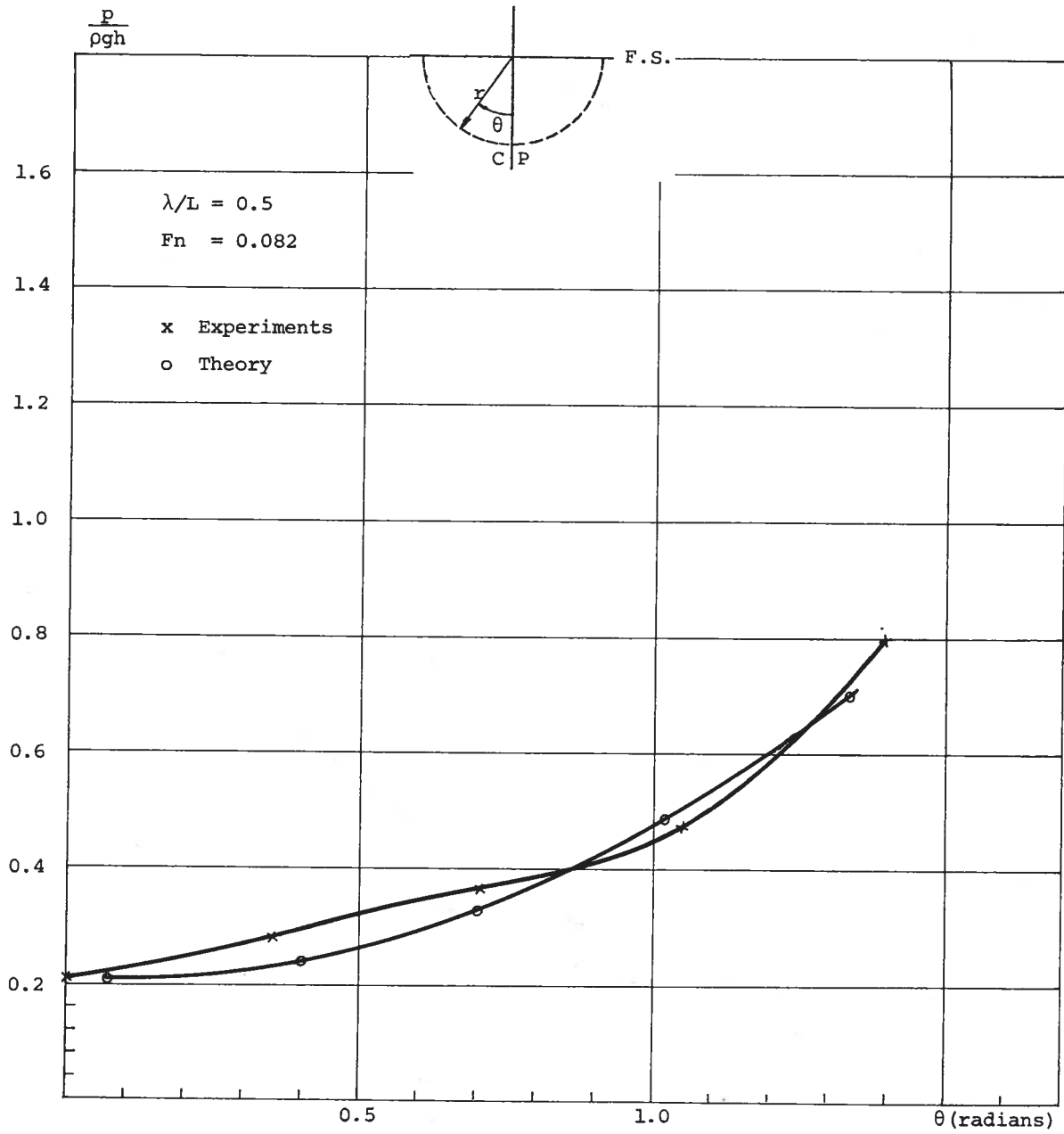


FIGURE 55
PRESSURE VARIATION ALONG THE CROSS-SECTION B_A

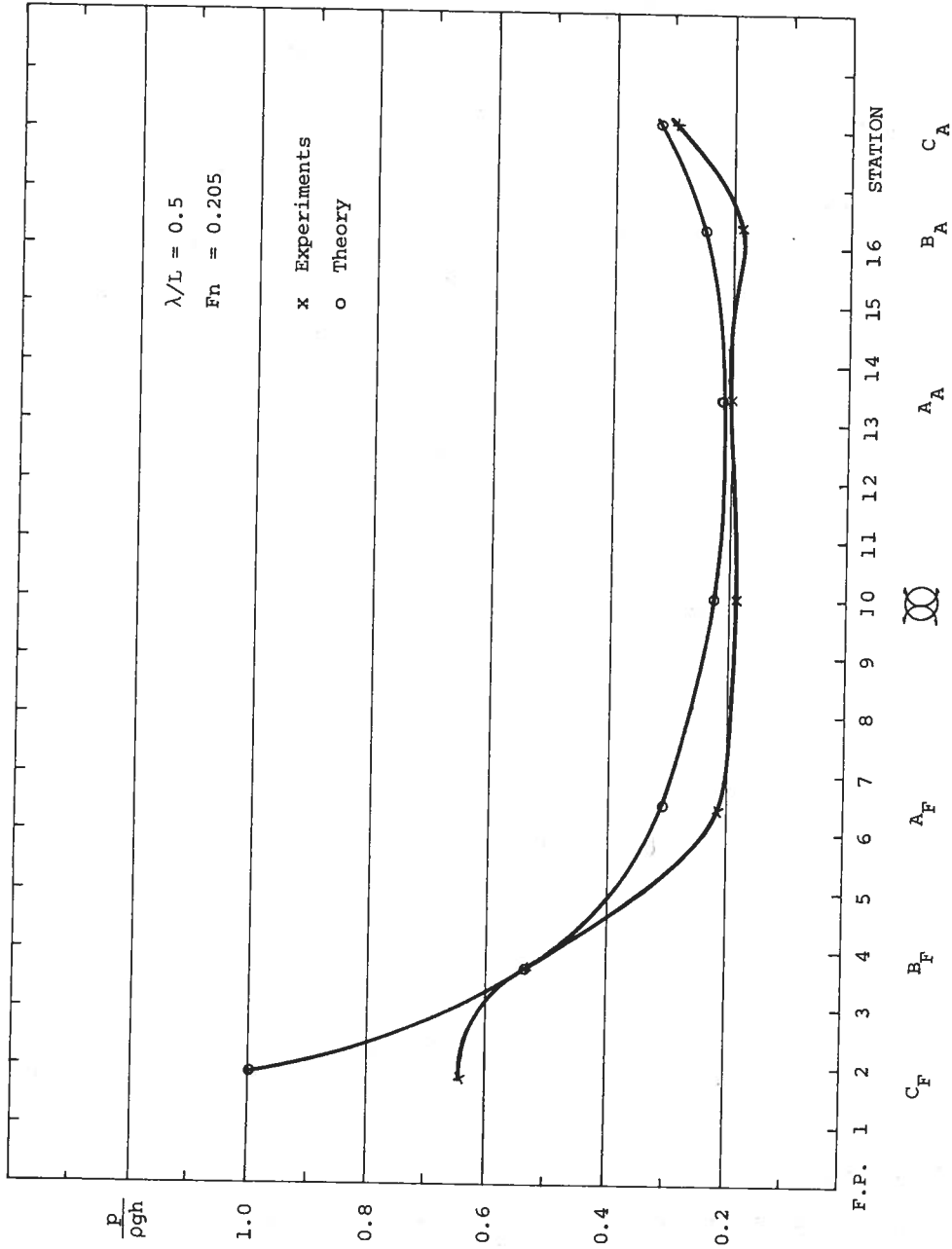


FIGURE 56
LONGITUDINAL DISTRIBUTION OF THE PRESSURE ALONG THE KEEL OF THE SPHEROID

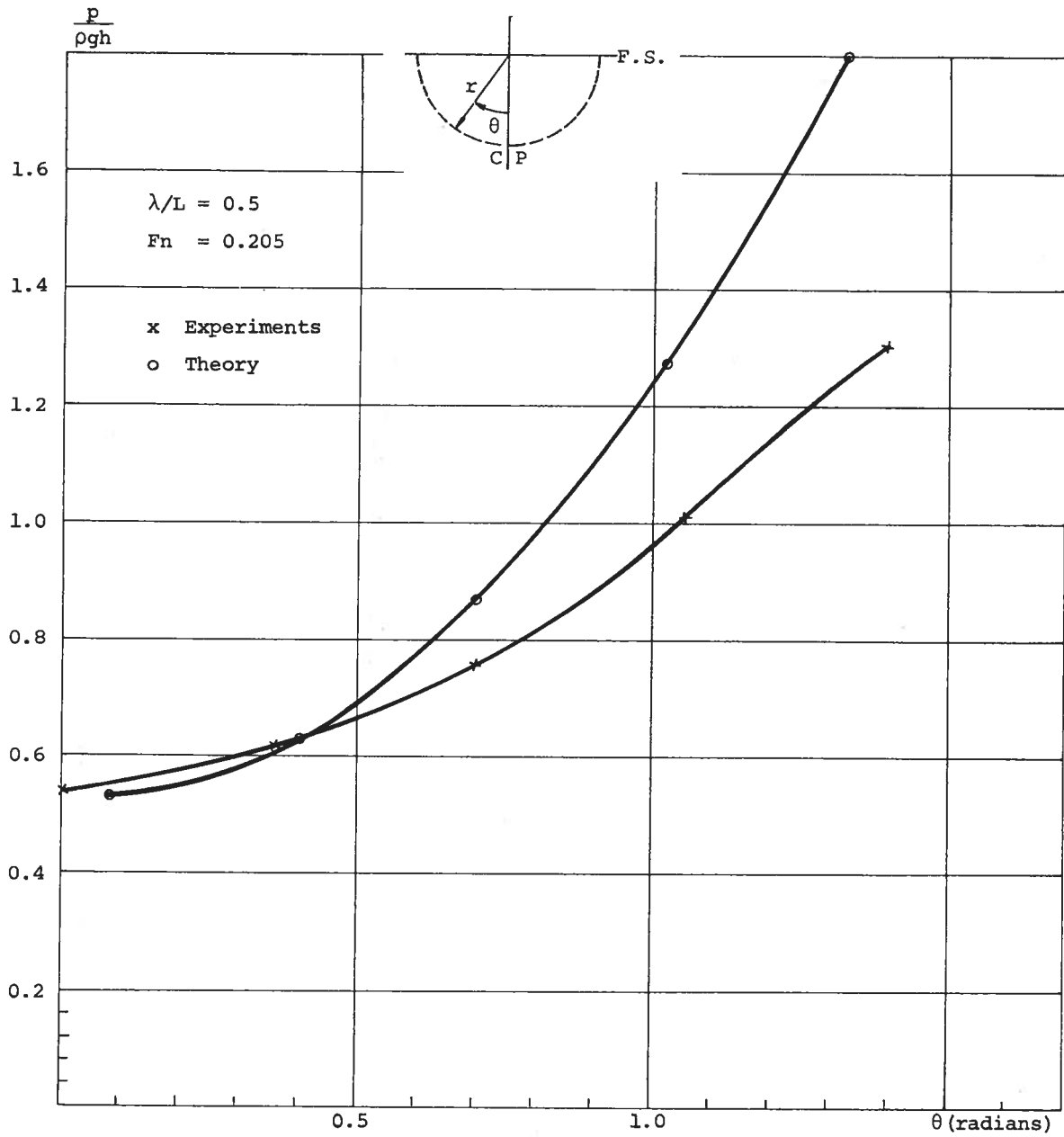


FIGURE 57

PRESSURE VARIATION ALONG THE CROSS-SECTION B_F

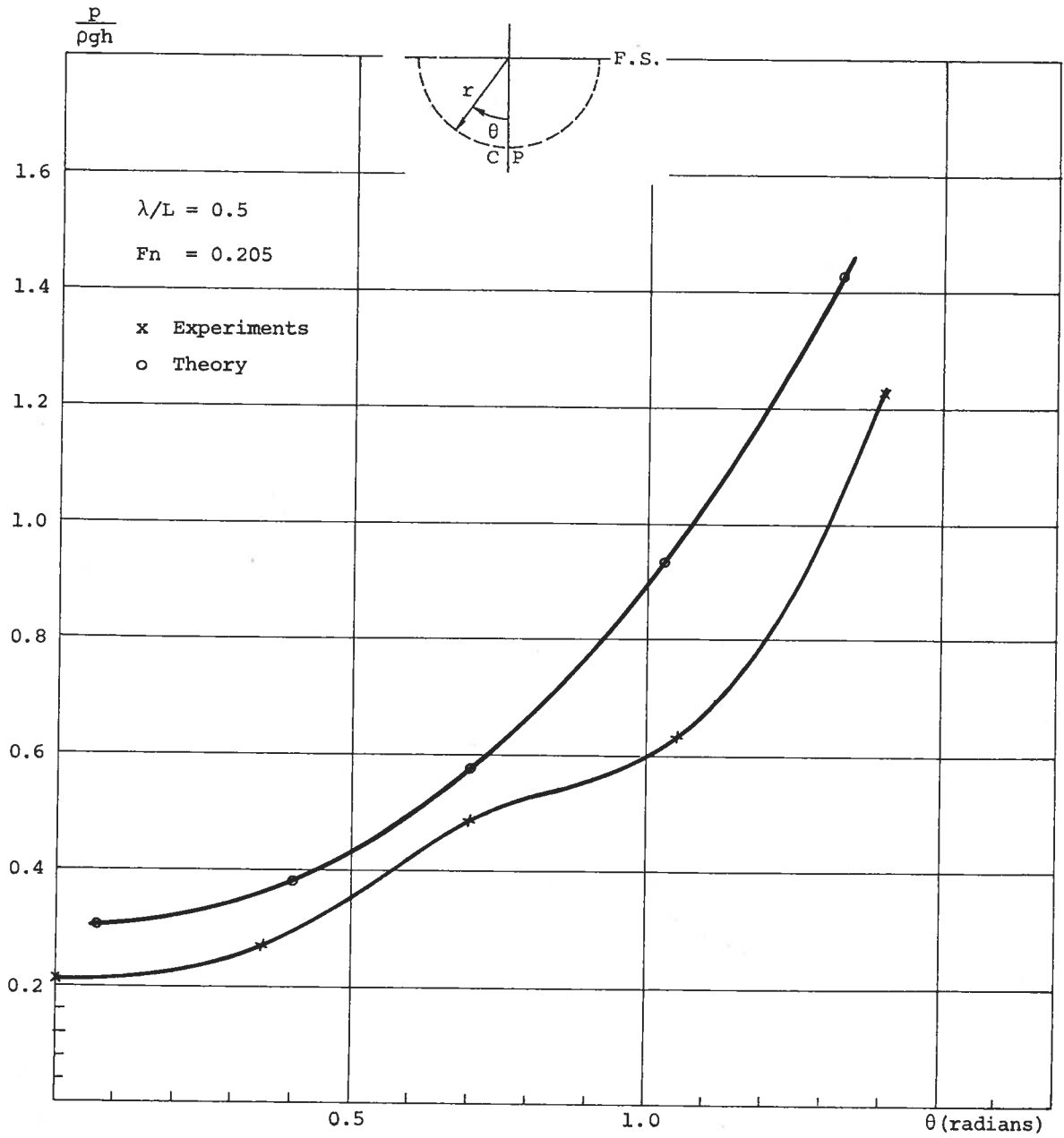


FIGURE 58

PRESSURE VARIATION ALONG THE CROSS-SECTION A_F

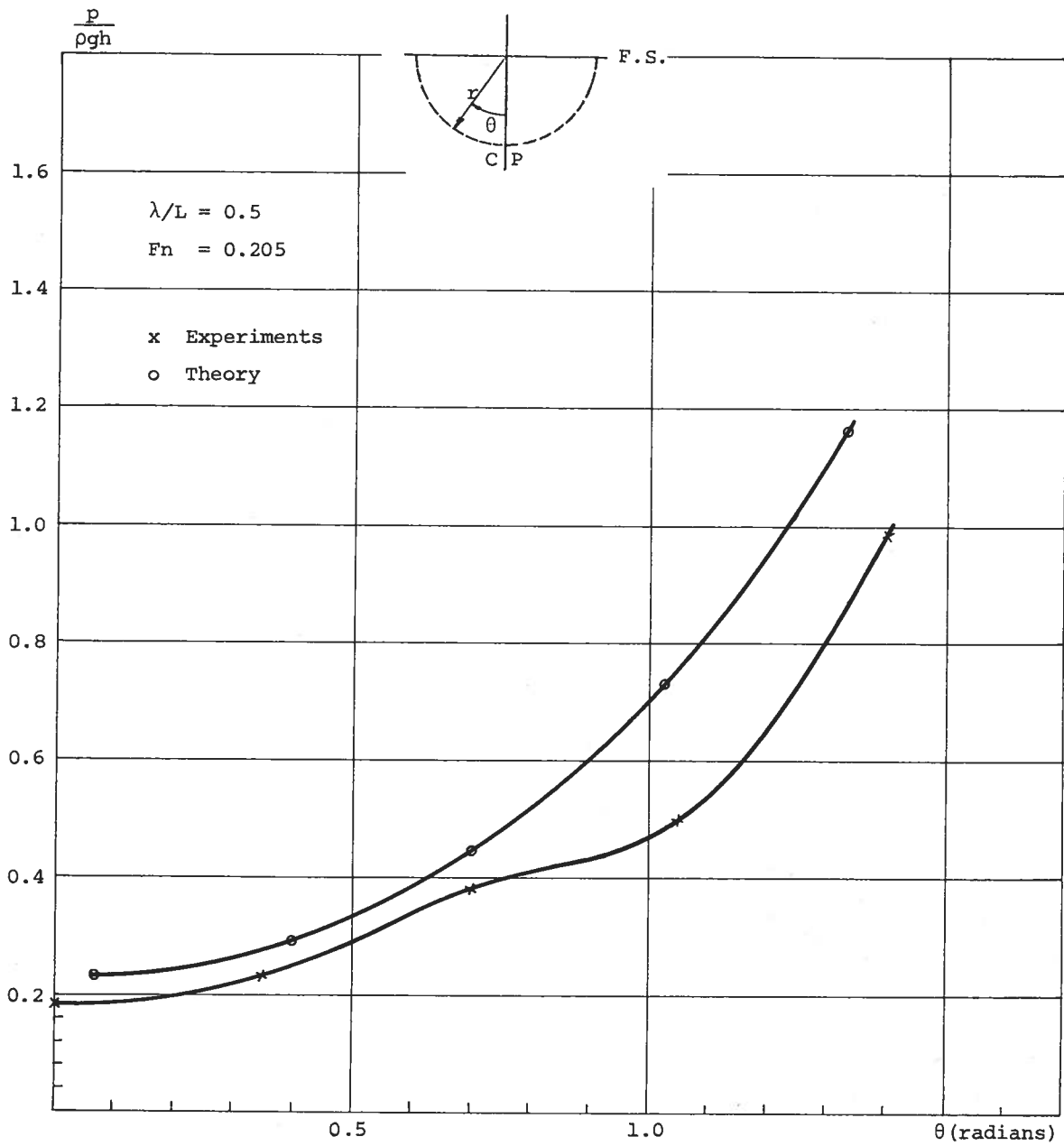


FIGURE 59

PRESSURE VARIATION ALONG THE CROSS-SECTION 

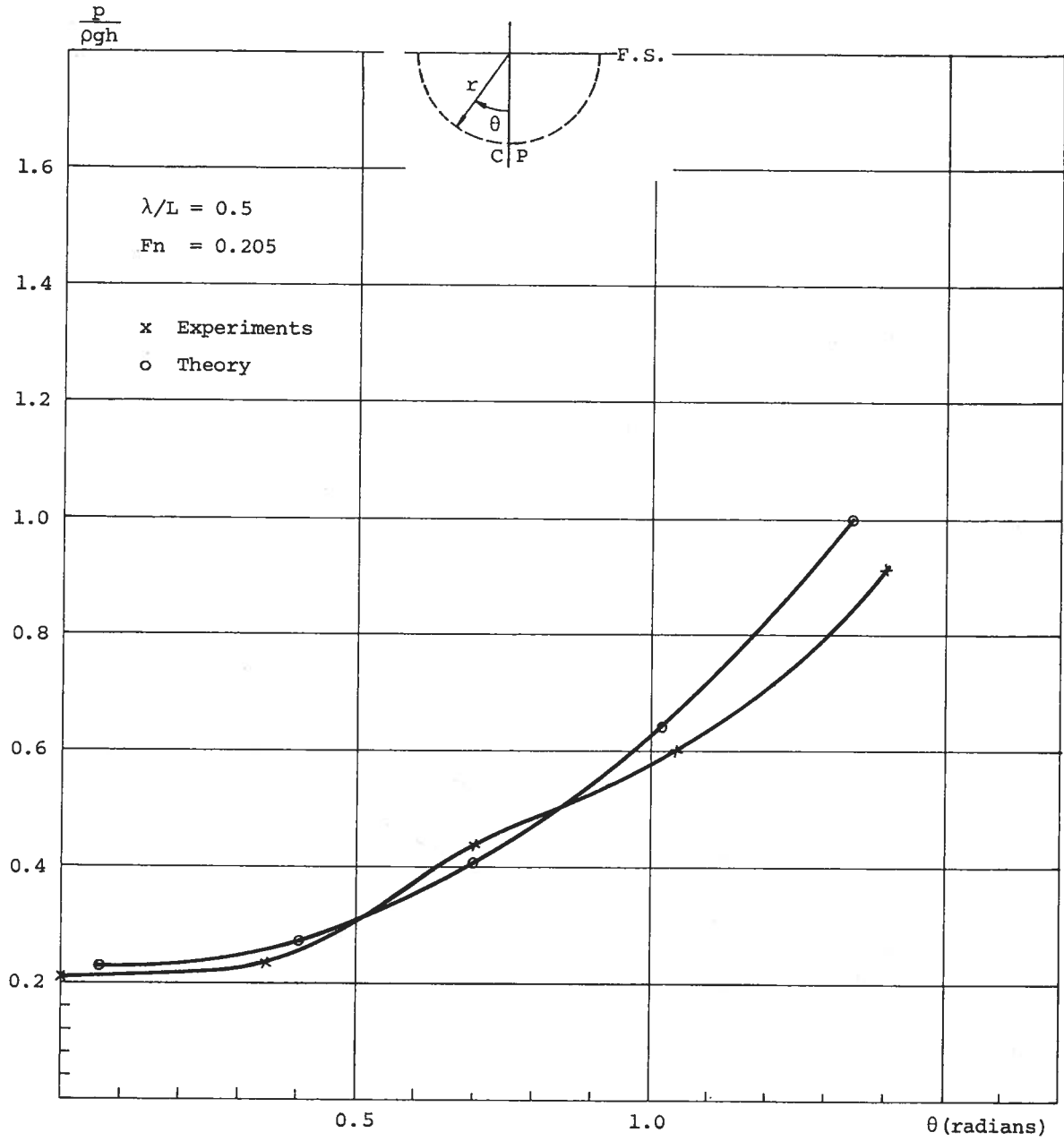


FIGURE 60

PRESSURE VARIATION ALONG THE CROSS-SECTION A_A

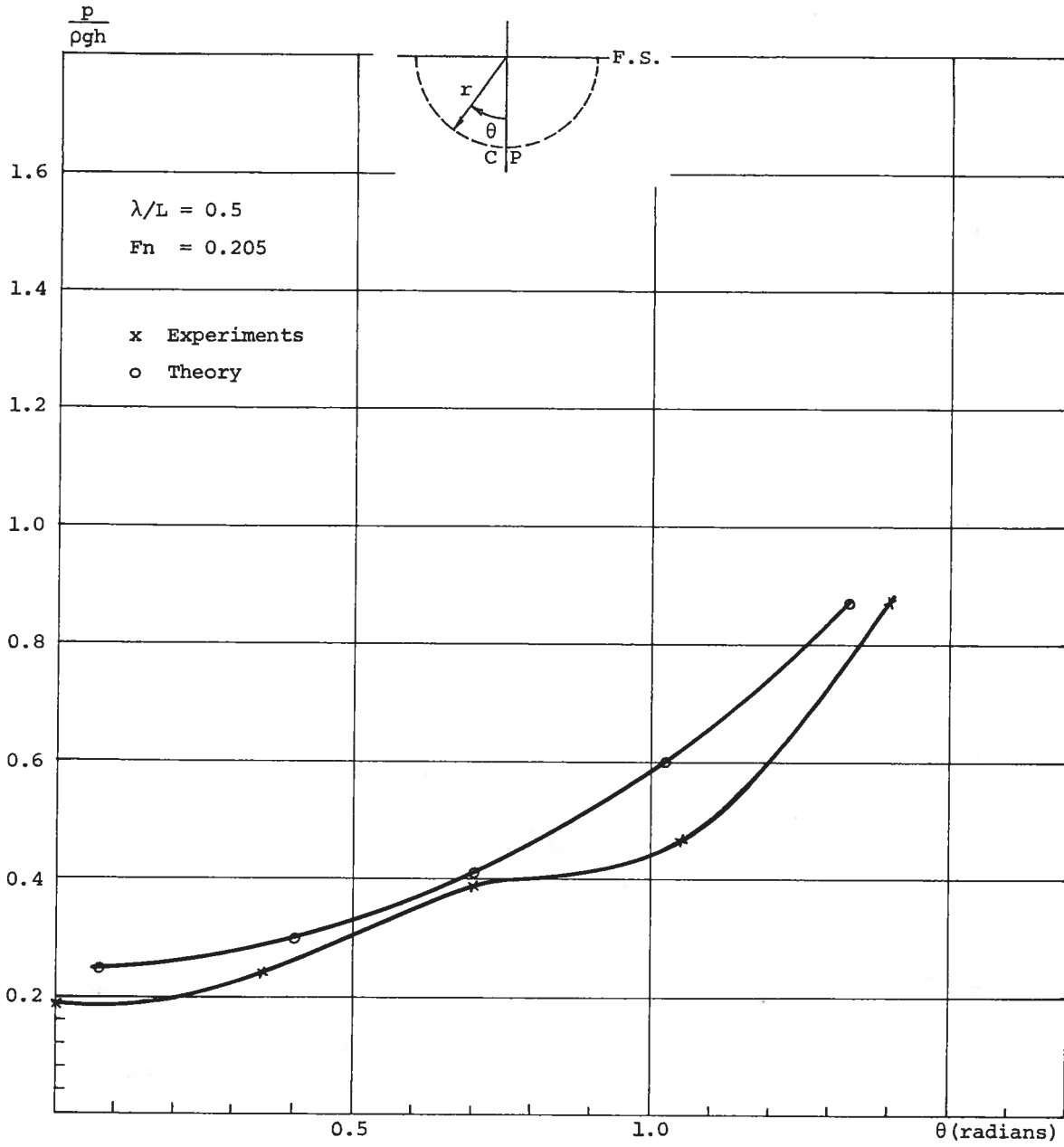


FIGURE 61

PRESSURE VARIATION ALONG THE CROSS-SECTION B_A

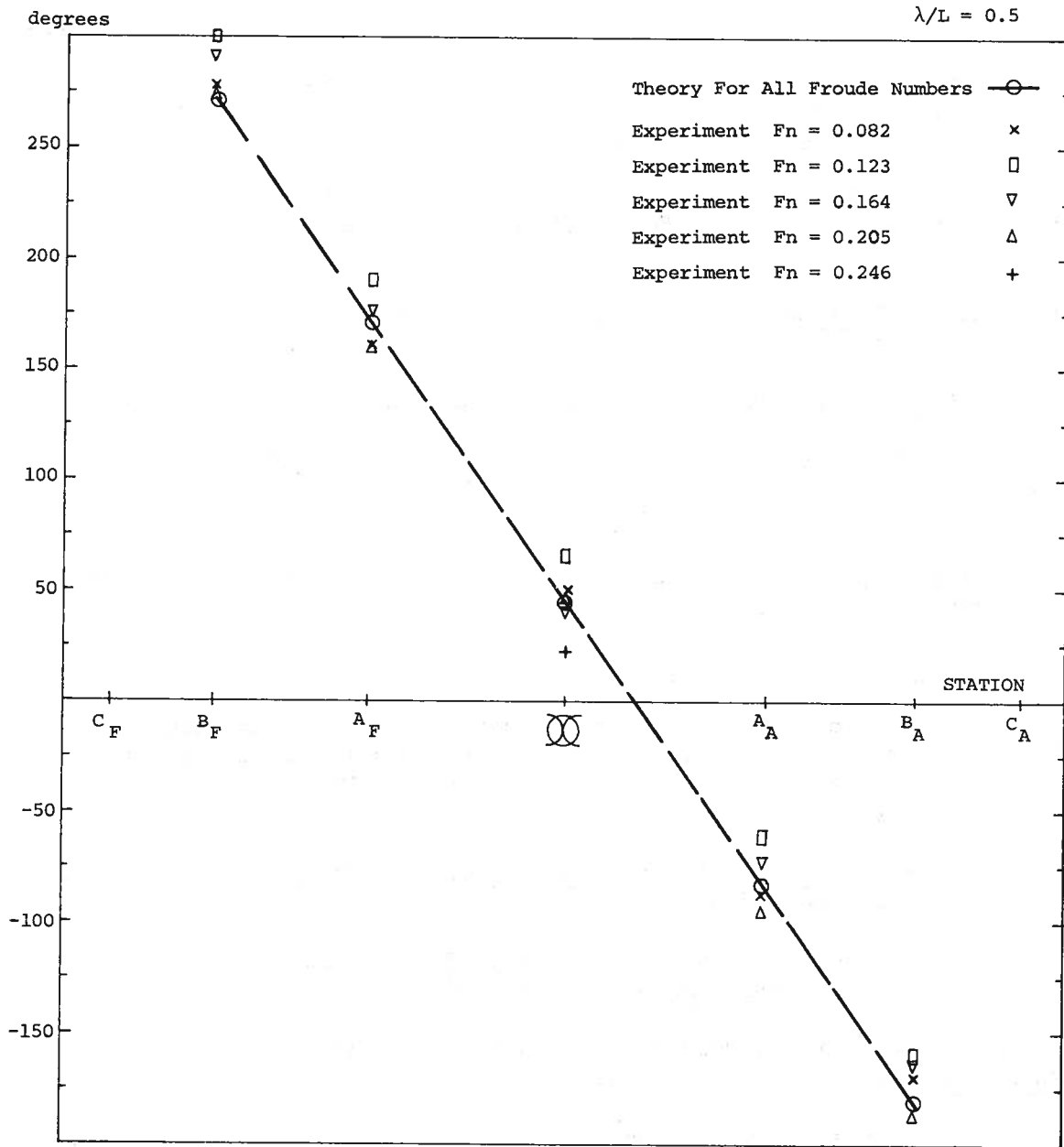


FIGURE 62

LONGITUDINAL DISTRIBUTION OF THE PHASE ANGLE
OF THE PRESSURE

VI. REFERENCES

- Abels, F; "Die Druckverteilung an einem festgehaltenen Schiffsmodell im regelmässigen Seegang," Jahrbuch der Schiffbautechnischen Gesellschaft, 53 (1959). Springer Verlag, Berlin /Göttingen/ Heidelberg.
- Abramowitz, M., and Stegun, I.A. Handbook of Mathematical Functions. National Bureau of Standards Mathematics Series, 55, Washington, D.C. (1964).
- Dettman, John W. Applied Complex Variables, The Macmillan Company, New York - Collier - Macmillan Limited, London (1965).
- Erdélyi, A. Asymptotic Expansions. Dover Publications, Inc., New York (1956).
- Faltinsen, O. "Comparison between theory and experiments of wave-induced loads for Series-60 hull with $C_B = 0.80$ ", Det norske Veritas, Oslo, Norway, Report No. 70-27-S, 1970.^B
- Gradshteyn, I.S., Ryzhik, I.M. Tables of Integrals, Series, and Products, Academic Press, New York and London, (1965).
- Jones, D.S. Generalized Functions. McGraw-Hill Book Co., New York, (1966).
- Lee, C.M. "Heaving Forces and Pitching Moments on a Semi-submerged and Restrained Prolate Spheroid Proceeding in Regular Head Waves", Report No. NA-64-2, Institute of Engineering Research, University of California, Berkeley, California, (1964).
- Lighthill, M.J. Fourier Analysis and Generalized Functions. Cambridge University Press, Cambridge (1958).
- Newman, J.N. "The Damping and Wave Resistance of a Pitching and Heaving Ship". Journal of Ship Research, 3:1 (1959).
- Newman, J.N. "The Exciting Forces on Fixed Bodies in Waves," Journal of Ship Research, 6:3 (1962) 10-17.
- Ogilvie, T.F. Unpublished work (1969).
- Ogilvie, T.F. and Tuck, E.O. "A Rational Strip Theory of Ship Motions: Part I." Department of Naval Architecture and Marine Engineering, College of Engineering, The University of Michigan, Ann Arbor, Michigan, Report No. 013, March 1969.
- Ogilvie, T.F. : "Singular Perturbation Problems in Ship Hydrodynamics", Department of Naval Architecture and Marine Engineering, College of Engineering, The University of Michigan, Ann Arbor, Michigan. Report No. 096, October 1970.

- Ogilvie, T.F. "On the Computation of Wave-Induced Bending and Torsion Moments" Journal of Ship Research, 15 (1971) 217-220.
- Salvesen, N., Tuck, E.O., Faltinsen, O. "Ship Motions and Sea Loads", SNAME Transactions, 78, (1970) 250-287.
- Ursell, F; "On Head Seas Travelling Along a Horizontal Cylinder." J. Inst. Maths. Applics., 4 (1968a) 414-427.
- Ursell, F. "The expansion of water-wave potentials at great distances". Proc.Camb.Phil.Soc. 64, (1968b), 811.
- Van Dyke, M. Perturbation Methods in Fluid Mechanics, 1964, Academic Press, New York and London.

DOCUMENT CONTROL DATA - R & D

(Security classification of title, body of abstract and indexing annotation must be entered when the overall report is classified)

1. ORIGINATING ACTIVITY (Corporate author) UNIVERSITY OF MICHIGAN, Dept. of Naval Architecture and Marine Engineering Ann Arbor, Michigan 48104	2a. REPORT SECURITY CLASSIFICATION UNCLASSIFIED
	2b. GROUP

3. REPORT TITLE
A RATIONAL STRIP THEORY OF SHIP MOTIONS: PART II

4. DESCRIPTIVE NOTES (Type of report and inclusive dates)
Interim Technical Report

5. AUTHOR(S) (First name, middle initial, last name)
Odd M. Faltinsen

6. REPORT DATE 1 December 1971	7a. TOTAL NO. OF PAGES 137 + vii	7b. NO. OF REFS 19
-----------------------------------	-------------------------------------	-----------------------

8a. CONTRACT OR GRANT NO. N00014-67-A-0181-0016	9a. ORIGINATOR'S REPORT NUMBER(S) No. 113 (Dept. of Nav. Arch. & Mar. Eng.)
b. PROJECT NO. SR 009 01 01	9b. OTHER REPORT NO(S) (Any other numbers that may be assigned this report) none
c.	
d.	

10. DISTRIBUTION STATEMENT
This document has been approved for public release and sale; its distribution is unlimited.

11. SUPPLEMENTARY NOTES	12. SPONSORING MILITARY ACTIVITY Naval Ship Research & Development Center, Bethesda, Md. 20034
-------------------------	--

13. ABSTRACT

The exact ideal-fluid boundary-value problem is formulated for the diffraction of head-sea regular waves by a restrained ship. The problem is then simplified by applying four restrictions: 1) the body must be slender; 2) the wave amplitude is small; 3) the wave length of the incoming waves is of the order of magnitude of the transverse dimensions of the ship; 4) the forward speed is zero or it is $O(\epsilon^{1/2-a})$, $0 < a \leq 1/2$, where ϵ is the slenderness parameter.

The problem is solved by using matched asymptotic expansions. The result shows that the wave is attenuated as it propagates along the ship. The result is not expected to be valid near the bow or stern of the ship.

The pressure distribution and force distribution along a ship model with circular cross-sections have been calculated. The total force on the ship has been compared with the value predicted by the Khaskind relation. The agreement is good.

The experimental and theoretical pressure distribution along a prolate spheroid have been compared. The predicted attenuation of the peak pressure is very well confirmed by the experiments. In addition, theory and experiment agree that the peak pressure near the ship generally leads the Froude-Kriloff pressure peak by 45° .

14. KEY WORDS	LINK A		LINK B		LINK C	
	ROLE	WT	ROLE	WT	ROLE	WT
Ship Motions Diffraction of Water Waves Asymptotic Expansions Slender-Body Theory						

University of Michigan, Department of Naval Architecture and Marine Engineering. A RATIONAL STRIP THEORY OF SHIP MOTIONS: PART II, by Odd Faltnesen. No. 113, December 1971. 137pp., 19 refs. UNCLASSIFIED

The exact ideal-fluid boundary-value problem is formulated for the diffraction of head-sea regular waves by a restrained ship. The problem is then simplified by applying four restrictions: 1) the body must be slender; 2) the wave amplitude is small; 3) the wave length of the incoming waves is of the order of magnitude of the transverse dimensions of the ship; 4) the forward speed is zero or it is $0(\epsilon^{1/2-a})$, $0 < a \leq 1/2$, where ϵ is the slenderness parameter.

The problem is solved by using matched asymptotic expansions. The result shows that the wave is attenuated as it propagates along the ship. The result is not expected to be valid near the bow or the stern of the ship.

Ship Motions
Strip Theory
Asymptotic Expansions
Slender-Body Theory

University of Michigan, Department of Naval Architecture and Marine Engineering. A RATIONAL STRIP THEORY OF SHIP MOTIONS: PART II, by Odd Faltnesen. No. 113, December 1971. 137pp., 19 refs. UNCLASSIFIED

The exact ideal-fluid boundary-value problem is formulated for the diffraction of head-sea regular waves by a restrained ship. The problem is then simplified by applying four restrictions: 1) the body must be slender; 2) the wave amplitude is small; 3) the wave length of the incoming waves is of the order of magnitude of the transverse dimensions of the ship; 4) the forward speed is zero or it is $0(\epsilon^{1/2-a})$, $0 < a \leq 1/2$, where ϵ is the slenderness parameter.

The problem is solved by using matched asymptotic expansions. The result shows that the wave is attenuated as it propagates along the ship. The result is not expected to be valid near the bow or the stern of the ship.

Ship Motions
Strip Theory
Asymptotic Expansions
Slender-Body Theory

University of Michigan, Department of Naval Architecture and Marine Engineering. A RATIONAL STRIP THEORY OF SHIP MOTIONS: PART II, by Odd Faltnesen. No. 113, December 1971. 137pp., 19 refs. UNCLASSIFIED

The exact ideal-fluid boundary-value problem is formulated for the diffraction of head-sea regular waves by a restrained ship. The problem is then simplified by applying four restrictions: 1) the body must be slender; 2) the wave amplitude is small; 3) the wave length of the incoming waves is of the order of magnitude of the transverse dimensions of the ship; 4) the forward speed is zero or it is $0(\epsilon^{1/2-a})$, $0 < a \leq 1/2$, where ϵ is the slenderness parameter.

The problem is solved by using matched asymptotic expansions. The result shows that the wave is attenuated as it propagates along the ship. The result is not expected to be valid near the bow or the stern of the ship.

Ship Motions
Strip Theory
Asymptotic Expansions
Slender-Body Theory

University of Michigan, Department of Naval Architecture and Marine Engineering. A RATIONAL STRIP THEORY OF SHIP MOTIONS: PART II, by Odd Faltnesen. No. 113, December 1971. 137pp., 19 refs. UNCLASSIFIED

The exact ideal-fluid boundary-value problem is formulated for the diffraction of head-sea regular waves by a restrained ship. The problem is then simplified by applying four restrictions: 1) the body must be slender; 2) the wave amplitude is small; 3) the wave length of the incoming waves is of the order of magnitude of the transverse dimensions of the ship; 4) the forward speed is zero or it is $0(\epsilon^{1/2-a})$, $0 < a \leq 1/2$, where ϵ is the slenderness parameter.

The problem is solved by using matched asymptotic expansions. The result shows that the wave is attenuated as it propagates along the ship. The result is not expected to be valid near the bow or the stern of the ship.

Ship Motions
Strip Theory
Asymptotic Expansions
Slender-Body Theory

(continued)
The pressure distribution and force distribution along a ship model with circular cross-sections have been calculated. The total force on the ship has been compared with the value predicted by the Khaskind relation. The agreement is good.
The experimental and theoretical pressure distribution along a prolate spheroid have been compared. The predicted attenuation of the peak pressure is very well confirmed by the experiments. In addition, theory and experiment agree that the peak pressure near the ship generally leads the Froude-Kriloff pressure peak by 45° .

(continued)
The pressure distribution and force distribution along a ship model with circular cross-sections have been calculated. The total force on the ship has been compared with the value predicted by the Khaskind relation. The agreement is good.
The experimental and theoretical pressure distribution along a prolate spheroid have been compared. The predicted attenuation of the peak pressure is very well confirmed by the experiments. In addition, theory and experiment agree that the peak pressure near the ship generally leads the Froude-Kriloff pressure peak by 45° .



(continued)
The pressure distribution and force distribution along a ship model with circular cross-sections have been calculated. The total force on the ship has been compared with the value predicted by the Khaskind relation. The agreement is good.
The experimental and theoretical pressure distribution along a prolate spheroid have been compared. The predicted attenuation of the peak pressure is very well confirmed by the experiments. In addition, theory and experiment agree that the peak pressure near the ship generally leads the Froude-Kriloff pressure peak by 45° .

(continued)
The pressure distribution and force distribution along a ship model with circular cross-sections have been calculated. The total force on the ship has been compared with the value predicted by the Khaskind relation. The agreement is good.
The experimental and theoretical pressure distribution along a prolate spheroid have been compared. The predicted attenuation of the peak pressure is very well confirmed by the experiments. In addition, theory and experiment agree that the peak pressure near the ship generally leads the Froude-Kriloff pressure peak by 45° .

University of Michigan, Department of Naval Architecture and Marine Engineering.
 A RATIONAL STRIP THEORY OF SHIP MOTIONS:
 PART II, by Odd Faltingsen.
 No. 113, December 1971. 137pp., 19 refs.
 UNCLASSIFIED

The exact ideal-fluid boundary-value problem is formulated for the diffraction of head-sea regular waves by a restrained ship. The problem is then simplified by applying four restrictions: 1) the body must be slender; 2) the wave amplitude is small; 3) the wave length of the incoming waves is of the order of magnitude of the transverse dimensions of the ship; 4) the forward speed is zero or it is $0(\epsilon^{1/2-a})$, $0 < a \leq 1/2$, where ϵ is the slenderness parameter.

The problem is solved by using matched asymptotic expansions. The result shows that the wave is attenuated as it propagates along the ship. The result is not expected to be valid near the bow or the stern of the ship.

Ship Motions
 Strip Theory
 Asymptotic Expansions
 Slender-Body Theory

University of Michigan, Department of Naval Architecture and Marine Engineering.
 A RATIONAL STRIP THEORY OF SHIP MOTIONS:
 PART II, by Odd Faltingsen.
 No. 113, December 1971. 137pp., 19 refs.
 UNCLASSIFIED

The exact ideal-fluid boundary-value problem is formulated for the diffraction of head-sea regular waves by a restrained ship. The problem is then simplified by applying four restrictions: 1) the body must be slender; 2) the wave amplitude is small; 3) the wave length of the incoming waves is of the order of magnitude of the transverse dimensions of the ship; 4) the forward speed is zero or it is $0(\epsilon^{1/2-a})$, $0 < a \leq 1/2$, where ϵ is the slenderness parameter.

The problem is solved by using matched asymptotic expansions. The result shows that the wave is attenuated as it propagates along the ship. The result is not expected to be valid near the bow or the stern of the ship.

Ship Motions
 Strip Theory
 Asymptotic Expansions
 Slender-Body Theory

University of Michigan, Department of Naval Architecture and Marine Engineering.
 A RATIONAL STRIP THEORY OF SHIP MOTIONS:
 PART II, by Odd Faltingsen.
 No. 113, December 1971. 137pp., 19 refs.
 UNCLASSIFIED

The exact ideal-fluid boundary-value problem is formulated for the diffraction of head-sea regular waves by a restrained ship. The problem is then simplified by applying four restrictions: 1) the body must be slender; 2) the wave amplitude is small; 3) the wave length of the incoming waves is of the order of magnitude of the transverse dimensions of the ship; 4) the forward speed is zero or it is $0(\epsilon^{1/2-a})$, $0 < a \leq 1/2$, where ϵ is the slenderness parameter.

The problem is solved by using matched asymptotic expansions. The result shows that the wave is attenuated as it propagates along the ship. The result is not expected to be valid near the bow or the stern of the ship.

Ship Motions
 Strip Theory
 Asymptotic Expansions
 Slender-Body Theory

University of Michigan, Department of Naval Architecture and Marine Engineering.
 A RATIONAL STRIP THEORY OF SHIP MOTIONS:
 PART II, by Odd Faltingsen.
 No. 113, December 1971. 137pp., 19 refs.
 UNCLASSIFIED

The exact ideal-fluid boundary-value problem is formulated for the diffraction of head-sea regular waves by a restrained ship. The problem is then simplified by applying four restrictions: 1) the body must be slender; 2) the wave amplitude is small; 3) the wave length of the incoming waves is of the order of magnitude of the transverse dimensions of the ship; 4) the forward speed is zero or it is $0(\epsilon^{1/2-a})$, $0 < a \leq 1/2$, where ϵ is the slenderness parameter.

The problem is solved by using matched asymptotic expansions. The result shows that the wave is attenuated as it propagates along the ship. The result is not expected to be valid near the bow or the stern of the ship.

Ship Motions
 Strip Theory
 Asymptotic Expansions
 Slender-Body Theory

(continued)
The pressure distribution and force distribution along a ship model with circular cross-sections have been calculated. The total force on the ship has been compared with the value predicted by the Khaskind relation. The agreement is good.
The experimental and theoretical pressure distribution along a prolate spheroid have been compared. The predicted attenuation of the peak pressure is very well confirmed by the experiments. In addition, theory and experiment agree that the peak pressure near the ship generally leads the Froude-Kriloff pressure peak by 45° .

(continued)
The pressure distribution and force distribution along a ship model with circular cross-sections have been calculated. The total force on the ship has been compared with the value predicted by the Khaskind relation. The agreement is good.
The experimental and theoretical pressure distribution along a prolate spheroid have been compared. The predicted attenuation of the peak pressure is very well confirmed by the experiments. In addition, theory and experiment agree that the peak pressure near the ship generally leads the Froude-Kriloff pressure peak by 45° .

(continued)
The pressure distribution and force distribution along a ship model with circular cross-sections have been calculated. The total force on the ship has been compared with the value predicted by the Khaskind relation. The agreement is good.
The experimental and theoretical pressure distribution along a prolate spheroid have been compared. The predicted attenuation of the peak pressure is very well confirmed by the experiments. In addition, theory and experiment agree that the peak pressure near the ship generally leads the Froude-Kriloff pressure peak by 45° .

(continued)
The pressure distribution and force distribution along a ship model with circular cross-sections have been calculated. The total force on the ship has been compared with the value predicted by the Khaskind relation. The agreement is good.
The experimental and theoretical pressure distribution along a prolate spheroid have been compared. The predicted attenuation of the peak pressure is very well confirmed by the experiments. In addition, theory and experiment agree that the peak pressure near the ship generally leads the Froude-Kriloff pressure peak by 45° .

+